Assessing Least Squares Monte Carlo for the Kulatilaka Trigeorgis General Real Options Pricing Model

Giuseppe Alesii*

18th June 2008

Abstract

We assess the applicability of (Longstaff and Schwartz, 2001) Least Squares Monte Carlo method (LSMC) to the General Real Options Pricing Model of (Kulatilaka and Trigeorgis, 1994) (KT). We propose some moment matching methods to get comparable results from KT model under different underlying stochastic processes for both LSMC and multivariate lattice methods.

We study LSMC under different stochastic processes, namely: GBM, up to three dimensions, and models 1, 2 and 3 in (Schwartz, 1997). Each LSMC application has been appropriately benchmarked by lattice methods.

We explore empirically a generalization of proposition 1 page 124 in (Longstaff and Schwartz, 2001) with respect to the number of discretization points K, of basis functions M, and of the number of simulated paths N for an individual estimate. Then, we study the speed precision tradeoff of LSMC when applied to the KT model with respect to the last two parameters just mentioned. Finally, we show the small and large sample statistical properties of LSMC estimates when these are replicated R times. We show how to make statistical inference on them, providing a practical application of proposition 2 page 125 in (Longstaff and Schwartz, 2001).

We conclude that LSMC can be conveniently used to estimate KT models in both univariate and multivariate frameworks, providing quick and unbiased estimates when some moment matching methods are adopted, an adequate number of replications is performed and the right least squares parameters are honed to choose consciously the appropriate trade off between precision and speed.

JEL classification code: G13, G31.
Keywords: Least Squares Monte Carlo (LSMC), Real Options, multi dimensional binomial lattices, moment matching, GBM, Geometric Ornstein Uhlenbeck, Two Factor Model, Three Factor Model, stochastic interest rates.

*Corresponding Author, **ADDRESS**: Universitá di L'Aquila, Faculty of Mathematics, Physics and Natural Sciences, Department of Pure and Applied Mathematics, Via Vetoio (Coppito 1), Coppito di L'Aquila 67010 AQ, Italy, Phone: (intl-code-for Italy) + 0862+433156; Fax idem+0862+433180; e-mail: galesii@luiss.it.

Assessing Least Squares Monte Carlo for the Kulatilaka Trigeorgis General Real Options Pricing Model

Abstract

We assess the applicability of (Longstaff and Schwartz, 2001) Least Squares Monte Carlo method (LSMC) to the General Real Options Pricing Model of (Kulatilaka and Trigeorgis, 1994) (KT). We propose some moment matching methods to get comparable results from KT model under different underlying stochastic processes for both LSMC and multivariate lattice methods.

We study LSMC under different stochastic processes, namely: GBM, up to three dimensions, and models 1, 2 and 3 in (Schwartz, 1997). Each LSMC application has been appropriately benchmarked by lattice methods.

We explore empirically a generalization of proposition 1 page 124 in (Longstaff and Schwartz, 2001) with respect to the number of discretization points K, of basis functions M, and of the number of simulated paths N for an individual estimate. Then, we study the speed precision tradeoff of LSMC when applied to the KT model with respect to the last two parameters just mentioned. Finally, we show the small and large sample statistical properties of LSMC estimates when these are replicated R times. We show how to make statistical inference on them, providing a practical application of proposition 2 page 125 in (Longstaff and Schwartz, 2001).

We conclude that LSMC can be conveniently used to estimate KT models in both univariate and multivariate frameworks, providing quick and unbiased estimates when some moment matching methods are adopted, an adequate number of replications is performed and the right least squares parameters are honed to choose consciously the appropriate trade off between precision and speed.

JEL classification code: G13, G31.

Keywords: Least Squares Monte Carlo (LSMC), Real Options, multi dimensional binomial lattices, moment matching, GBM, Geometric Ornstein Uhlenbeck, Two Factor Model, Three Factor Model, stochastic interest rates.

Contents

List of Figures

List of Tables

Introduction

Early approaches to real option valuation were derived on a close parallelism with financial options models. These are simply inadequate to describe the complexities of intertwined decisions concerning an industrial project flexibilities. (Kulatilaka and Trigeorgis, 1994) provide, instead, a framework for pricing real options which is general enough to entail a wide variety of decisions and to evaluate them all in one model without *ad hoc* solutions which strive to find the financial option which best resembles to the real one under exam. Hence, in section 1 we motivate the choice of the Kulatilaka Trigeorgis (henceforth, KT) model, providing a brief review and stressing its advantages over other switching options valuation frameworks as applied to real options.

In extant literature, the KT model has been often implemented in univariate frameworks. Instead, we aim to extend the applicability of the KT model to multi variate frameworks.[1] This is necessary to get realistic results since industrial projects are planned over long horizons over which all cost and revenue drivers become stochastic. Pursuing this aim, numerical methods previously used in the literature, such as binomial lattices or grids, are not the most promising approaches, being affected by the well known curse of dimensionality. Therefore, we chose to apply the most suitable Monte Carlo method for pricing American options among those available in current literature, namely (Longstaff and Schwartz, 2001) Least Squares Monte Carlo (henceforth, LSMC). Hence, in section 2, we motivate the choice of LSMC. Moreover, we derive discrete time methods necessary to implement correctly the KT model in both a LSMC framework and multivariate lattices to be used as benchmarks. In section 3 a numerical example is reported in which we progressively increase the complexity of the underlying data generating process (DGP) in the same risk mapping equation.

Assessing the applicability of LSMC to the KT model means to test whether and how the method of (Longstaff and Schwartz, 2001) provides accurate results with respect to lattice valuations used as benchmarks. For this purpose, we have set up a series of real options non coordinated numerical examples which verifies the applicability when the underlying DGP is specified as a univariate GBM, a bivariate and a trivariate GBM with correlated Wiener processes, a Geometric Ornstein Uhlenbeck with spring effect on the log of normal values, model 1 in (Schwartz, 1997), a GBM with convenience yield generated by an Arithmetic Ornstein Uhlenbeck, model 2 in (Schwartz, 1997), a GBM with both convenience yield and risk free rates

[1] Among mayor analytic approaches to real options analysis reviewed by (Borison, 2005), the methods proposed in this paper can be classified in the *integrated approach*. As a matter of fact, every source of risk is singled out and the investment project is valued in a "deconstructed state". The alternative approach – MAD, *marketed asset disclaimer* – followed among the others by (Copeland and Antikarov, 2005) and (Mun, 2002) derives the volalitily – including techical uncertainties and other private risks – of the investment project as a whole, a sort of notional pseudo asset value, and then implements a martingale pricing model on it. In this paper we follow the former approach but unlike (Borison, 2005) only for market risks.

generated by Arithmetic Ornstein Uhlenbeck with correlated Wiener processes, model 3 in (Schwartz, 1997).

We have pursued the following approach in assessing accuracy of LSMC valuations. To begin with, we have checked whether LSMC is actually a convergent algorithm in this application, see section 4.1. To be specific, after choosing, with hindsight with respect to the ensuing steps in this research, the number of Monte Carlo simulations and the order of the polynomial equation estimated in the regression, we let $\Delta t \rightarrow 0$. We find that LSMC is not a convergent algorithm with respect to models with underlying, univariate or multivariate, GBM. Instead it converges asymptotically when the underlying DGP presents a mean reverting feature, both directly, model 1 (Schwartz, 1997), or indirectly, model 2 or 3 (Schwartz, 1997).

Secondly, following a standard approach in extant literature, we have studied the trade off between accuracy, represented by RMSE, and the number of paths simulated together with the order of the polynomial estimated, see section 4.2. Our results do not confirm in all the cases (Longstaff and Schwartz, 2001) propositions about convergence of LSMC. Instead, for the case of GBMs, (Glasserman and Yu, 2004) "divergence after a threshold" effect is observed with respect to both the number of paths and the order of the polynomial. Finally, for model 1 (Schwartz, 1997) accuracy depends very much on the number of paths simulated but not much on the order of the polynomial estimated. Instead, for models 2 and 3 (Schwartz, 1997), (Longstaff and Schwartz, 2001) proposition about convergence of LSMC is confirmed with respect to both the number of paths simulated and the order of the polynomial in the equation used to estimate continuation values.

Thirdly, we have studied the trade off between accuracy and computational time. Results for underlying GBM DGPs confirm findings provided by extant literature for different applications: even for very high orders of the regression polynomial after some threshold there is no gain in accuracy due to the increase in the number of paths simulated. Results for model 1 (Schwartz, 1997) shows that the trade off between accuracy and speed is very much the same for different orders of the polynomial. Instead, for models 2 and 3 (Schwartz, 1997), better trade off properties are shown for a high order of the regression polynomial. To sum up, in all three DGPs of (Schwartz, 1997), accuracy can be improved for very high orders of the polynomial increasing the number of paths simulated, confirming the convergence properties.

Fourtly, we have tackled the issue of making statistical inference on LSMC results. Using bootstrapping methods, we show that it is actually appropriate to apply statistical inference methods to verify that LSMC estimates are unbiased with respect to their respective lattice benchmarks. Consequently, we find that LSMC produces estimates that are significantly different from lattice benchmarks, mostly biased low. Although

that is true, LSMC estimates distributions are entailed in a strict neighborhood of their respective lattice benchmarks. Hence, we conclude that, although statistically different from their lattice benchmarks, LSMC estimates are economically useful in valuing investmen projects.

In section 7 we derived the main conclusions of this paper and stress the limits of LSMC applicability to the KT model. Moreover, we set up the blueprint for several side applications of LSMC to the Kulatilaka Trigeorgis general model of real options.

1 The Kulatilaka Trigeorgis General Model of Real Options

In this section we introduce the reader to the Kulatilaka Trigeorgis General Model of Real Options. We start with the familiar risk adjusted discount rate approach in traditional capital budgeting to be used as benchmark of comparison in order to stress the differences and analogies with the KT model. We position the KT model in the class of the Bellman Dynamic Programming applications describing the solution offered by this strand of literature. We sketch the previous versions of the model and show how applying LSMC to the KT model is simply the natural evolution of the general model of real options.

For just to start basic, traditional NPV implies that forecasted cash flows are discounted according to an asset pricing model, e.g. a CAPM, which derives the risk adjusted discount rate (henceforth, RADR) from the expected return of a corresponding twin security traded in financial markets, see expression (1). Without any loss of generality, NPV can be expressed simply discounting period by period cash flows, the *running present value*, (henceforth, RPV_t) see expression (2).[2]

$$NPV = \sum_{t=0}^{T} \frac{E(CF_t)}{(1+E(R_j))^t} \tag{1}$$

$$RPV_t = E(CF_t) + \frac{RPV_{t+1}}{1+E(R_j)} \; \forall t = T-1, \ldots, 0 \tag{2}$$

being for $t = T$ $RPV_t = E(CF_T)$ and for $t = 0$, $RPV_0 \equiv NPV$.

Apart from the implied passive behaviour in managing the investment project – which is the usual main motivation of a real option valuation, traditional NPV presents several other shortcomings. To begin with, cash flows forecasting is completely decoupled from the asset pricing model used to compute the RADR. Their relation is allegorical at best. As a matter of fact, RADR is determined based on the more or less subjective choice of a twin security or pure play from which risk return features of the industrial project

[2]Previous applications of running present value in both traditional NPV and real options frameworks can be found in (Luenberger, 1998).

can be gleaned. This makes very cumbersome to specify analytically the various risk drivers which affect cash flows. As a matter of fact, in most of the cases, both the cash flow figure $E(CF_t)$ and the interest rate $E(R_j)$ are considered respectively as sufficient statistics to describe expected profitability and the risk return features of the project as a whole.[3]

Instead, the advantage of real options is not only to accomodate an optimal dynamic management of the industrial project but also to specify a pricing framework in which both cash flows and interest rates used to discount them are derived consistently. As a matter of fact, most real options models are derived in a martingale pricing framework in which expected cash flows are computed on an equivalent martingale measure –$E^*(/)$ – and discounted at the risk free rate.[4] Moreover, in multivariate real options models, it is easy to specify analytically the stochastic properties of the various risk drivers of cash flows. For instance, cost, volume and price drivers in equation (3), which yield cash flows from operations, can each be specified as generated by the most appropriate stochastic process.

$$CF_t(\boldsymbol{\theta_t}, m, t) = Q \cdot (P - Uvc) - F \tag{3}$$

where:

$CF_t(/) \equiv EBIT$	:	cash flow from operations or earnings before interest and taxes, under the assumption that working capital does not change;
Q	:	volume produced and sold, in units used to specify prices and variable costs;
P	:	unit price;
Uvc	:	unit variable cost;
F	:	fixed – with respect to volume produced and sold – costs.

In the KT model cash flows are specified not only as a function of at least one risk driver but also according to the operating mode m in which the investment project is managed, i.e. waiting to invest, producing, being idle, expanded, contracted, etc. In a more general form, RPV_t reported in expression (2) can be rewritten as

$$RPV_t(\boldsymbol{\theta_t}, m, t) = CF_t(\boldsymbol{\theta_t}, m, t) + \frac{E^*\left(RPV_{t+1}(\boldsymbol{\theta_{t+1}}, m, t+1)\right)}{e^{r_f \cdot \Delta t}} \; \forall t = T-1, \ldots, 0 \tag{4}$$

where:

$\boldsymbol{\theta_t}$	:=	vector of stochastic state variable, e.g. price of goods sold, cost of raw materials;
m	:=	operating modes, waiting to invest, producing, being idle, producing in an expanded scale plant, producing in a contracted scale plant;
$E^*(/)$	:=	expectation operator on an equivalent martingale measure, hence starred;
r_f	:=	risk free rate.

Traditional NPV is then a particular case of the general specification given in (4) being simply the $RPV_{t=0}$ obtained managing the project in the same operating mode over the whole planning horizon.

[3] See (McDonald, 2006) for a review of traditional NPV and a comparison with martingale pricing adopted by real options analysis. For simplicity in this paper we do not report all the particular cases in which discounted cash flows can be articulated.

[4] See (Hodder et al., 2001) for real options modelling in a RADR framework.

Instead, both technological flexibilities and organizational capabilities can be conveniently exploited changing the operating mode depending on the stochastic state variable θ_t. This takes place at a cost. For instance, the cost of passing from the wait to invest mode to the production mode is given by the sum necessary to purchase the industrial plant. Suspending production and keeping the plant idle implies mothballing costs for the plant and severance payments for the workforce. By the same token, restarting production implies costs for re hiring workforce and refurbish plant and machinery. Finally, in most of the cases, abandoning the project implies cashing in the salvage value of the industrial plant. In conclusion, in addition to the cash flows produced by operating modes at every epoch, an investment project can yield non recurrent cash flows due to asset play, purchase or sale of the plant, and to changing modes of operation. These transition costs are usually summarized in a transition cost matrix, see expression (5).

$$c_{m,\ell}\left(\boldsymbol{\theta_t}, \ell, t\right) = \begin{pmatrix} 0 & c_{1,2} & c_{1,3} & c_{1,3} & \infty \\ \infty & 0 & c_{2,3} & c_{2,4} & \infty \\ \infty & c_{3,2} & 0 & c_{3,4} & \infty \\ \infty & c_{4,2} & \infty & 0 & c_{4,5} \\ \infty & \infty & \infty & \infty & 0 \end{pmatrix} \tag{5}$$

where, being m the initial mode, rows, and ℓ the final mode, columns:

$m = 1$:= wait to invest mode;
$m = 2$:= production mode;
$m = 3$:= being idle mode, production suspended;
$m = 4$:= expanded production mode;
$m = 5$:= abandoned mode;

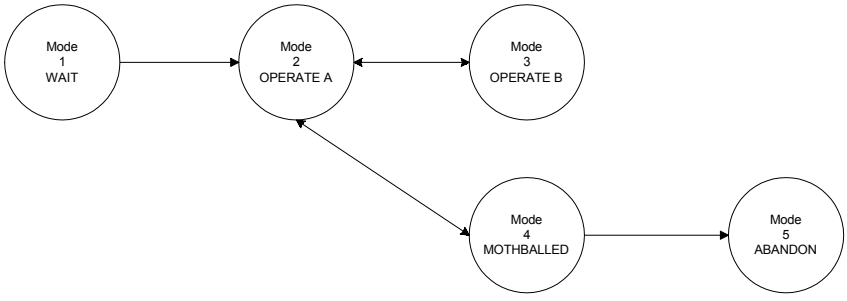

Figure 1: Accessibility of operating modes.

Legend: Recurrent modes are linked by arrows with pointed heads on both sides. Reflecting modes are linked by a one side pointed head arrow originating from them. Absorbing modes are linked by a one side pointed head arrow originating from a recurrent mode.

Adopting a terminology used in the description of Markov chains, it is worth noting that according to their accessibility, operating modes can be classified in three categories, see figure 1. Reflecting modes,

like the waiting to invest mode; Recurrent modes, like the production or being idle mode; and Absorbing modes, like the abandonment one. The first and the last can be easily recognized simply observing that their respective column or row has infinite transition costs in expression (5). Moreover, transition costs too can depend on some stochastic state variable in $\boldsymbol{\theta_t}$. For instance, the salvage value of a plant can be specified as dependent on the price of the land on which it has been built and its alternative uses, e.g. residential or commercial building.

Directed graph representation of the KT model, like the one proposed in figure 1, neglects the fact that operating modes can have different time horizons and switching opportunity frequencies. In other words, a project can be kept in the wait to invest mode over a time horizon different from the life of the industrial plant.[5] On the other hand, the options to mothball and to restart production can be taken with a different frequency depending on both technological and institutional constraints over the technical life of the project. Considering all real options in an investment project as if they have the same time to maturity and the same exercise frequency leads to an overvaluation of the investment opportunity.

(Vollert, 2002), pages 104-116, provides a time scaled graphical decomposition method originally concieved for describing the interacting options approach of (Trigeorgis, 1991) but easily adapted to the KT model, see for instance figure 2 for a representation of the specification of the model considered in this section. Hence, directed graph and time scaled representations for the KT model are complementary in representing thoroughly the optionalities offered by an investment project.

Assuming as objective function the net present value (or equivalently, the running present value at time zero) for the plant kept in the wait to invest mode, management faces the problem of determining the *optimal policy* or *control law* according to which optimal switches between operating modes are chosen in every epoch and for every level of the state variable. Had transition costs been nil, switching decisions could have been taken according to a myopic criterion just comparing each mode payoff at each epoch, switching opportunity, a *Marshallian thresholds* approach as defined by (Dixit and Pindyck, 1994).

Since switching cost are important in describing asset play and actual management of an industrial plant, any switching decision in each epoch should take into due account the previous and the following, in other words it has to be optimal with respect to the whole sequence of switching decisions. Bellman Optimum principle provides a criterion for determining the optimal policy or control law, see page 16 in (Bertsekas, 1995).[6]

[5] The latter is dependent on obsolescence and other technical considerations, the former tipically depends on institutional and legal contraints such as building permits, patent rights or exploration leases.

[6] An alternative approach to dynamic optimization is pursued by (Brennan and Schwartz, 1985), (Dixit, 1989), chapter 7 in (Dixit and Pindyck, 1994), (Brekke and Oksendal, 1994), (Duckworth and Zervos, 2001). There a partial differential equation (pde) is derived and it is solved numerically or analytically. Certainly, their approach cannot be easily generalized

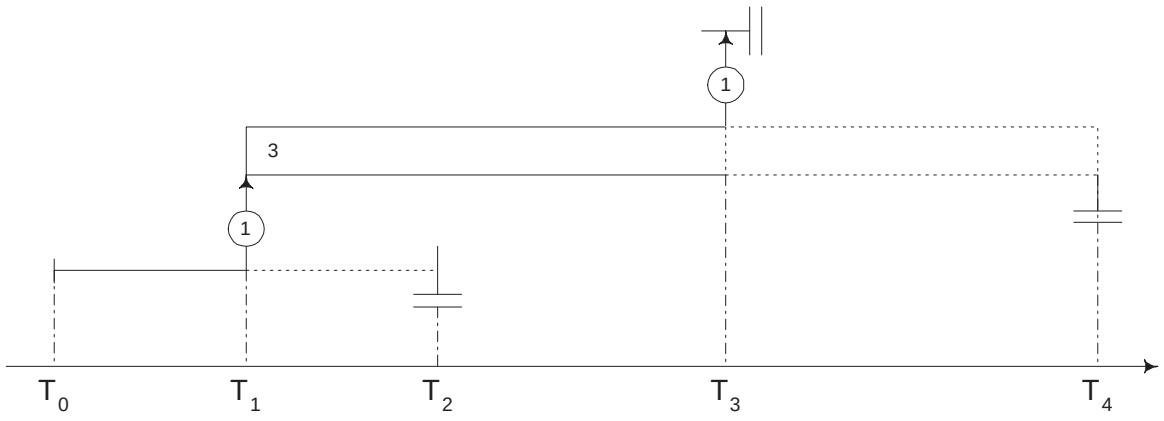

Figure 2: Graphical Representation of a KT model according to (Vollert, 2002).
Legend: horizontal axis represents time. The lower left hand side segment represents the time horizon over which the investment project can be kept in a *wait to invest* mode. Dashed lines represent inactive operating modes after an irreversible switch has occurred. Segments with an arrow and a solid circle represent American type switching over the number of modes reported in the circle. When the option to invest is exercised, the project in switched over the 3 recurrent modes grouped in a box. If at time T_3 salvage value is greater than continuation value, the project is abandoned. In any case, the project is terminated if it happens to be in the wait to invest mode at time T_2 or in one of the three recurrent production / mothballed plant at time T_4.

As a matter of fact, the optimal sequence of switching decisions is determined thanks to Bellman Dynamic Programming over a finite horizon solved using a value iteration algorithm applied in a backward induction process. More specifically, as noted by (Vollert, 2002), an optimal switching problem is a particular kind of impulse control problem.[7]

In continuos time modeling the proof of the existence of an optimal solution for a general optimal switching problem is not available yet in extant literature (Gamba, 2002). In discrete time modelling, instead, a solution always exists. Hence, the methods proposed in the following sections should not be interpreted as continuous time approximations but as solutions for discrete time real options problems.

In general, – leaving aside any consideration about discretization methods – the value iteration algorithm on a finite horizon works as described in equations (6)-(9). Starting from the end and going backward, equation (6) represents the boundary condition of the dynamic programming algorithm. It is independent from the entering mode m. The function $S(/)$ picks up from the state variables vector the salvage value of the plant.

in a multivariate framework. For instance, (Geltner et al., 1996), (Brekke and Schieldrop, 2000) in (Brennan and Trigeorgis, 2000), (Cortazar et al., 1998), (Cortazar et al., 2001) do not deal with more than bivariate cases. Moreover, the analytical solution pde approach does not accomodate a wide variety of stochastic processes. Finally, it requires a good familiarity with Ito's calculus which is far beyond most of practictioners capability and intuition.

[7]For an introduction to continuos time modelling of impulse control problems see page 347-369 in (Miranda and Fackler, 2002). For a review of the applications of impulse control to management, economics and finance problems see page 55 in (Vollert, 2002).

In equation (7) the ending mode ℓ is chosen in the set of available modes $\ell \epsilon L = \{1, 2, 3, 4, 5\}$, as previously listed, in order to maximize the sum of the last but one cash flow net of transition costs and the present value of the last value function. At time $t = T - 2$, see equation (8), for any entering mode m it is necessary to chose the maximizing mode ℓ in order to maximize the sum of the current cash flow net of transition costs and the present value of a value function which is dependent on the mode too. The general expression – Bellman Equation – for the backward induction procedure is represented by expression (9).

$$
\begin{aligned}
t &= T \\
F(\boldsymbol{\theta_T}, m, t) &= F(\boldsymbol{\theta_T}, T) = S(\boldsymbol{\theta_T}) && (6) \\
t &= T-1 \\
F(\boldsymbol{\theta_{T-1}}, m, T-1) &= \underset{\ell \epsilon L}{max} \left\{ \pi(\boldsymbol{\theta_{T-1}}, \ell, T-1) - c_{m,\ell}(\boldsymbol{\theta_{T-1}}, \ell, T-1) + \frac{E^*_{T-1}[S(\boldsymbol{\theta_T})]}{e^{r_f \cdot \Delta t}} \right\} && (7) \\
t &= T-2 \\
F(\boldsymbol{\theta_{T-2}}, m, T-2) &= \underset{\ell \epsilon L}{max} \left\{ \pi(\boldsymbol{\theta_{T-2}}, \ell, T-2) - c_{m,\ell}(\boldsymbol{\theta_{T-2}}, \ell, T-2) + \frac{E^*_{T-2}[F(\boldsymbol{\theta_{T-1}}, \ell, T-1)]}{e^{r_f \cdot \Delta t}} \right\} && (8) \\
\forall t &< T-2 \\
F(\boldsymbol{\theta_t}, m, t) &= \underset{\ell \epsilon L}{max} \left\{ \pi(\boldsymbol{\theta_t}, \ell, t) - c_{m,\ell}(\boldsymbol{\theta_t}, \ell, t) + \frac{E^*_t[F(\boldsymbol{\theta_{t+1}}, \ell, t+1)]}{e^{r_f \cdot \Delta t}} \right\} && (9)
\end{aligned}
$$

where:

$\boldsymbol{\theta_t}$	=	state variables vector;
$S(/)$	=	salvage value;
L	=	set of available modes of the dynamic system: $m = 1$, waiting; $m = 2$, mothballed; $m = 3$, operate A; $m = 4$, operate B; $m = 5$, abandoned;
$F(\boldsymbol{\theta_t}, m, t)$	=	value function at epoch t, for operating mode m and for a state variable level $\boldsymbol{\theta_t}$;
$\pi(\boldsymbol{\theta_t}, \ell, t)$	=	profit for a level of the state variable $\boldsymbol{\theta_t}$, for an operating mode ℓ, at epoch t;
$E^*_t[F(\boldsymbol{\theta_{t+1}}, \ell, t+1)]$	=	expected value on the equivalent martingale measure of the value function in the following epoch for the operating mode ℓ;
$c_{m,\ell}(\boldsymbol{\theta_t}, \ell, t)$	=	transition costs from mode m to mode ℓ, dependent on the state variable $\boldsymbol{\theta_t}$, e.g. SHS price of the more than five years old ship and wreckage value of the vessel.

In the first version of the KT model, (Kulatilaka and Marcus, 1988) strived to derive analytical solutions for the problem described in equations (6)-(9) in the spirit of (Black and Scholes, 1973), hence in a univariate framework with a Geometric Brownian Motion specified as data generating process. That solution was limited to a two mode, three period problem and is was not so easy to generalize. Instead, a grid, Markov chain approach is used by (Kulatilaka, 1988) and (Kulatilaka, 1993) to discretize a univariate Arithmetic Ornstein Uhlenbeck. In these versions, the procedure is easy to generalize to more than two modes but not to more than one source of risk being grid discretization approach very similar to pde numerical solution, i.e. unsuitable for multivariate problems. Another numerical approach is adopted by (Kulatilaka and Trigeorgis, 1994).[8] A (Cox et al., 1979) binomial lattice is used to discretize a univariate GBM while the model is proposed in a two modes version. A grid approach to discretize a GBM is proposed by (Kulatilaka, 1995)

[8]The same approach is pursued in (Trigeorgis, 1996) pages 171-196.

in (Trigeorgis, 1995) to price a multiple mode version although numerical examples are not provided. In the same framework (Alesii, 2000) proposes, instead, numerical examples deriving numerically thresholds for optimal switching over the whole planning horizon. Finally, (Gamba, 2002) proposes a bivariate version of the KT model implemented in both a (Boyle et al., 1989) bivariate binomial lattice and a LSMC discretization framework, the former being the benchmark to the latter.

The common feature of the previous versions of the KT model is the implementation of Bellman Dynamic Programming (DP) in the contingent claim (CC) discretization approach which was most fashionable at that time. In other words, the most important flaw of Dynamic Programming – the determination in a subjective way of the expected value function and of the interest rate to be used to discount it – is corrected borrowing from option pricing literature the principles of martingale pricing.[9] Following this line of reasoning, LSMC application to the KT model appears as a "Back to the Future" operation. As a matter of fact, a method very similar to (Longstaff and Schwartz, 2001) was proposed back in the '50s by (Bellman and Dreyfus, 1959) and was well known in operation research as *approximate value iteration*. Although that is true, the detour into contingent claims literature of the '70s and the '80s now allows us to apply the method of (Bellman and Dreyfus, 1959) in a no arbitrage framework, i.e. martingale pricing or in an equivalent risk neutral valuation, general equilibrium economy à la (Cox et al., 1985).

2 Applying LSMC to the KT model

In this section we motivate the choice of LSMC in the wide variety of Monte Carlo methods that extant literature offers for pricing American options. We provide a short review of previous methodological extensions and applications of LSMC in the field of real options. We then highlight some problems in applying LSMC in a discrete time KT model and provide some new methods to solve them. These same methods are then tested in the ensuing sections.

2.1 LSMC and other Monte Carlo Methods for Pricing American Options

LSMC is the least problem dependent modelling method among those using Monte Carlo to price American options. As a matter of fact, competing methods present some peculiarities and rigidities which prevent a flexible and thorough application to approximate value iteration in KT model.[10] For instance, the version of

[9] According to (Knudsen et al., 1999) page 435: "Dynamic Programming and contingent claim pricing are essentially equivalent and can be considered just *two faces of the same coin*". To quote (Dixit and Pindyck, 1994) page 121: "the two methods have offsetting advantages and disadvantages and together they can handle a wide variety of applications. In specific applications one may be more convenient that the other, but *there is no difference in principle between the two on their common ground*".

[10] For a review of Monte Carlo methods applied to American Option pricing see chapter 6 in (Tavella, 2002) and chapter 8 in (Glasserman, 2004).

LSMC by (Tsitsiklis and Van Roy, 2001) implies a generalization of both state space and time of approximate value iteration which is untenable for the KT model. The version proposed by (Andersen, 2000) implies an early exercise parametrization which is not applicable in the general real options model setting.

Alternative Monte Carlo methods are unapplicable either: (Barraquand and Martineau, 1995) state stratification along the payoff is not suitable for RPV_t based models like the KT one, in which streams of cash flows are compared at every epoch;[11] (Broadie and Glasserman, 1997) simulated bushy tree cannot be implemented for more than five epochs, see page 431 in (Glasserman, 2004); dual approach, pursued by (Rogers, 2002) through the optimal choice of a Lagrangian martingale and by (Haugh and Kogan, 2004) through neural nets, is too much problem dependent to accomodate the generality of KT model specifications. Although that is true, stochastic mesh method by (Broadie and Glasserman, 2004) and quantization method by (Bally et al., 2002) can be considered competitive methods with respect to LSMC, even better for KT model implementations in which current state variables depend on earlier states if not on the whole path.[12]

In extant literature, LSMC has been applied to real options problems in general and to switching real options (KT model) in particular. Although that is true, to the best of our knowledge, there is not a thorough analysis of LSMC applied to KT model in discrete time. For instance, in the pioneering work by (Gamba, 2002) LSMC is applied only to a bivariate case in switching options being the main contribution of the paper the decomposition approach of complex optionalities in an investment project. (Rodrigues and Rocha Armada, 2005) applied low discrepancy methods for LSMC to the same decomposition approach suggested by (Gamba, 2002). (Cortazar et al., 2005) and (Tsekrekos et al., 2006) applied LSMC in the context of three and two factor models to the well known (Brennan and Schwartz, 1985) copper mine valuation. Finally, (Imai, 2006) applies LSMC to the valuation of switching options although in a destructured model which does not resemble to the KT approach.

None of the references just mentioned tackles the problem of applying in discrete time methods which were originally concieved as continuous time approximations. Moreover, none tackles the problem of valuations comparability accross different discretization granularities and different stochastic specifications. In addition, only a few, namely (Tsekrekos et al., 2006) and (Rodrigues and Rocha Armada, 2005) propose convergence experiments of LSMC applied to switching options. Finally, LSMC applicability to the KT model in a

[11] The same line of reasoning applies to variants of state stratification method in which other dimensions in state space partitioning are added (Raymar and Zwecher, 1997). An application of this Monte Carlo method to real options by (Cortazar and Schwartz, 1998) deals only with timing options on a MAD like approach, see footnote 1.

[12] A Dynamic Optimization problem is path dependent in the sense that the decision taken in one epoch should be consistent with an optimal policy, hence with the previous and the following decision. In addition to that, some dynamic systems have state variables which depend on the earlier if not the whole history of the dynamic model. In a state augmentation approach, see page 30 in (Bertsekas, 1995), this would imply computing expected value functions for all the possible levels that the path dependent variable could possibly have reached in each epoch. Obviously this is not the task for LSMC but for other methods such as those mentioned in the text.

multivariate framework is often dismissed as being computationally unfeasible, page 3 (Gamba, 2002), page 1 in (Rodrigues and Rocha Armada, 2005).

Parallel to the methodological extensions, several applications of LSMC to real options valuations case studies have been published. A copper mine has been valued in a more realistic setting by (Abdel Sabour and Poulin, 2006) having as benchmark of comparison (Brennan and Schwartz, 1985). Another case study in mining is provided by (Lemelin et al., 2006) in which a multi mineral mine is valued. Other applications can be found in natural gas (Abadie and Chamorro, 2006), nuclear reactors (Oduntan and Fuller, 2005), real estate (Kalligeros, 2005), infrastructure valuation (Chiara, 2006), oil refining (Imai and Nakajima, 2000). Finally, the same method is applied to fundamental security analysis (Schwartz and Moon, 2000), (Schwartz and Moon, 2001) and (Baule and Tallau, 2006).

In the remaining part of this section we describe some problems in applying the KT model in discrete time and suggest some solutions.

2.2 Lattice and Least Squares Monte Carlo Methods for KT Model in Discrete Time

Management decisions modelled as real options do occur in discrete time for both technological and institutional reasons. Hence, it is worth studying discrete time models by themselves and not as approximations of continuous ones, page 670 (Sick, 1995) in (Jarrow et al., 1995).

The choice of the optimal resetting period –Δt– of the dynamic system representing the optionalities embedded in an investment project implies the comparison of results derived for different discretizations of the data generating processes underlying the project. While for stock variables these comparisons are trivial and do not require any further comment, for flow variables – whether deterministic or stochastic – some adjustment is necessary in order to obtain comparable results for different Δt. As a matter of fact, the question is how the flow variable for finer discretizations –$\Delta t \to 0$ – should be rescaled in order to get results which are comparable to those derived from coarser ones.[13] In addition to the normative use of the methods proposed below, these results are also important to test convergence of our numerical methods for the Kulatilaka Trigeorgis model as $\Delta\, t \to 0$. We will show that the straightforward solution of dividing the annual figure for the number of intervals in the year is correct only for the univariate geometric brownian motion (GBM) discretized in a (Cox et al., 1979) binomial lattice but not for deterministic variables in the same model. Instead, for multivariate GBMs or univariate geometric Ornstein Uhlenbeck (GOU) processes,

[13]This question would arise also in the case in which a monthly discretization is used while the initial data are annual. This in turn means that even resetting the dynamic system with a frequency lower than the actual discretization of the stochastic process would not solve the problem of getting the right figure to be placed at the initial node of the lattice or at time $t = 0$ of the Monte Carlo simulation.

sub annual equivalent figures should be derived taking into account how the expected value of the stochastic variable behaves within different discretizations.

	Discretization and Pricing Models	
Stochastic Process	**LSMC (Longstaff and Schwartz, 2001)**	**Lattice**
univariate GBM	analytic solution of GBM eq. in univariate LSMC	univariate lattice (Cox et al., 1979)
bivariate and trivariate GBMs with correlated Wiener processes	analytic solution of GBM eq. with Cholesky transformation of independent Wiener processes in multivariate LSMC	multivariate lattices (Boyle et al., 1989),(Kamrad and Ritchken, 1991),(Ekvall, 1996),(Gamba and Trigeorgis, 2005)
univariate Geometric Ornstein Uhlenbeck (GOU), model 1 in (Schwartz, 1997)	analytic solution of GOU eq., model 1 (Schwartz, 1997), in univariate LSMC	univariate censored lattice (Sick, 1995)
two factor model: univariate GBM with mean reverting convenience yield	analytic solution of GBM eq. in univariate LSMC with convenience yield DGP as an arithmetic Ornstein Uhlenbeck, model 2 (Schwartz, 1997) or (Gibson and Schwartz, 1990)	our two variable extension of page 177 (Schulmerich, 2005) univariate lattice with Monte Carlo simulated underlying factors
three factor model: univariate GBM with mean reverting convenience yield and risk free rate	analytic solution of GBM eq. in univariate LSMC with convenience yield and risk free DGPs as correlated arithmetic Ornstein Uhlenbeck, model 3 (Schwartz, 1997), stochastic discounting	our three variable extension of page 177 (Schulmerich, 2005) univariate lattice with Monte Carlo simulated underlying factors

Table 1: Synopsis of the stochastic processes covered and their respective discretization

We have dealt with the problem of comparability of results for different Δt for both lattice and Monte Carlo discretizations for most of the DGPs dealt with in this paper, see synopsis in table 1. This is necessary being results obtained from one approach benchmarked with those obtained from the other. For multivariate GBMs we have used binomial lattices provided by extant literature choosing those with best convergence properties, namely (Gamba and Trigeorgis, 2005). For GOUs, instead, we have used censored binomial lattices provided by extant literature only for the univariate case by (Sick, 1995).[14] For two and three factors models in (Schwartz, 1997), we have derived benchmarks for the uncorrelated factors cases modifying the binomial lattice with Monte Carlo simulated convenience yield and risk free rate by (Schulmerich, 2005), page 177. For the last three models, we do not provide PV matching solutions for the problem of figures comparability for results derived for different Δt.

To begin with, it is worth remembering that real options are simply the capabilities to switch between different streams of cash flows, (Vollert, 2002) page 17. The present value of these streams – i.e. the cash flows yielded by an investment project in each individual operating mode in a KT model, see expression (4)

[14] We have discarded the bivariate censored lattice proposed by (Hahn and Dyer, 2008) since, to the best of our efforts, we did not manage to get accurate benchmarks.

– should not depend on Δt adopted in uni or multi variate lattices or Monte Carlo simulations used to discretize the underlying stochastic process.

In principle, in order to get comparable results from lattices or simulations with different Δt we need to have that present values of flow variables stay constant when $\Delta t \to 0$, see expression (10) in which the left hand side represents the present value computed on # n annual figures Cash Flows, while the right hand side represents the present value computed on # $n \cdot m$ sub annual $(1/m)$ figures Cash flows, being $\Delta t = 1$ for the LHS and $\Delta t = 1/m$ for the RHS.

$$PV_n = \overline{R}_0 + \overline{R}_1 \cdot v + \overline{R}_2 \cdot v^2 + \ldots + \overline{R}_n \cdot v^{n-1} = PV_{m \cdot n} = \overline{R}_{0,1/m} + \overline{R}_{1,1/m} \cdot v' + \overline{R}_{2,1/m} \cdot v'^2 + \ldots + \overline{R}_{n \cdot m,1/m} \cdot v'^{n \cdot m-1} \quad (10)$$

where:

PV_n	:=	the present value of a variable discretized on an annual basis, $\Delta t = 1$;
$\overline{R}_t$	:=	expected annual figure at epoch t;
$v = e^{-r_f}$	:=	present value factor on an annual basis;
$PV_{n \cdot m}$	:=	the present value of a variable discretized on a sub annual basis, $\Delta t = 1/m$;
$\overline{R}_{t,1/m}$	:=	expected $1/m$ subperiod figure at epoch t;
$v' = e^{-r_f \cdot \Delta t}$	:=	present value factor on a sub annual $\Delta t = 1/m$ basis.

Expression (10) is assumed to hold for both deterministic and stochastic flow variables specified in a KT real option model, whatever the underlying stochastic process. The methods we propose below strive to find $\overline{R}_{0,1/m}$ to be used at the initial node of the lattice or as starting observation of a Monte Carlo simulation which satisfy equation (10).

For stochastic cash flows, in a martingale pricing framework, the expected value of $\overline{R}_{t,1/m}$ for the next epoch is the compound value of the present one – submartingale with drift $\mu = r_f$ in the expected values, see expression (11).[15]

$$\overline{R}_{t+\Delta t,1/m} = e^{r_f \cdot \Delta t} \cdot \overline{R}_{t,1/m} \quad (11)$$

In the actual implementation of a martingale pricing model, the submartingale property in expected values, equation (11), does not hold exactly. As a matter of fact, both lattice and Monte Carlo discretizations do not show completely accurate moment matching properties. In general, in any multivariate lattice, the expected value of the variable grows at a rate $\hat{\mu} \ll r_f$, see expression (12). Moreover, for finer discretizations $\Delta t \to 0$ or number of intervals $m \to \infty$, the drift on the lattice $\hat{\mu}$ approximates better the risk free rate r_f. Hence, a finer discretization would yield higher valuations, blurring the contribution of a more frequent resetting period – real options exercise frequency – with the mere numerical effect.

[15] Without any loss of generality, in order to simplify notations, dealing with GBMs and GOUs, we do not consider constant convenience yields to be subtracted from the risk free rate.

$$\hat{\mu}_{\frac{1}{m}} = \ln\left(\frac{E\left(V_{t+\Delta t}\right)}{V_t}\right) \cdot \frac{1}{\Delta t} \tag{12}$$

where:

V_t := scaleless variable, $V_0 = 1$;
$E\left(V_{t+\Delta t}\right)$:= expected value computed on adjacent nodes;
Δt := $= \text{life}/(n \cdot m) = 1/m$, life of the project in years divided by the number of intervals;

Being this bias so crucial for the implementation of the KT model in discrete time, we examine how the submartingale property is approximated for bivariate, trivariate and tetravariate cases of four different multivariate binomial and trinomial lattices, namely (Boyle et al., 1989) (Kamrad and Ritchken, 1991), (Ekvall, 1996), (Gamba and Trigeorgis, 2005) adjusted generalized log transformed (AGLT). To the best of our knowledge, moment matching properties of multivariate lattices have never been explored before in extant literature.

In tables 2-4, it should be noticed that (Boyle et al., 1989) (Kamrad and Ritchken, 1991) volatilities and correlations are just the same being the latter a variant of the former with an horizontal movement.[16] Instead, volatilities and correlations obtained from (Ekvall, 1996), (Gamba and Trigeorgis, 2005) are both exactly equal to the moments of the correlated GBMs. Therefore, they are reported in two groups.

Blatantly enough, the last two models have better moment matching and faster convergence properties than the first ones. Moreover, they can be applied even in cases in which the first two give negative probabilities, because discretization is too coarse with respect to low volatilities and high correlations, see for instance table 4 for $\Delta t = 2/1$. Therefore, in the ensuing assessment of LSMC applicability to the KT model, we will benchmark Monte Carlo results with (Gamba and Trigeorgis, 2005) adjusted generalized log transformed (AGLT) modified as shown below.

For any of the four multivariate lattice methods cited above, remembering expression (11), i.e. being the submartingale property verified locally,[17] period by period for each node in the lattice, each side of expression (10) can be rewritten as an increasing annuity, see expression (13).

$$\begin{aligned} PV_n &= \overline{R}_0 + \overline{R}_0 \cdot (q \cdot v) + \overline{R}_0 \cdot (q \cdot v)^2 + \ldots + \overline{R}_0 \cdot (q \cdot v)^{n-1} = \\ PV_{m \cdot n} &= \overline{R}_{0,1/m} + \overline{R}_{0,1/m} \cdot (q' \cdot v') + \overline{R}_{0,1/m} \cdot (q' \cdot v')^2 + \ldots + \overline{R}_{0,1/m} \cdot (q' \cdot v')^{n \cdot m - 1} \end{aligned} \tag{13}$$

where, in addition to previous notation:

$q = e^{\hat{\mu}}$:= drift of the expected values on the annual discretization;
$q' = e^{\hat{\mu}_{1/m} \cdot \Delta t}$:= drift of the expected values on the sub-annual discretization.

[16] see footnote 19.
[17] Together with variances and correlations of the multivariate GBMs, see page 670 (Sick, 1995).

In the cases in which $\hat{\mu} \neq r_f$, expression (13) can be rewritten as in (14).

$$PV_n = \overline{R}_0 \cdot \frac{1-(q \cdot v)^n}{1-q \cdot v} = PV_{m \cdot n} = \overline{R}_{0,1/m} \cdot \frac{1-(q' \cdot v')^{n \cdot m}}{1-q' \cdot v'} \tag{14}$$

Hence, $\overline{R}_{0,1/m}$ is simply derived as follows:

$$\overline{R}_{0,1/m} = \overline{R}_0 \cdot \frac{\frac{1-(q \cdot v)^n}{1-q \cdot v}}{\frac{1-(q' \cdot v')^{n \cdot m}}{1-q' \cdot v'}} \tag{15}$$

Expression (15) is applicable for stochastic flow variables discretized in a multivariate lattice in which the risk free rate is approximated from below, $\hat{\mu} \ll r_f$ and for deterministic flow variables which have a grow rate exogenously determined greater or smaller than r_f. In the case of annual figures of non growing deterministic variables, i.e. $\hat{\mu} = \hat{\mu}_{1/m} = 0$, expression (15) becomes simply (16). In other words, annual figures should be rescaled in a way that resembles uniform annuity series used in traditional capital budgeting to compare investments with different lives, see page 260 (Rao, 1992).

$$\overline{R}_{0,1/m} = \overline{R}_0 \cdot \frac{\frac{1-v^n}{1-v}}{\frac{1-v'^{\,n \cdot m}}{1-v'}} \tag{16}$$

Instead, for cases in which $\hat{\mu} = \hat{\mu}_{1/m} = r_f$, as in the (Cox et al., 1979) univariate binomial lattice, expression (14) simplifies to

$$PV_n = \overline{R}_0 \cdot n = PV_{m \cdot n} = \overline{R}_{0,1/m} \cdot (m \cdot n) \tag{17}$$

Hence, in this case, and only in this case, it is possible to get the equivalent figure for the sub period Δt as in expression (18), simply dividing the annual figure for the number of subperiods in a year.

$$\overline{R}_{0,1/m} = \overline{R}_0 \cdot \frac{n}{(m \cdot n)} = \overline{R}_0 \cdot \frac{1}{m} = \overline{R}_0 \cdot \Delta t \tag{18}$$

A. drifts:

$\widehat{\mu}$	$\Delta t = 2/1$	$\Delta t = 1/1$	$\Delta t = 1/2$	$\Delta t = 1/3$	$\Delta t = 1/4$
BEG	4.8141%	4.9045%	4.9515%	4.9675%	4.9756%
	4.8409%	4.9184%	4.9587%	4.9723%	4.9792%
KR	4.8171%	4.9060%	4.9523%	4.9681%	4.9760%
	4.8456%	4.9208%	4.9599%	4.9732%	4.9798%
NEK	4.9739%	4.9868%	4.9934%	4.9956%	4.9967%
	4.8736%	4.9354%	4.9673%	4.9781%	4.9836%
GT	4.9755%	4.9876%	4.9938%	4.9958%	4.9969%
	4.8727%	4.9349%	4.9670%	4.9779%	4.9834%

B. volatilities and correlations:

σ_1 $\rho_{1,2}$ σ_2	$\Delta t = 2/1$		$\Delta t = 1/1$		$\Delta t = 1/2$		$\Delta t = 1/3$		$\Delta t = 1/4$	
BEG / KR	.19545	−.10748	.19887	−.10369	.19774	−.10183	.19925	−.10122	.19944	−.10091
		.29992		.29996		.29998		.29999		.29999
NEK / GT	.20000	−.10000	.20000	−.10000	.20000	−.10000	.20000	−.10000	.20000	−.10000
		.30000		.30000		.30000		.30000		.30000

Table 2: Moment Estimation on Multivariate Lattices: Bivariate Cases

Legend: multivariate lattice models are: BEG: (Boyle et al., 1989); KR: (Kamrad and Ritchken, 1991); NEK: (Ekvall, 1996); GT: (Gamba and Trigeorgis, 2005). drifts, volatilities and correlations have been computed according to the following expressions on adjacent nodes:

$$\widehat{\mu} = \ln\left(\frac{E(P_{t+\Delta t})}{P_t}\right)\cdot\frac{1}{\Delta t}$$

$$\widehat{\sigma} = \sqrt{\frac{\left\{E\left(\ln(P_{t+\Delta t})^2\right) - \left[E\left(\ln(P_{t+\Delta t})\right)\right]^2\right\}}{\Delta t}}$$

$$\widehat{\rho}_{1,2} = \frac{E\left(\ln(P_{1,t+\Delta t}\cdot\ln(P_{2,t+\Delta t})\right) - E\left(\ln(P_{1,t+\Delta t})\right)\cdot E\left(\ln(P_{2,t+\Delta t})\right)}{\Delta t}\cdot\frac{1}{\widehat{\sigma}_1\cdot\widehat{\sigma}_2}$$

A. drifts:

$\widehat{\mu}$	$\Delta t = 2/1$	$\Delta t = 1/1$	$\Delta t = 1/2$	$\Delta t = 1/3$	$\Delta t = 1/4$
BEG	4.8141% 4.8409% 4.8137%	4.9045% 4.9184% 4.9043%	4.9515% 4.9587% 4.9515%	4.9675% 4.9723% 4.9675%	4.9756% 4.9792% 4.9756%
KR	4.8171% 4.8456% 4.8166%	4.9060% 4.9208% 4.9059%	4.9523% 4.9599% 4.9523%	4.9681% 4.9732% 4.9681%	4.9760% 4.9798% 4.9760%
NEK	4.9739% 4.8736% 4.6231%	4.9868% 4.9354% 4.8041%	4.9934% 4.9673% 4.9001%	4.9956% 4.9781% 4.9329%	4.9967% 4.9836% 4.9495%
GT	4.9768% 4.8839% 4.6169%	4.9883% 4.9407% 4.8008%	4.9941% 4.9700% 4.8984%	4.9961% 4.9799% 4.9318%	4.9970% 4.9849% 4.9487%

B. volatilities and correlations:

σ_1 $\rho_{1,2}$ $\rho_{1,3}$ σ_2 $\rho_{2,3}$ σ_3	$\Delta t = 2/1$	$\Delta t = 1/1$	$\Delta t = 1/2$	$\Delta t = 1/3$	$\Delta t = 1/4$
BEG/KR	.1954 −.1075 .1261 .2999 .1031 .3977	.1977 −.1037 .1128 .3000 .1016 .3989	.1989 −.1018 .1064 .3000 .1008 .3994	.1992 −.1012 .1042 .3000 .1005 .3996	.1994 −.1009 .1032 .3000 .1004 .3997
NEK / GT	.2000 −.1000 .1000 .3000 .1000 .4000	.2000 −.1000 .1000 .3000 .1000 .4000	.2000 −.1000 .1000 .3000 .1000 .4000	.2000 −.1000 .1000 .3000 .1000 .4000	.2000 −.1000 .1000 .3000 .1000 .4000

Table 3: Moment Estimation on Multivariate Lattices: Trivariate Cases

Legend: see table 2.

A. drifts:

$\widehat{\mu}$	$\Delta t = 2/1$	$\Delta t = 1/1$	$\Delta t = 1/2$	$\Delta t = 1/3$
BEG	0.0000%	4.9045%	4.9515%	4.9675%
	0.0000%	4.9184%	4.9587%	4.9723%
	0.0000%	4.9043%	4.9515%	4.9675%
	0.0000%	4.8866%	4.9424%	4.9614%
KR	0.0000%	4.9060%	4.9523%	4.9681%
	0.0000%	4.9208%	4.9599%	4.9732%
	0.0000%	4.9059%	4.9523%	4.9681%
	0.0000%	4.8870%	4.9426%	4.9615%
NEK	4.9739%	4.9868%	4.9934%	4.9956%
	4.8736%	4.9354%	4.9673%	4.9781%
	4.6231%	4.8041%	4.9001%	4.9329%
	4.9984%	4.9992%	4.9996%	4.9997%
GT	4.9769%	4.9883%	4.9941%	4.9961%
	4.8839%	4.9407%	4.9700%	4.9799%
	4.6167%	4.8007%	4.8983%	4.9318%
	4.9985%	4.9992%	4.9996%	4.9997%

B. volatilities and correlations:

σ_1 $\rho_{1,2}$ $\rho_{1,3}$ $\rho_{1,4}$ σ_2 $\rho_{2,3}$ $\rho_{2,4}$ σ_3 $\rho_{3,4}$ σ_4	$\Delta t = 2/1$				$\Delta t = 1/1$				$\Delta t = 1/2$				$\Delta t = 1/3$			
BEG / KR	.0000	.0000	.0000	.0000	.0000	−.1037	.1128	−.1897	.0000	−.1018	.1064	−.1419	.0000	−.1012	.1042	−.1273
		.0000	.0000	.0000		.3000	.1016	.1036		.3000	.1008	.1015		.3000	.1005	.1010
			.0000	.0000			.3989	−.0744			.3994	−.0878			.3996	−.0920
				.0000				.0893				.0948				.0966
NEK / GT	.2000	−.1000	.1000	−.1000	.2000	−.1000	.1000	−.1000	.2000	−.1000	.1000	−.1000	.2000	−.1000	.1000	−.1000
		.3000	.1000	.1000		.3000	.1000	.1000		.3000	.1000	.1000		.3000	.1000	.1000
			.4000	−.1000			.4000	−.1000			.4000	−.1000			.4000	−.1000
				.1000				.1000				.1000				.1000

Table 4: Moment Estimation on Multivariate Lattices: Tetra-variate Cases

Legend: see table 2.

To analyze the same moment matching properties for Monte Carlo discretizations of GBM processes, we have devised the following experiment design which to the best of our knowledge is novel in extant literature, see for instance page 288 in (Gourieroux and Jasiak, 2001). Over a 20 years horizon, being this the likely life of an industrial investment project, we have simulated the analytic solution of GBMs with correlated Wiener processes in the same bivariate, trivariate and tetra variate cases previously discretized in multivariate lattices. Monte Carlo observations at each epoch are obtained from the analytic solution (20) of the GBM equation (19).

$$dS = \mu\, S\, d\, t + \sigma\, S\, d\, z \tag{19}$$

$$\begin{aligned} S_t &= S_{t-1} \cdot e^{\nu \Delta t + \sigma \epsilon_t \sqrt{\Delta t}} \\ S_t &= S_{t-1} \cdot e^{\left(\mu - 1/2\sigma^2\right)\Delta t + \sigma \epsilon_t \sqrt{\Delta t}} \end{aligned} \tag{20}$$

where, in addition to previous notation:

$\epsilon_t \sim N(0,1)$:= shocks drawn from a standardized normal distribution, in the case of correlated Wiener processes they have been transformed using a Cholesky decomposition of the correlation matrix;

This has been performed for different $\Delta\, t$ and for different batches of simulated paths. While for lattices estimated figures were reported directly, in this case we have chosen to report relative $RMSE_r$, see expression (21), rescaled for the results obtained from the most coarse discretization $\Delta\, t = 2$ and the smallest batch $L = \#\text{paths}{=}5.000$.

$$RMSE_r = \sqrt{\frac{1}{L} \cdot \sum_{j=1}^{L} \frac{\left[\widehat{\theta}_j - \theta\right]^2}{\theta}} \tag{21}$$

where:

L : number of paths simulated in the individual batch;
$\widehat{\theta}_j$: estimates of $\widehat{\mu} = \widehat{\nu} + \frac{1}{2}\widehat{\sigma}^2$, $\widehat{\sigma}^2$, $\widehat{\rho}$;
θ : parameters used in the Monte Carlo simulation, μ, σ^2 and ρ;

Moreover, we have repeated the same experiment 10 times to get less noisy relationships between $RMSE_r$, $\Delta\, t$ and $L = \#\text{paths}$. Therefore, tables 5-7 report average values of $RMSE_r$ rescaled for the least computationally intensive discretization, upper left hand corner. Although intuitively immediate, these table can be better interpreted with a simple OLS regression of the $RMSE_r$ on respective $\Delta\, t$ and $L = \#\text{paths}$. Hence, we have estimated equation (22) on 350 observations, obtained from repeating 10 times the same experiment.

$$\ln(RMSE_r) = \alpha + \beta_L \cdot \ln(L) + \beta_{\Delta t} \cdot \ln\left(\frac{T}{\Delta t}\right) + \epsilon \tag{22}$$

where, in addition to previous notation:

T : life of the investment project, 20 years;
$n = \frac{T}{\Delta t}$: number of observations for each simulated time series;

From tables 5-7 moment matching properties of simulated GBMs can be summarized as follows. For drifts, see panels A in the tables just cited, the increase in the number of paths per batch is definetly effective in reducing $RMSE_r$. Instead, as (Jiang and Knight, 1999) page 12 notice, there are not efficiency gains in approximating drifts on simulated series if we increase the sample size by reducing the sampling interval Δt over a fixed horizon. This is confirmed by regression estimates of equation (22), see expression (23), t-stats are reported in parentheses. As a matter of fact, the number of paths coefficients are always highly significant, while the number of observations in a path ones are not. Moreover, it is worth noting that number of path coefficients stay the same for the three multivariate cases. The level of β_L indicates a $\sqrt{L}$ consistency as it is well known for Monte Carlo estimates of European Options.[18] Finally, another pattern emerges. Results for tetra variate cases are much more stable than for the other two. This is due to the fact that $RMSE_r$ are the average of the individual parameters figures which are noisier.

$$\begin{aligned}
\text{bivariate: } \ln(RMSE_r) &= \underset{(0.23)}{0.08} + \underset{(-14.11)}{-0.49}\cdot\ln(L) + \underset{(-1.35)}{-0.05}\cdot\ln\left(\tfrac{T}{\Delta t}\right) \quad R^2 = .37 \\
\text{trivariate: } \ln(RMSE_r) &= \underset{(1.35)}{0.46} + \underset{(-15.52)}{-.50}\cdot\ln(L) + \underset{(0.48)}{0.02}\cdot\ln\left(\tfrac{T}{\Delta t}\right) \quad R^2 = .41 \\
\text{tetravariate: } \ln(RMSE_r) &= \underset{(1.91)}{0.65} + \underset{(-16.01)}{-0.51}\cdot\ln(L) + \underset{(-2.17)}{-0.07}\cdot\ln\left(\tfrac{T}{\Delta t}\right) \quad R^2 = .43
\end{aligned} \tag{23}$$

For volatilities, instead, the increase in the number of paths is almost irrelevant, see panels B in tables 5-7 while increased sampling is very effective in reducing $RMSE_r$. This is confirmed by regression estimates of equation (22), see expression (24). Differently from drift and correlations estimates, this pattern stays the same in all three cases, bivariate, trivariate and tetravariate as can be observed from R^2 and coefficient estimates too.

$$\begin{aligned}
\text{bivariate: } \ln(RMSE_r) &= \underset{(-9.33)}{-1.29} + \underset{(0.995)}{0.013}\cdot\ln(L) + \underset{(-82.136)}{-1.049}\cdot\ln\left(\tfrac{T}{\Delta t}\right) \quad R^2 = .95 \\
\text{trivariate: } \ln(RMSE_r) &= \underset{(-12.071)}{-1.286} + \underset{(0.324)}{0.00324}\cdot\ln(L) + \underset{(-104.567)}{-1.02652}\cdot\ln\left(\tfrac{T}{\Delta t}\right) \quad R^2 = .97 \\
\text{tetravariate: } \ln(RMSE_r) &= \underset{(-14.6703)}{-1.32325} + \underset{(0.573085)}{0.004836}\cdot\ln(L) + \underset{(-122.795)}{-1.01991}\cdot\ln\left(\tfrac{T}{\Delta t}\right) \quad R^2 = .98
\end{aligned} \tag{24}$$

[18] As a matter of fact, $\ln RMSE = -\frac{1}{2}\cdot\ln L \;\Rightarrow\; \ln RMSE = \ln L^{-1/2} \;\Rightarrow\; RMSE = \frac{1}{\sqrt{L}}$

For correlations both increased number of paths and finer sampling are effective in reducing $RMSE_r$, see panel C in tables 5-7. Although that is true, the former is less effective than the latter, see equations (25). As can be observed from panel C, increased size batch is much more effective for finer sampling discretization schemes. Moreover, in this case $RMSE_r$ is the average of the whole correlation matrix. Hence, comparison accross the three multivariate specifications help us to single out how much noisy is the estimate of individual correlation coefficients, as in the bivariate case, when compared to the estimates of three and six for the trivariate and tetravariate cases respectively.

$$\begin{aligned}
\text{bivariate: } \ln(RMSE_r) &= \underset{(-1.06141)}{-0.547} + \underset{(2.043)}{0.0986} \cdot \ln(L) + \underset{(-22.107)}{-1.050} \cdot \ln\left(\tfrac{T}{\Delta t}\right) \quad R^2 = .58 \\
\text{trivariate: } \ln(RMSE_r) &= \underset{(3.590)}{0.668} + \underset{(-2.590)}{-0.045} \cdot \ln(L) + \underset{(-55.382)}{-0.949} \cdot \ln\left(\tfrac{T}{\Delta t}\right) \quad R^2 = .89 \\
\text{tetravariate: } \ln(RMSE_r) &= \underset{(5.051)}{0.669} + \underset{(-3.853)}{-0.047} \cdot \ln(L) + \underset{(-77.317)}{-0.943} \cdot \ln\left(\tfrac{T}{\Delta t}\right) \quad R^2 = .94
\end{aligned} \tag{25}$$

Obviously, this reduction in $RMSE_r$ takes place at a cost. CPUs time between upper right hand corner and lower righ hand corner experiments in tables 5-7 increases respectively 13, 15 and 18 times. In any case, even after reduction in $RMSE_r$ for drifts due to increased number of path or finer sampling, the submartingale property, equation (11) does never hold exactly.

A. drifts:

	2/1	1/1	1/2	1/3	1/4	1/6	1/12
5,000	100.00	113.06	111.04	160.41	86.73	101.59	109.79
10,000	78.39	74.02	68.30	76.23	88.45	67.30	83.24
20,000	62.36	47.62	41.00	48.24	51.75	66.12	59.82
40,000	53.90	49.69	47.79	40.89	28.84	36.39	41.07
80,000	34.07	36.05	21.15	23.67	38.31	22.63	21.27

B. volatilities:

	2/1	1/1	1/2	1/3	1/4	1/6	1/12
5,000	100.00	50.29	21.69	14.84	11.70	10.11	3.17
10,000	96.68	45.79	23.34	14.74	9.02	7.90	3.46
20,000	95.59	45.78	23.08	16.18	10.58	7.63	3.62
40,000	96.38	46.90	22.15	14.48	11.52	8.17	3.78
80,000	95.48	46.56	22.56	14.86	11.44	7.59	3.59

C. correlations:

	2/1	1/1	1/2	1/3	1/4	1/6	1/12
5,000	100.00	56.12	24.91	20.28	15.90	12.87	10.79
10,000	108.74	63.03	29.96	15.37	15.34	9.17	7.42
20,000	107.50	52.27	24.93	20.26	16.37	8.49	6.87
40,000	111.03	56.63	27.74	17.60	14.48	9.53	4.44
80,000	116.99	55.72	27.01	20.45	15.75	10.52	4.28

Table 5: Moment Estimation on Monte Carlo Simulations: Bivariate Cases

Legend: Analytic solutions of correlated GBMs have been simulated spanning a $T = 20$ years horizon, with different samples as reported in the first column and different Δt as reported in the first row. Drifts, volatilities and correlations have been computed according to the following expressions on simulated time series:

$$\widehat{\nu}_i = \left\{ \frac{1}{obs} \sum_{k=0}^{obs-1} \ln \left[\frac{S_{i,t_{k+1}}}{S_{i,t_k}} \right] \right\} \cdot \frac{1}{\Delta t}$$

$$\widehat{\sigma}_i = \sqrt{\frac{1}{obs-1} \sum_{k=0}^{obs-1} \left(\ln \left[\frac{S_{i,t_{k+1}}}{S_{i,t_k}} \right] - \widehat{\nu}_i \cdot \Delta t \right)^2} \cdot \frac{1}{\sqrt{\Delta t}}$$

$$\widehat{\mu}_i = \widehat{\nu}_i + \frac{1}{2} \cdot \widehat{\sigma}_i^2$$

$$\widehat{\rho}_{i,j} = \frac{\frac{1}{obs-1} \sum_{k=0}^{obs-1} \left[\left(\ln \left[\frac{S_{i,t_{k+1}}}{S_{i,t_k}} \right] - \widehat{\nu}_i \cdot \Delta t \right) \cdot \left(\ln \left[\frac{S_{j,t_{k+1}}}{S_{j,t_k}} \right] - \widehat{\nu}_j \cdot \Delta t \right) \right]}{\widehat{\sigma}_i \cdot \widehat{\sigma}_j \cdot \Delta t}$$

Relative $RMSE$ has been computed according to expression:

$$RMSE_r = \sqrt{\frac{1}{L} \cdot \sum_{j=1}^{L} \frac{\left[\widehat{\theta}_j - \theta \right]^2}{\theta}}$$

This experiment has been repeated 10 times. Average values have been computed and they have been rescaled for the upper left hand side corner $RMSE_r$.

A. drifts:

	2/1	1/1	1/2	1/3	1/4	1/6	1/12
5,000	100.00	83.54	83.89	102.39	113.29	134.57	119.58
10,000	68.81	51.00	66.86	75.69	58.97	60.10	77.69
20,000	48.97	65.34	39.73	55.86	55.34	49.25	64.80
40,000	37.60	29.50	43.19	38.20	33.21	29.79	31.65
80,000	24.16	23.73	25.58	22.96	21.36	26.38	20.77

B. volatilities:

	2/1	1/1	1/2	1/3	1/4	1/6	1/12
5,000	100.00	52.16	23.46	13.90	11.51	8.66	4.30
10,000	98.71	46.22	24.47	15.11	12.52	7.01	4.06
20,000	101.99	47.11	23.52	15.99	11.29	7.99	3.82
40,000	99.09	47.94	24.65	15.18	11.37	7.67	3.84
80,000	99.62	46.81	23.06	15.98	11.86	7.65	3.89

C. correlations:

	2/1	1/1	1/2	1/3	1/4	1/6	1/12
5,000	100.00	52.34	24.69	16.63	12.41	10.77	8.03
10,000	95.04	48.23	20.10	17.61	14.31	7.99	5.22
20,000	96.01	45.12	23.38	14.02	11.14	7.11	4.99
40,000	91.69	45.09	22.75	15.77	10.18	8.76	4.10
80,000	93.20	45.49	23.30	15.85	11.64	7.58	4.40

Table 6: Moment Estimation on Monte Carlo Simulations: Trivariate Cases
Legend: see table 5.

A. drifts:

	2/1	1/1	1/2	1/3	1/4	1/6	1/12
5,000	100.00	77.62	70.24	78.15	90.35	71.33	83.63
10,000	61.42	50.37	58.85	49.45	53.43	45.15	60.15
20,000	55.17	36.75	38.26	55.32	43.74	31.20	30.21
40,000	32.24	26.55	40.66	27.64	21.22	24.61	23.40
80,000	19.47	14.66	21.46	17.79	23.52	18.83	19.33

B. volatilities:

	2/1	1/1	1/2	1/3	1/4	1/6	1/12
5,000	100.00	45.85	24.69	15.88	11.54	8.53	3.65
10,000	100.74	46.15	23.15	15.13	12.08	8.03	4.52
20,000	100.47	47.04	23.30	15.50	11.18	7.72	3.88
40,000	99.60	48.77	24.02	15.50	12.08	7.63	4.08
80,000	100.42	48.42	23.48	15.63	11.47	7.67	3.90

C. correlations:

	2/1	1/1	1/2	1/3	1/4	1/6	1/12
5,000	100.00	47.16	24.97	20.15	13.75	10.44	7.70
10,000	97.09	44.49	24.14	14.36	12.80	10.25	5.67
20,000	94.80	47.54	22.29	16.15	12.34	9.80	4.15
40,000	99.39	51.25	24.17	16.49	12.39	7.45	4.34
80,000	97.56	47.80	24.57	17.57	12.91	7.89	3.92

Table 7: Moment Estimation for Monte Carlo Simulations: Tetra-variate Cases
Legend: see table 5.

Therefore, for Monte Carlo simulations of GBMs, both univariate and multivariate with correlated Wiener processes, the method we propose in order to get comparable present values for cash flow streams discretized with different granularities hinges on the same principle, equation (10), but cannot rely on the nice properties of growing annuities present values which we have used for lattice discretizations. Simulating S_t recursively with equation (20), setting $\mu = r_f$, we get the following expected value for each epoch t.

$$E\left(S_t\right) = S_0 \cdot e^{\hat{\mu}_t \cdot \Delta t \cdot t} \tag{26}$$

From equation (26), drifts $\hat{\mu}_t$ computed for state variable S_t in each epoch are different from r_f, see expression (27). As shown above, the drift $\hat{\mu}_t$ approximates r_f as the number of simulated time series increases and, with a smaller extent, as $\Delta t \to 0$.

$$\hat{\mu}_t = \ln\left(\frac{E\left(S_t\right)}{S_0}\right) \cdot \frac{1}{\Delta t \cdot t} \tag{27}$$

where:

S_t	:=	actual variable, being S_0 the initial figure of each simulated time series;
$E\left(S_{t+\Delta t}\right)$	:=	expected value computed cross sectionally on observations taken from simulated time series at epoch t;
Δt	:=	$= \text{life}/(n \cdot m) = 1/m$, life of the project in years divided by the number of intervals, increment of the Monte Carlo simulation;

We have noticed previously that rescaling can take place simply multiplying annual figures for Δt or the fraction of the year, see expression (18), only when the drift of the expected values computed on discretization – whether lattice or Monte Carlo – is exactly $\hat{\mu} = r_f$. We observe that, according to the Doob Meyer decomposition, a stochastic process which is not a martingale can be transformed into one simply subtracting its predictable part, see page 133 (Neftci, 2000). Moreover, we remark that random variable distributions at any epoch t resulting from Monte Carlo simulations just approximate the martingale in the present values property, being the drift $\hat{\mu} \ll r_f$. Consequently, in a sort of moment matching method, see page 153 (Tavella, 2002), in order to rescale simulated time series resulting from Monte Carlo experiments to be used in (Longstaff and Schwartz, 2001), we proceed as follows:

1. deflate, hence the superscript ^{d} for S_t, each observation at epoch t $\forall t = 0, \ldots, T$ for the estimated drift $\hat{\mu}_t$ from equation (27),

$$S_t^d = \frac{S_t}{e^{\hat{\mu} \cdot \Delta t \cdot t}} \tag{28}$$

2. reinflate, hence the superscript ^{r} for S_t, each observation at epoch t $\forall t = 0, \ldots, T$ for the risk neutral drift $\mu = r_f$.

$$S_t^r = S_t^d \cdot e^{\mu \cdot \Delta t \cdot t} \tag{29}$$

If simulated figures for any Δt are rescaled as in the previous two steps, then initial values S_0 for a subperiod Δt can be computed simply multiplying the annual figure as in expression (18). This assures that present value computation would not be sensitive to discretization granularity. After the deflating reinflating process, both univariate and multivariate GBM keep the same stochastic properties in terms of volatilities and correlations, the only difference being that drifts $\mu = r_f$ are exactly equal to the risk free rate.[19]

The same procedure can be applied also to the multivariate lattices previously described. For brevity, we do not report these results which differ from those reported in tables 2-4 only for the fact that after rescaling computed drifts are exactly equal to the risk free rate. From a comparison of these rescaled lattice discretizations the (Gamba and Trigeorgis, 2005) or the (Ekvall, 1996) can be considered a sort of "perfect lattice" since they replicate exactly in any interval all the statistics of the multivariate GBM – drifts, volatilities and correlations.

In the remaining part of this section, we report a PV matching method to apply KT model when the underlying DGP is a Geometric Ornstein Uhlenbeck. Moreover, we show that PV matching methods are not suitable for the last two models reported in table 1. We have specified mean reverting processes using model 1 page 926 in (Schwartz, 1997) which is the same as expression (65) page 665 in (Sick, 1995), see expression (30).[20]

$$d\,P_t = \eta\left(\overline{L} - \ln P_t\right)\cdot P_t \cdot d\,t + \sigma \cdot P_t \cdot d\,z \tag{30}$$

where, in addition to previous notation, we have:

$$\begin{array}{rcl} \overline{L} & := & \ln \overline{P} + \frac{\sigma_P^2}{2\cdot\eta}, \text{ normal value of the log transform to which the process tends to revert;} \\ \ln P_t & := & \text{logarithm of the price;} \end{array}$$

The reasons for this choice are that (Sick, 1995) provides for this process a nice censored binomial lattice approximation, see expression (35) and, together with (Schwartz, 1997), some analytical expressions for expected values of spot prices, see expression (34).[21]

[19] This result is easy to explain remembering that $Var(a + b\tilde{X}) = b^2 \cdot Var(\tilde{X})$ and $Cov(a + b\tilde{X}, c + d\tilde{Y}) = b \cdot d \cdot Cov(\tilde{X}, \tilde{Y})$.

[20] We have discarded the geometric Ornstein Uhlenbeck with the spring effects on normal levels and not on their log transforms, see page 78 (Øksendal, 2001) eq. (5.3.9) for its analytical solution suitable for Monte Carlo simulations, because an analytical expression for the expected value of the spot price following that process is not available in the literature. Moreover, differently for the process used in the text, parameters of GOUP with spring effects on normal levels are difficult to estimate. Finally, a binomial lattice discretization is not available in extant literature.

[21] It should be noticed that $\ln(\overline{P})$ is the expected value of a normally distributed variable. As such, the expected value of the corresponding lognormal distribution – the figure that we actually estimate empirically – can be expressed as a function of it as in expression (31). Substituting the *arithmetic Ornstein Uhlenbeck* variance for $T \to \infty$ $\sigma^2(p_t) = \frac{\sigma^2}{2\cdot\eta}$, we get the value $\overline{P}$ to be substituted in the (Sick, 1995) binomial discretization, see (32).

$$\widehat{P} \quad = \quad e^{\ln(\overline{P}) + \frac{1}{2}\cdot\sigma^2} \tag{31}$$

$$E_t\left(P(T)\right) = \overline{P} \cdot \left(\frac{P_t}{\overline{P}}\right)^{e^{-\eta\,(T-t)}} \cdot \exp\left[\frac{\sigma^2}{4\cdot\eta}\cdot\left(1-e^{-2\cdot\eta\cdot(T-t)}\right)\right] \tag{34}$$

In (Sick, 1995) lattice for the natural probability measure, hence excluding the risk premium correction, binomial movements are the same as in a (Cox et al., 1979) model while the probability of an up movement is given by expression (35) in which probabilities greater than one or lower than zero are censored. This Binomial lattice provides a benchmark to LSMC.

$$p_t^* = \max\left(0, \min\left(1, \frac{\left(\frac{P_t}{\overline{P}}\right)^{e^{-\eta\,\Delta t}-1} \cdot \exp\left[\frac{\sigma^2}{4\cdot\eta}\cdot\left(1-e^{-2\cdot\eta\cdot\Delta t}\right)\right] - e^{-\sigma\cdot\Delta t}}{e^{\sigma\cdot\Delta t} - e^{-\sigma\cdot\Delta t}}\right)\right) \tag{35}$$

The arithmetic Ornstein Uhlenbeck process of the log tranform of model 1 (Schwartz, 1997), expression (36), has an analytical solution, see expression (37), which can be conveniently used for Monte Carlo simulations of the log of prices, $p_t = \ln P_t$. These results are then exponentiated in order to estimate real options values in the (Longstaff and Schwartz, 2001) framework. This framework prevents us getting mired into approximate discretization schemes, e.g. Euler.

$$d\,p_t = \eta\left(\overline{p} - p_t\right)\cdot d\,t + \sigma\cdot d\,z \tag{36}$$

where:

$$\begin{aligned}
\ln(\overline{P}) &= \ln(\widehat{P}) - \frac{1}{2}\cdot\sigma^2 \\
\overline{P} &= \exp\left(\ln(\widehat{P}) - \frac{1}{2}\cdot\sigma^2\right) \\
\overline{P} &= \exp\left(\ln(\widehat{P}) - \frac{\sigma^2}{4\cdot\eta}\right) \\
\overline{P} &= \widehat{P}\cdot\exp\left(-\frac{\sigma^2}{4\cdot\eta}\right)
\end{aligned} \tag{32}$$

As a matter of fact, substituting the value $\overline{P}$ just derived in the expected value expression (34) we get $\widehat{P}$ as expected value over the long run on the binomial lattice and on the Monte Carlo simulations, see (33).

$$\begin{aligned}
\lim_{T\to\infty} E_t\left(P(T)\right) &= \overline{P}\cdot\exp\left[\frac{\sigma^2}{4\cdot\eta}\right] \\
&= \widehat{P}\cdot\exp\left(-\frac{\sigma^2}{4\cdot\eta}\right)\cdot\exp\left[\frac{\sigma^2}{4\cdot\eta}\right] \\
&= \widehat{P}
\end{aligned} \tag{33}$$

p_t := $\ln P_t$, logarithm of the price;
η := the speed of reversion, e.g. for $\eta = 0$ the process becomes a driftless geometric Brownian motion while for $0 < \eta < 1$ the process tends to be mean reverting, negative levels are excluded to avoid mean aversion, one is excluded to avoid overshooting;
$\overline{p}$:= normal level of the logarithm transform;

$$p_t = \overline{p} \cdot \left(1 - e^{-\eta \cdot \Delta t}\right) + e^{-\eta \cdot \Delta t} \cdot p_{t-1} + \epsilon_t \tag{37}$$

where,

$\epsilon_t \sim N\left(0, \sigma_\epsilon^2 = \frac{\sigma_0^2}{2 \cdot \eta} \cdot \left(1 - e^{-2 \cdot \eta \Delta t}\right)\right)$;
p_t := $\ln P_t$, logarithm of the price;

Mean values computed at each epoch on both binomial lattices and exponentiated Monte Carlo simulations of equation (37) approximate expected value closed form (34). This is the expectation of the process under the natural probability measure. We can derive the certainty equivalent just subtracting the risk premium. In the numerical examples which follow this section we have assumed an underlying with zero sistematic risk hence no need to subtract a risk premium.

The problem of finding the value of $\overline{R}_{1/m,t}$ which verifies equation (10) for variables generated by a GOU can be solved only numerically. Equation (10) is rewritten as (38) and expected values are computed with the closed form reported in expression (34). To set up a numerical solution, it is important to express the normal value $\overline{P}_{1/m}$ as a multiple of the initial value $\overline{R}_{1/m,t=0}$. In this way the zero of the function is found only with respect to the latter.

$$PV_n = \sum_{t=0}^{n} \overline{R}_t \cdot v^t = PV_{m \cdot n} = \sum_{t=0}^{n \cdot m} \overline{R}_{1/m,t} \cdot v'^t \tag{38}$$

We conclude this section showing how to construct a lattice benchmark for LSMC valuations of KT model when the underlying follows a two or a three factor model, model 2 and model 3 in (Schwartz, 1997) respectively. As a matter of fact, while LSMC application is plain, requiring just the simulation of a GBM with nested stochastic convenience yield, model 2, see equations (39) and (40), and risk free rate, model 3, see equations (41)-(43), a lattice counterpart is not frequently used in the literature being the model proposed by (Schulmerich, 2005) page 177 a notable exception.

$$d\,S_t = (\mu - \delta_t)\; S_t\, dt + \sigma_1\, S_t\, dz_1 \tag{39}$$

$$d\,\delta_t = \eta_2\,(\alpha - \delta_t)\; dt + \sigma_2\, dz_2 \tag{40}$$

being $\mathrm{cov}\,(dz_1 \cdot dz_2) = \rho_{1,2} \cdot dt$

$$
\begin{aligned}
d\,S_t &= (r_t - \delta_t)\; S\,dt + \sigma_1\, S\,dz_1 && (41)\\
d\,\delta_t &= \eta_2\,(\alpha - \delta_t)\; dt + \sigma_2\, dz_2 && (42)\\
d\,r_t &= \eta_3\,(m - r_t)\; dt + \sigma_3\, dz_3 && (43)
\end{aligned}
$$

being the variance covariance matrix:

$$
\mathrm{cov}\,(dz_i \cdot dz_j) = \begin{pmatrix} 1 & \rho_{1,2} & \rho_{1,3} \\ & 1 & \rho_{2,3} \\ & & 1 \end{pmatrix} \cdot dt
$$

Following a solution originally proposed by (Hull, 2000) page 401, (Schulmerich, 2005) substitutes a deterministic term structure of interest rates for a path of spot rates simulated according to a wide variety of interest rate models, to name a few (Vasicek, 1977) or (Hull and White, 1990). A (Cox et al., 1979) is then constructed with up state probabilities varying with time. This lattice is recombinant in any case since binomial movements are not affected by the change in each epoch of the risk free rate. A valuation of the real option model is obtained for each simulated path/lattice. The average of all the valuations obtained as just shown is proposed by (Schulmerich, 2005) as the expected value of a real option model with time varying interest rates.

We extend the framework just depicted and we consider as time varying not only the risk free rate but also the convenience yield. Pursuing the same procedure just described, we obtain a lattice benchmark for both model 2 and model 3 of (Schwartz, 1997). It is worth noting that in this way we are able to benchmark only cases in which the state variable is uncorrelated with the underlying factor, being it either a convenience yield and/or a risk free rate, while these two factors can be correlated in the Monte Carlo simulations to benchmark model 3.

3 Numerical example

In this section we describe a numerical example which will be analized thoroughly in the following sections.

The specification of the KT model we propose aims to show LSMC estimates properties and not to provide a realistic application. For instance, in order to estimate value functions in a state of hysteresis of the dynamic system[22], transition costs have been set unrealistically high. This is necessary because only in

[22]The investment project when managed according to a dynamic programming algorithm is a dynamic system.

hysteresis regions value functions differ for less than transition costs and their valuations would be actually distinct for each mode. Instead, in one mode regions[23] value functions differ exactly for the transition costs and this case would be of no interest for studying LSMC estimates properties. Moreover, in order to observe how LSMC behaves with optionalities deep out of money and in the money, the cash flow equation variables have been set up to get two different plants, one very profitable and another completely unprofitable. Finally, we have considered both reversible optionalities – switching real options – and irreversible optionalities, i.e. real options to wait and to abandon, in order to observe LSMC in both cases.

Hence, the reader should not expect individual real options valuations within the ensuing model. We save their computation for another paper being the focus of the present one just to show the properties of the value functions LSMC valuations.

As sketched above, in a KT model the production technology is described by two expressions, one for the recurrent cash flows, i.e. those generated by every day activity, and one for the non recurrent ones, i.e. those generated by asset play. Usually, decisions concerning the first one are reversible and correspond to switching options while decisions concerning the latter are irreversible and they correspond to plain vanilla options akin to calls or puts.

The investment project we consider in this numerical example has two different production technologies, see expressions (44)-(45). The latter is conceived as a sort of expanded plant with respect to the former, showing economies of scale. As a matter of fact, while production volume doubles, fixed costs increase only 150%. The former, instead, is a sort of pilot production plant which produces at a loss. In case it becomes convenient, the pilot plant can be doubled, exercising an option to expand. In both plants, production can be suspended, exercising the real option to mothball, or resumed, exercising the option to restart. In mothballed state, maintenance costs are given by expression (46). Both plants can be sold for their initial value, depreciated to yield wreckage value at the end of the life of the project, being either in mothballed or in production state, see directed graph in figure 3 which summarizes the modes accessibility.

$$
\begin{aligned}
CF_t\left(\boldsymbol{\theta_t}, m, t\right) &= Q \cdot (P - Vc) - F \\
CF_t\left(\boldsymbol{\theta_t}, m = \text{Plant } 1, t\right) &= 80\% \cdot (95 - 78) - 16 \qquad (44) \\
CF_t\left(\boldsymbol{\theta_t}, m = \text{Plant } 2, t\right) &= 200\% \cdot 80\% \cdot (95 - 78) - 150\% \cdot 16 \qquad (45) \\
CF_t\left(\boldsymbol{\theta_t}, m = \text{Mothballed}, t\right) &= -3 \qquad (46)
\end{aligned}
$$

where:

[23] We define one mode regions those levels of the state variable for which only one mode of the dynamic system is optimal.

Q : expected capacity utilization;
P : revenue per year for 100% capacity utilization;
Vc : Variable costs per year for 100% capacity utilization;
F : fixed costs per year corresponding to the plant structure;

The actual construction of both plants can be postponed over a period of 20 years, exercising the option to wait. After a period of 20 years both plants are decommitted. Hence, postponing the construction of the production plant in this setting means curtailing its useful life. In conclusion, for simplicity we have set up a specification in which every option is exercised with the same frequency over the same span of time. Transition costs for exercising options are reported in expression (47)

$$c_{m,l} = \begin{pmatrix} 0 & 500 \cdot e^{r_f \cdot t} & 1000 \cdot e^{r_f \cdot t} & +\infty & +\infty & +\infty \\ +\infty & 0 & 20 & 2 & +\infty & -\text{Ab. Val.} \\ +\infty & +\infty & 0 & +\infty & 5 & -\text{Ab. Val.} \\ +\infty & 7 & +\infty & 0 & +\infty & -\text{Ab. Val.} \\ +\infty & +\infty & 14 & +\infty & 0 & -\text{Ab. Val.} \\ +\infty & +\infty & +\infty & +\infty & +\infty & 0 \end{pmatrix} \tag{47}$$

where,

1. modes are ordered in the following sequence: W: wait to invest mode; A: Plant 1 mode; B: Plant 2 mode; C: Plant 1 mothballed mode; D: Plant 2 mothballed mode; E: abandoned mode.

2. the abandonment value is computed depreciating the initial investment sum taking into due account the wreckage value.

$$\begin{aligned} \text{Cum. Depr.} &= \frac{\text{Ini.Invest.}_0 \cdot e^{r_f \cdot \Delta t \cdot t} - \text{Wreck.Value}_0 \cdot e^{r_f \cdot \Delta t \cdot t}}{\text{intervals}} \\ \text{Ab. Val.} &= \left(\text{Ini.Invest.} \cdot e^{r_f \cdot \Delta t \cdot t} - \text{Cum. Depr.}\right) \cdot 10\% \end{aligned}$$

It is important to notice that both the initial investment sum and the wreckage value, $\text{Wreck.Value}_0 = 2$, are increased for the risk free rate to consider the opportunity cost of postponing actual investment. Risk free rate is held fixed in all specifications at the level of $r_f = 5\%$ or at a time varying interest rate generated by a (Vasicek, 1977) model with a normal value of $\overline{r}_f = 4\%$, an initial value of $r_{f,t=0} = 6\%$, a mean reversion speed of $\eta_3 = .44$ and a volatility term of $\sigma_3 = .0025$. In the latter case, a risk premium $RP = 0.0025$ is included in the computation of the up state probability and in the drift term of the equation simulated in Monte Carlo experiments.

The model depicted above has been estimated for different underlying data generating processes. They are summarized in table 8.

The multivariate GBMs with correlated Wiener processes, models # 1 through # 4 in table 8 are described in expression (48), where figures refer to variables ordered in the following sequence, P, Vc, F.

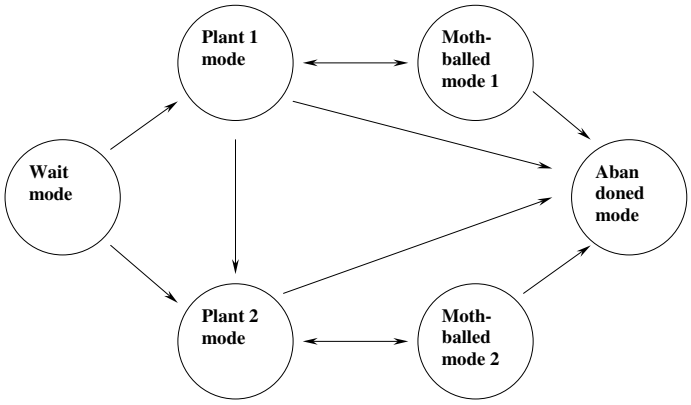

Figure 3: Directed Graph Representation of the 6 modes specification KT model.

	Data Generating Process Specification					
variable	# 1	# 2	# 3	# 4	# 5	# 6
Q						
P	GBM	GBM	GBM	GOU	GBM	GBM
Vc		GBM	GBM			
F			GBM			
Mtn						
δ_P					AOU	AOU
r_f						AOU

Table 8: Data Generating Process Specifications

Legend: processes # 1 through # 3 are univariate or multivariate Geometric Brownian Motions with correlated Wiener processes; # 4 specifies Price as a Geometric Ornstein Uhlenbeck; # 5: a two factor model (Schwartz, 1997); # 6: a three factor model (Schwartz, 1997).

Convenience yields have been set to zero for all three variables. Instead, in models #5 and #6 a time varying convenience yield is generated by an Arithmetic Ornstein Uhlenbeck with a normal value of $\overline{r}_f = -2\%$, an initial value of $r_{f,t=0} = 2\%$, a mean reversion speed of $\eta_2 = .2$ and a volatility term of $\sigma_2 = .2$.

$$\sum = \begin{pmatrix} 0.15 \\ 0.25 \\ 0.20 \end{pmatrix} \quad \rho = \begin{pmatrix} 1.00 & 0.20 & 0.30 \\ & 1.00 & 0.30 \\ & & 1.00 \end{pmatrix} \tag{48}$$

4 Assessing Applicability of LSMC to the KT model

The research question we address in applying LSMC to the KT model is how to "fine tune" the least squares Monte Carlo method in order to get more accurate results, i.e. to minimize $RMSE_r$ – and not the expected bias as explained below – in the most efficient way. There are many ways to address this problem and we had to chose some and discard some others.

To begin with, one way would be to test which family of polynomials is best in our application. In most of the previous literature the choice of different families of polynomials has been shown to be not so crucial in getting more accurate results, see for instance (Moreno and Navas, 2001), (Stentoft, 2004) pag. 142, or lately (Areal et al., 2007) pag.16 Table 6. Hence, we have followed (Stentoft, 2004) in focusing on the *complete set of polynomials* as a specification of the equation adopted to estimate continuation value in LSMC.

Moreover, another setting which has been explored in the literature is the way random numbers are generated applying, see for instance (Areal et al., 2007), quasi random numbers instead of pseudo random numbers generated by a congruential random number generator in any programming language. Because of the novelty of our application, we decided not to mingle together several issues. Hence, we have adopted plain pseudo random numbers as generated in Gauss^{tm} programming language in performing our Monte Carlo simulations.

Finally, another issue which has been addressed in fine tuning LSMC is the choice of the actual least squares method. We have to dismiss the simple `x/y` command and substitute it for the `olsqr2(y,x)` instruction which uses the QR decomposition, slower than the previous but yielding better results for near singular matrices which may occur expecially near time $t = 0$. Moreover, the command adopted handles matrices which do not have full rank returning zeros for the coefficients that cannot be estimated. This means that in our application the order of the polynomial fitted is variable being set only its maximum.

In the setting just described, LSMC method is applied to the numerical example DGPs listed in table 8, choosing properly some parameters in order to get accurate results, namely: for an individual estimate, the number of discretization points K, of basis functions M, and the number of simulated paths N. Moreover, an estimate can be replicated several times, taking as final result the average of a number R of replications.

To begin with, we verify whether LSMC is actually a convergent valuation method for $\Delta t \to 0$ or $K \to \infty$, as in (Broadie and Detemple, 1996) page 1222. Then, we test what is the accuracy of LSMC method for different combinations of basis functions M, and the number of simulated paths N. Hence, the original contribution of this section is a generalized, although empirical, exploration of proposition 1 page

124 (Longstaff and Schwartz, 2001) as another small step towards a general convergence result which is not available to date in extant literature. As a matter of fact, (Tsitsiklis and Van Roy, 2001), (Longstaff and Schwartz, 2001), (Clément et al., 2002) provide convergence results with respect to the number of simulated paths holding the number of basis functions fixed. (Glasserman and Yu, 2004), instead, provide convergence results with respect to polynomial regression coefficients in a setting in which the number of paths and the number of basis functions increase together. Moreover, it should be noticed that the previous convergence results are derived in a univariate setting assuming that they could be "*relevant for higher dimensional problems*" page 3 (Glasserman and Yu, 2004). Instead, we verify empirically what (Longstaff and Schwartz, 2001) page 125 define "*only conjectures about higher dimensional problems*".

In the next two sections, then, we analyze the trade off between accuracy and computational time, see section 5 and we explore the statistical properties of LSMC estimates, see section 6.

4.1 The Asymptotic Behavior of LSMC

In this section we try to answer the following question: what is the asymptotic behavior of the LSMC algorithm ? In other words, what happens when $\Delta t \to 0$. As a matter of fact, a convergent asymptotic behavior of LSMC valuations may help in getting less biased estimates, together with the choice of the two most important parameters of the model, namely order of the polynomial and number of paths simulated. We would not have been able to tackle this problem without the rescaling methods proposed above in order to compare results for different Δt. We find that LSMC is not a convergent algorithm in this application when the underlying is a GBM, both univariate or correlated multivariate. Instead, when the underlying DGP is a model 1, 2 or 3 in (Schwartz, 1997) LSMC valuations converge asymptotically.

In order to observe the asymptotic behavior of LSMC we have pursued the following experiment design. To begin with we have estimated KT model value functions with lattice methods letting $\Delta t \to 0$, see figures 4-9. In the univariate case, GBM discretization has been performed using (Cox et al., 1979). In multivariate cases, correlated GBMs discretization has been performed using (Boyle et al., 1989) and (Gamba and Trigeorgis, 2005) where one cross-checks the other. In the univariate GOU case, (Sick, 1995) censored lattice has been applied. For model 2 and 3 in (Schwartz, 1997) a generalization of the (Schulmerich, 2005) page 177 approach has been deviced.

At first glance, observing the graphs just mentioned, lattice methods produce asymptotically convergent valuations. This happens even though drift adjustment methods proposed in the previous sections have been implemented[24] and even though the optionalities in the model are bermudan, i.e. the number of epochs in

[24]For all but the last two DGPs for which flows were rescaled simply multiplying annual figures for Δt.

which the industrial plant can be managed –dates in which it is possible to exercise real options – remain fixed while the number of epochs which discretize the underlying stochastic process grows to infinity.

The previous lattice benchmarks have been compared with LSMC valuations. For univariate GBM, these have been obtained through two different discretization methods, namely a Brownian Bridge and a pde solution simulation. Instead, for all the remainind DGPs, only the latter discretization method has been adopted. From a computational point of view, it is worth mentioning that while the former does not require much RAM and much HD space, the latter requires much of both, needing to simulate forward the underlying stochastic process and storing it in view of its use in the backward induction process. For path dependent stochastic processes, like the last three DGPs, the latter is the only simulation method available to date.

For choosing the order of the polynomial and the number of simulated paths we referred to the combination which gives the lowest RMSE among the combinations examined in section 4.2. There, the number of discretization points has been chosen taking into account the results of this section. In short, one choice is consistent with the other since, after some trial and error, we converged on the LSMC configuration reported in table 9

data generating process	N	M
GBM 1	640.000	5
GBM 2	80.000	6
GBM 3	320.000	5
model 1 in (Schwartz, 1997)	320.000	2
model 2 in (Schwartz, 1997)	320.000	9
model 3 in (Schwartz, 1997)	320.000	6

Table 9: LSMC Configurations used to test the Asymptotic Behavior for KT model.
Legend: N=number of paths; M=order of the polynomial.

Results are reported in figures 4-9. In the univariate case, LSMC results obtained through Brownian bridge and through direct simulation of the pde solution are remarkably similar. Although that is true, Brownian Bridge estimates show a positive bias for a low number of discretization epochs, while pde estimates are much more stable for different Δt. For this reason, we do not use Brownian Bridge in the multivariate GBM applications of LSMC. In any case, none of them shows a clear asymptotic convergence as, instead, lattice benchmarks. A more rigorous proof of the non significant difference between the valuations for different Δt could be achieved using a simple bootstrapping design, see page 221 chapter 16 (Efron and Tibshirani, 1993). Since this would require much more CPU time, we save this proof for the following draft.

In conclusion, it is not necessary to discretize univariate GBMs letting the number of intervals go to

infinity. As a matter of fact results are not much different. In other words, like Sherlock Holmes, what we propose as a proof of the non convergent behavior of LSMC in our application is a sort of "the dog that didn't bark".[25]

About multivariate correlated GBMs, between the two multivariate lattice methods adopted, we observe that (Gamba and Trigeorgis, 2005) converges much faster than (Boyle et al., 1989). Moreover, convergence is remarkably smooth and monotonic allowing the use of Richardson extrapolation in both its simple and repeated versions. This would have been required for the tetravariate GBM case. For both to contain the size of the paper and to propose examples in which we rely only on lattice methods to obtain benchmarks, we decided to drop tetravariate GBM case also because convergence pattern of LSMC as dimensionality increases can be gleaned from a comparison of univariate with bivariate and trivariate GBM cases.

About models 1, 2 and 3 (Schwartz, 1997), figures 7-9 show a clear asymptotic convergence of LSMC estimates as $\Delta t \to 0$. We conjecture that this happens because the mean reverting properties of the three processes are better approximated by a finer discretization.

In conclusion, LSMC asymptotic convergence property depends on the underlying data generating process. When this is a GBM in both its univariate and multivariate versions, LSMC is not a convergent valuation method. Therefore, it is not necessary a fine discretization and the mere exercise frequency would be enough to get accurate results.

Instead, when the underlying data generating process has direct or indirect mean reverting properties, like respectively, model 1 in (Schwartz, 1997), a mean reverting process with spring effect on the log of the normal value, and models 2 or 3 in (Schwartz, 1997), a two and three factor model with mean reverting drift, then LSMC should be used with a fine discretization in order to obtain accurate results.

[25] Arthur Conan Doyle, Silver Blaze, published in The Memoirs of Sherlock Holmes, 1892.

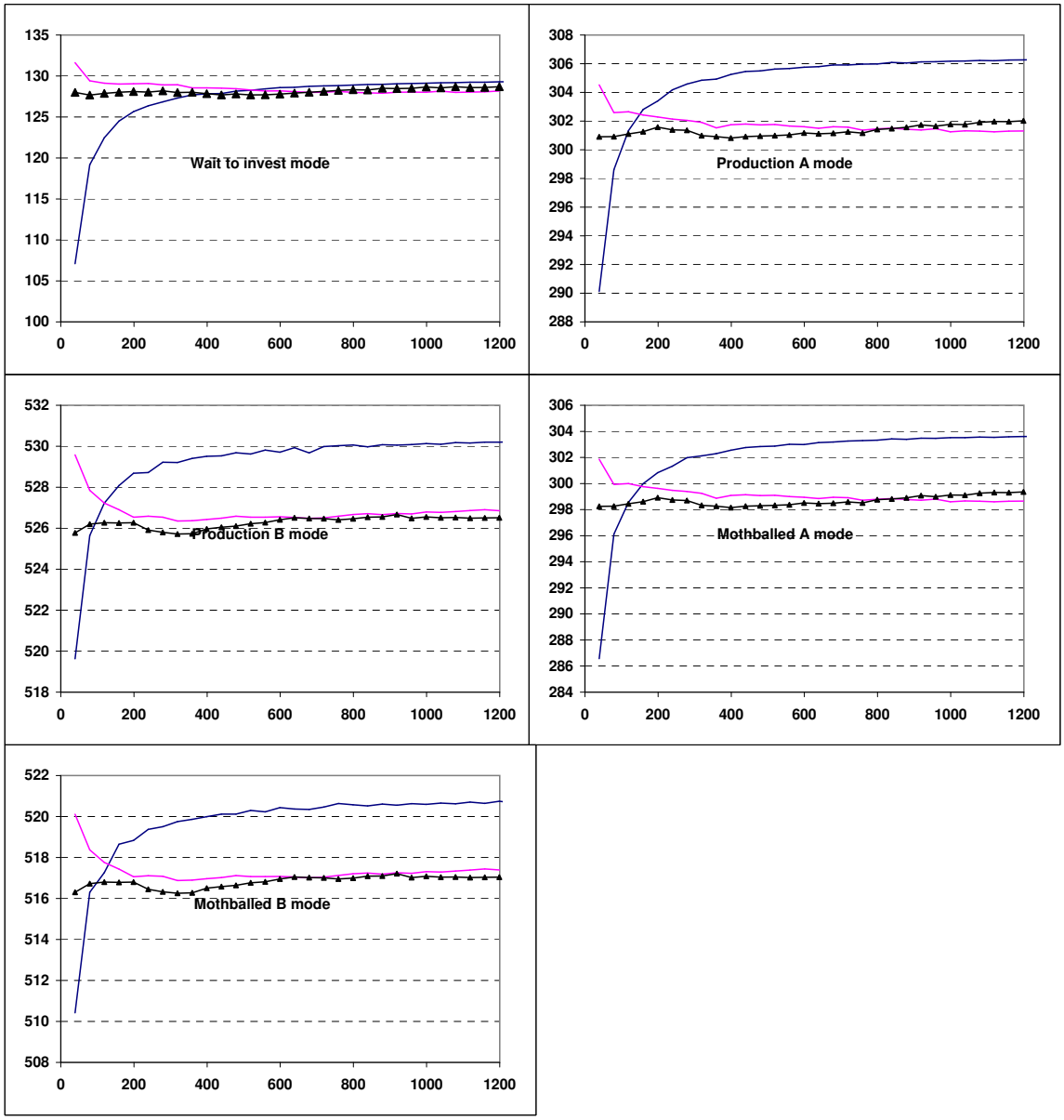

Figure 4: Asymptotic Behavior of GBM 01 estimates.
Legend: graphs report different valuations for an increasing number of epochs in which the life of the investment project, $life = 20\ years$, is discretized, for a corresponding interval of $1/2 \leq \Delta t \leq 1/60$. Lattice results are reported in a bold line. LSMC with pde simulation results are represented by a line with triangles. LSM with BB simulation results are represented by a lighter line. Lattice method adopted is (Cox et al., 1979). LSMC simulating pde has been implemented for a polynomial order $ord = 5$ and a number of paths $nms = 640 \cdot 10^3$. LSMC simulating Brownian Bridge has been implemented for a polynomial order $ord = 5$ and a number of paths $nms = 800 \cdot 10^3$. Correction methods reported in section 2.2 above have been applied to both methods to obtain comparable results.

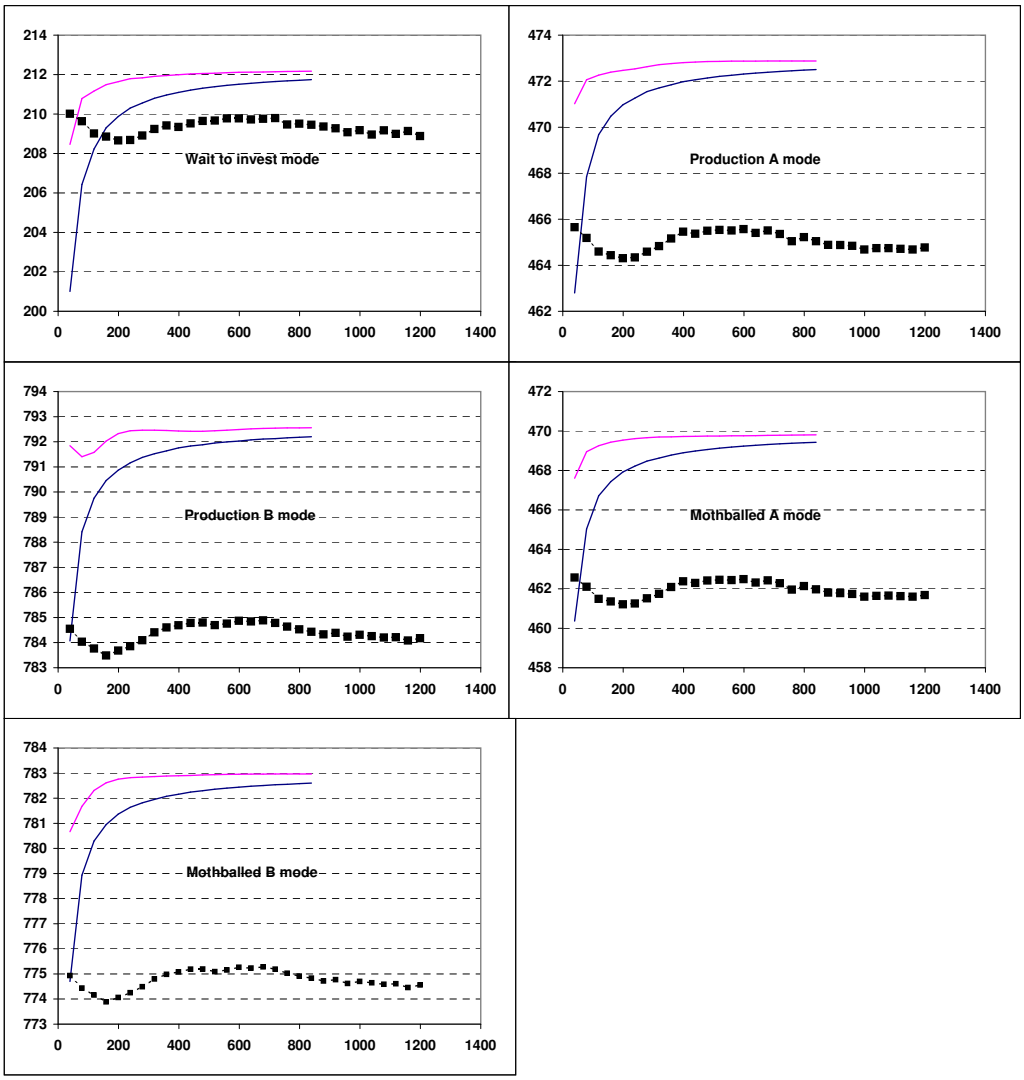

Figure 5: Asymptotic Behavior of GBM 02 estimates.
Legend: graphs report different valuations for an increasing number of epochs in which the life of the investment project, $life = 20\ years$, is discretized, for a corresponding interval of $1/2 \leq \Delta t \leq 1/40$. Lattice method adopted are (Gamba and Trigeorgis, 2005) upper curves, (Boyle et al., 1989), lower curves. LSMC has been implemented for the order of the polynomial to be $ord = 6$ and the number of paths to be $nms = 80 \cdot 10^3$ over the same discretization intervals. Correction methods reported in section 2.2 above have been applied to both methods to obtain comparable results.

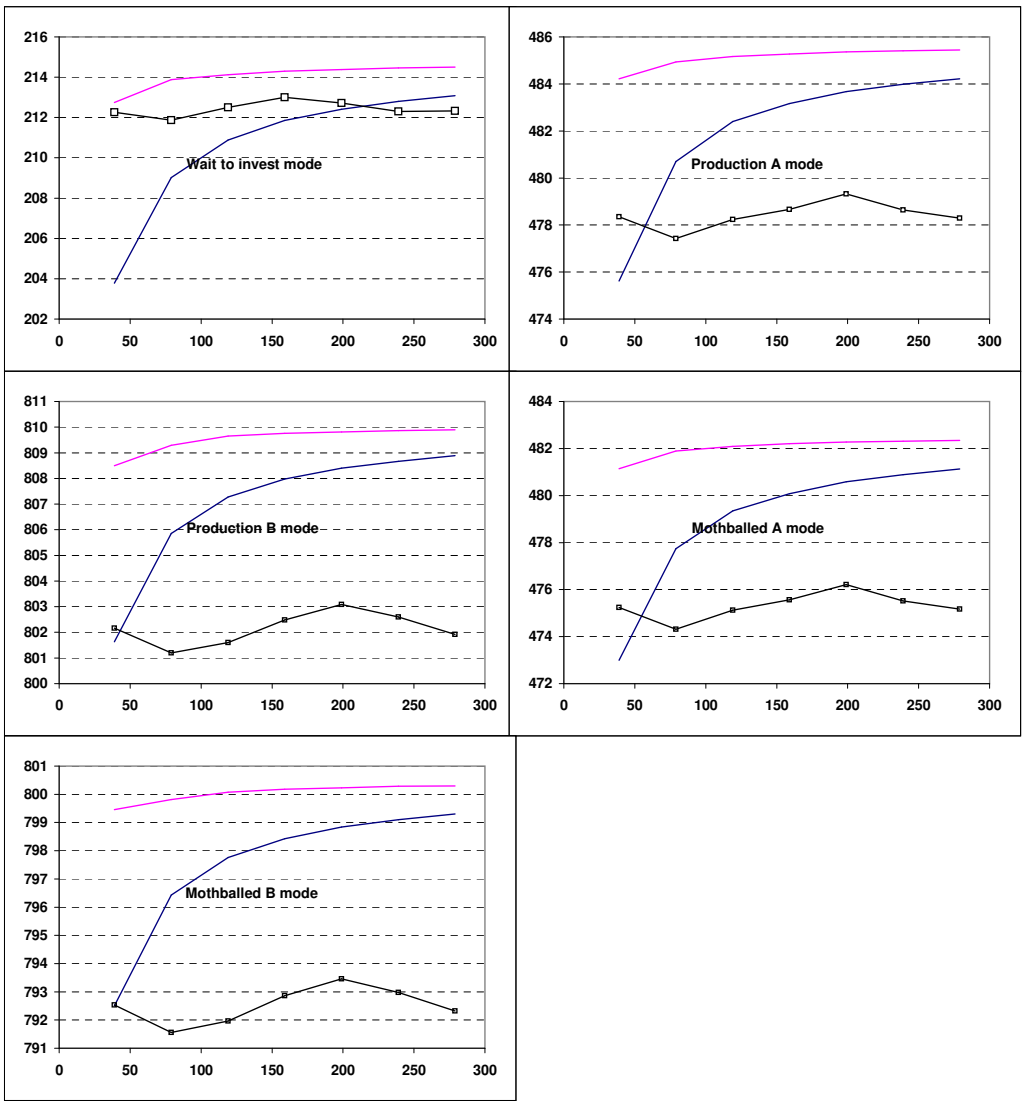

Figure 6: Asymptotic Behavior of GBM 03 estimates.
Legend: graphs report different valuations for an increasing number of epochs in which the life of the investment project, $life = 20\ years$, is discretized, for a corresponding interval of $1/2 \leq \Delta t \leq 1/14$. Lattice method adopted are (Gamba and Trigeorgis, 2005) upper curves, (Boyle et al., 1989), lower curves. LSMC has been implemented for the order of the polynomial to be $ord = 5$ and the number of paths to be $nms = 320 \cdot 10^3$ over the same discretization intervals. Correction methods reported in section 2.2 above have been applied to both methods to obtain comparable results.

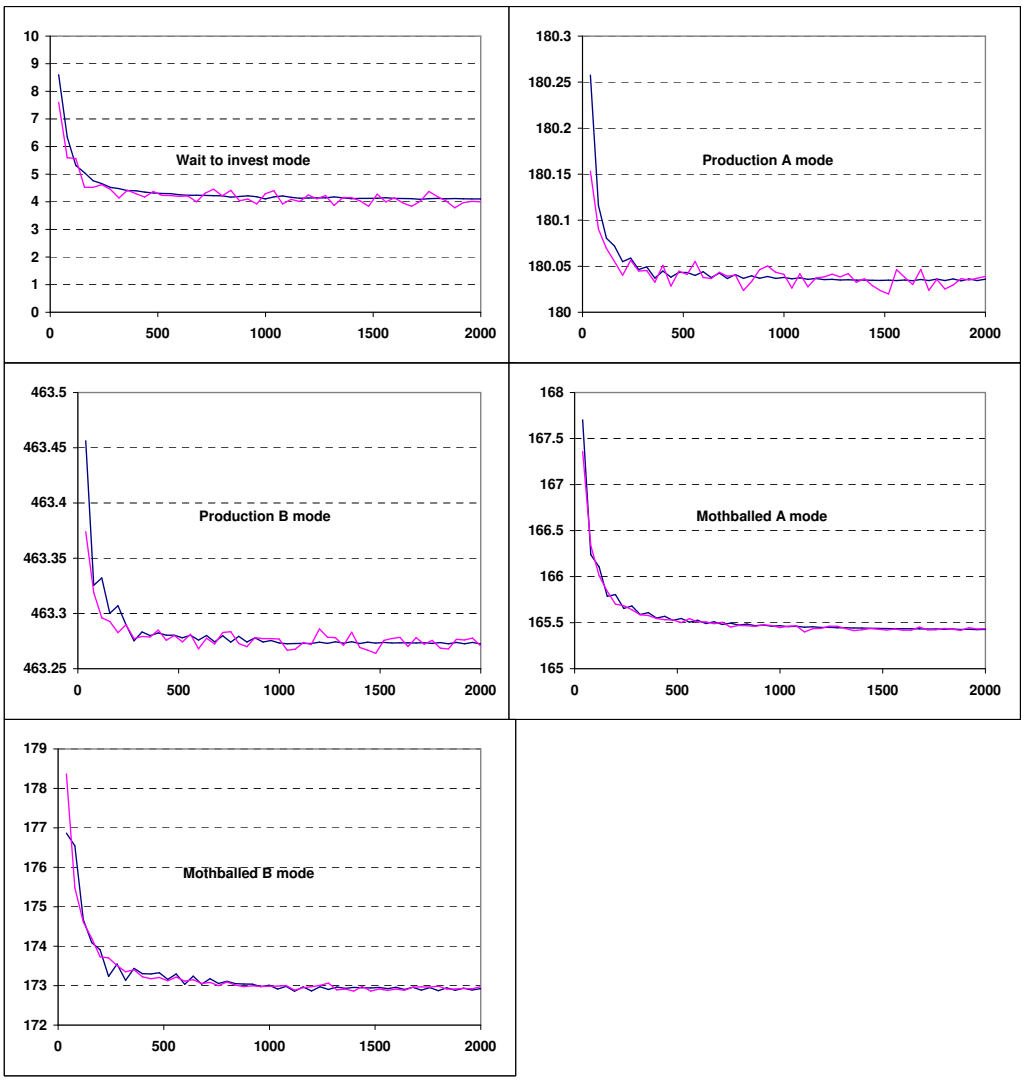

Figure 7: Asymptotic Behavior of Geometric Ornstein Uhlenbeck, model 1 in (Schwartz, 1997). Legend: graphs report different valuations for an increasing number of epochs in which the life of the investment project, $life = 20\ years$, is discretized, for a corresponding interval of $1/2 \leq \Delta t \leq 1/100$. Lattice method adopted are (Sick, 1995), represented in squares. LSMC has been implemented for the order of the polynomial to be $ord = 2$ and the number of paths to be $nms = 320 \cdot 10^3$ over the same discretization intervals. Correction methods reported in section 2.2 above have been applied to both methods to obtain comparable results.

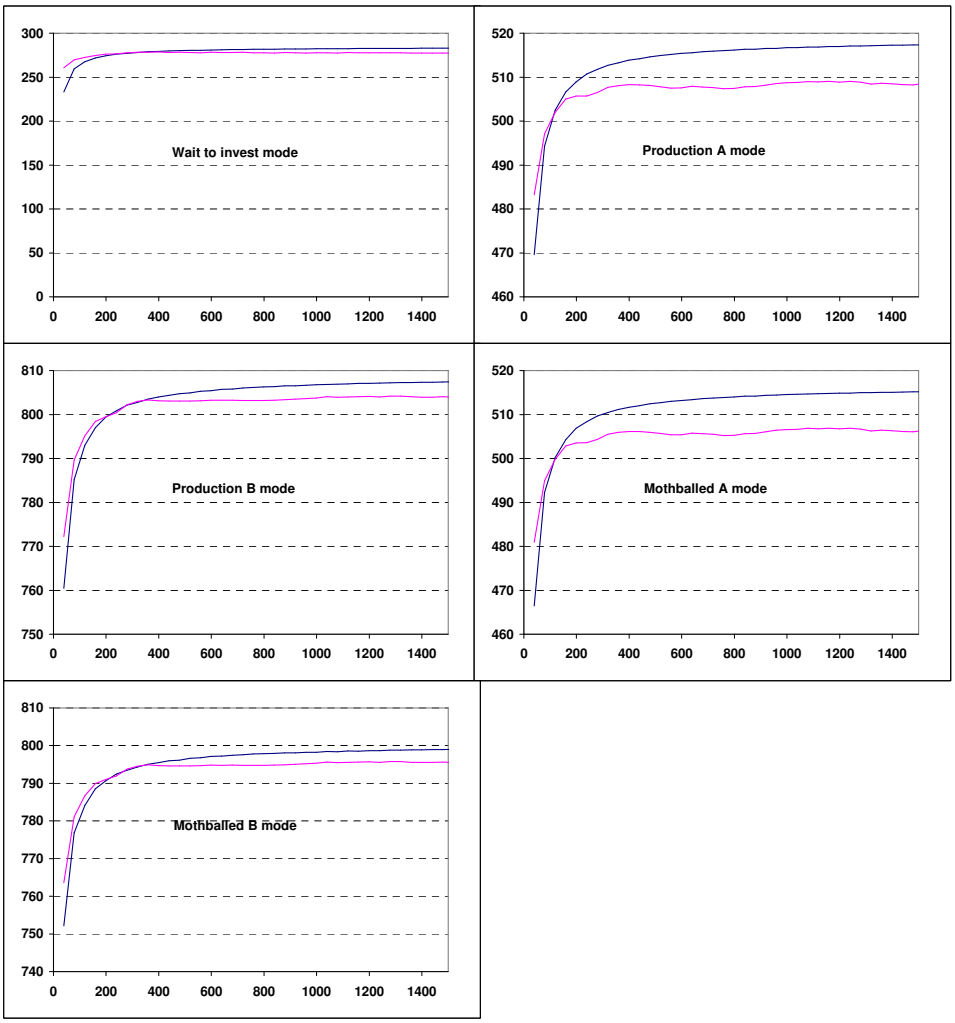

Figure 8: Asymptotic Behavior of Two Factor Model, model 2 in (Schwartz, 1997).
Legend: graphs report different valuations for an increasing number of epochs in which the life of the investment project, $life = 20\ years$, is discretized, for a corresponding interval of $1/2 \leq \Delta t \leq 1/76$. Lattice method adopted is (Schulmerich, 2005), represented in light line. LSMC has been implemented for the order of the polynomial to be $ord = 9$ and the number of paths to be $nms = 320 \cdot 10^3$ over the same discretization intervals. Correction methods reported in section 2.2 above have been applied to both methods to obtain comparable results.

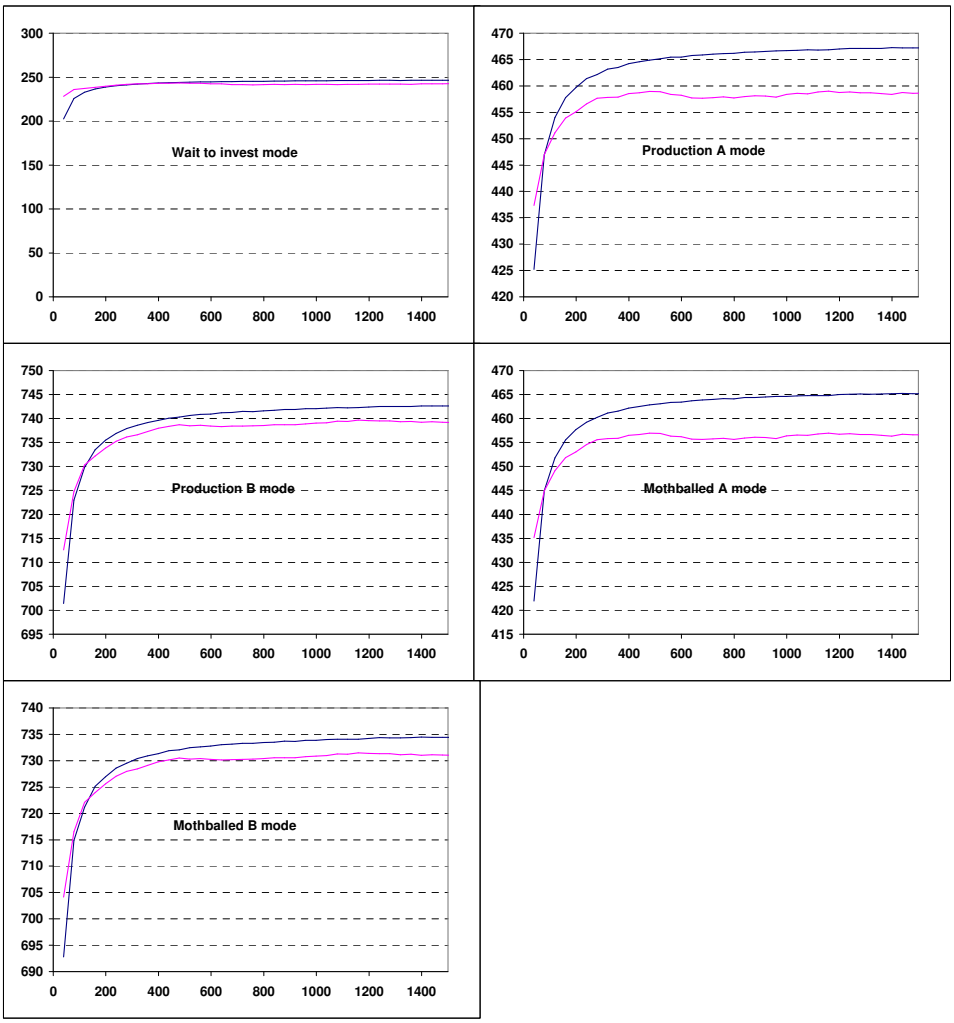

Figure 9: Asymptotic Behavior of Three Factor Model, model 3 in (Schwartz, 1997).
Legend: graphs report different valuations for an increasing number of epochs in which the life of the investment project, $life = 20\ years$, is discretized, for a corresponding interval of $1/2 \leq \Delta t \leq 1/80$. Lattice method adopted is (Schulmerich, 2005), represented in light line. LSMC has been implemented for the order of the polynomial to be $ord = 6$ and the number of paths to be $nms = 320 \cdot 10^3$ over the same discretization intervals. Correction methods reported in section 2.2 above have been applied to both methods to obtain comparable results.

4.2 The Choice of LSMC Parameters

In this section we explore the sensitivity of LSMC to the choice of its two most important parameters, namely the order of the polynomial used in the regression and the number of simulated paths. The different combinations of the two mentioned parameters have been tested with respect to the most used criterion: Root Mean Squared Error (RMSE), relative to the benchmark, see expression (49).[26]

$$RMSE = \sqrt{\frac{\left(\widetilde{F}_{m,lsmc} - F_{m,b}\right)^2 + Var\left(\widetilde{F}_{m,lsmc}\right)}{F_{m,b}}} \tag{49}$$

where:

$\widetilde{F}_{m,lsmc}$:= LSMC estimate of mode m value function;
$F_{m,b}$:= Lattice benchmark.

Dimension	Intervals	Wait	Produce A	Produce B	Mothballed A	Mothballed B
GBM 1	4999	129.819800	306.675950	530.438210	304.022380	520.979250
GBM 2	839	211.744380	472.505540	792.199920	469.429730	782.600810
GBM 3	239	212.80664	483.98359	808.67086	480.8921	799.10293
GOU 1	4999	4.0606302	180.03288	463.27087	165.39738	172.83802
TwoFm	1599	283.00908	517.40216	807.48896	515.25179	799.04503
ThreeFm	2279	246.83917	467.64133	743.01833	465.60727	734.84563

Table 10: Lattice Benchmarks.
Legend: univariate GBM uses a (Cox et al., 1979) lattice, multivariate GBMs (Gamba and Trigeorgis, 2005), GOU 1 (Sick, 1995). Two and Three Factor models estimates are provided by extensions of (Schulmerich, 2005) page 177.

RMSE is used in extant literature, see for instance (Stentoft, 2004) and (Areal et al., 2007), as a loss function, instead of the average error, see page 97 (Greene, 1994), because, as shown in section 6, LSMC provides a random biased estimate of the option price. Hence, focussing on the unbiasedness may preclude the choice of a LSMC specification providing a tolerably biased estimator with a much smaller variance. Therefore, the mean squared error is chosen as a criterion that recognizes this possible tradeoff between unbiasedness and variance of the estimator. As a matter of fact, it may be more convenient to have a

[26] Expression (49) and expression (21) are exactly equivalent, see page 293 (Mood et al., 1974).

biased but less variable estimator than an unbiased but very volatile estimator. In the case of the various parameter combinations of LSMC, among the biased low estimators we would prefer to get those with the lowest variance, being the estimates that they yield more probably in a close neighborhood of the benchmark value, as shown in section 6.

Therefore, we have computed RMSE of LSMC estimates around their benchmark values, see table 10, simply replicating 100 times LSMC valuations for a combination of order of the polynomial used in the regression and number of paths simulated as reported in table 11. These results are depicted in surface plots in figures 10-14. Moreover, in order to give a one equation portrayal of the influence of the two parameters on RMSE and tackling its statistical significance, we have computed a multiple regression on the average RMSE of the main value functions estimated, see table 12-16 where, for brevity, we report equations only for three value functions out of five. As a matter of fact, the first value function stays as a sort of summary of all the others, Wait mode, while the other two represent respectively an out of the money switching option, plant 1 mode, and an in the money switching option, plant 2 mode.

data generating process	N ($\cdot 10^3$)	M	K	$argmin_{(N,M)}$	$min(RMSE)$ Wait Mode
GBM 1	20-640	2-9	40	640.000, 5	.0061906
GBM 2	20-640	2-9	40	80.000, 6	.0134957
GBM 3	10-320	1-8	40	320.000, 5	.0083723
model 1 in (Schwartz, 1997)	10-320	2-9	2000	320.000, 2	.0224053
model 2 in (Schwartz, 1997)	10-320	2-9	1520	320.000, 9	.0050930
model 3 in (Schwartz, 1997)	10-320	2-9	1600	320.000, 6	.0060304

Table 11: LSMC Configurations used to Study the influence on RMSE of N and M.
Legend: N=number of paths; M=order of the polynomial; K= discretization epochs; $argmin_{(N,M)}$: the number of simulated paths and the order of the complete set of polinomials for which $min(RMSE)$ is achieved.

Differently from what finds (Stentoft, 2004) for LSMC pricing of an American Put written on an underlying asset following a univariate GBM, we do not find always a monotonic negative relation between both the order of the polynomial and the number of paths simulated. In that application, proposition 2 of (Longstaff and Schwartz, 2001) is confirmed. This is not always the case when LSMC is applied to the KT model. Results depend very much on the underlying DGP.

For GBMs, the parameter which affects most RMSE is M, the order of the complete set of polynomials. This is true for all three cases, and within them for each value function. As is depicted in figures 10-12 and summarized by regressions in table 12-14, the order of the complete set of polynomials contributes significantly to the reduction of RMSE up to some threshold level after which, instead, M increases significantly RMSE. This happens for any level of N, number of paths simulated. This parameter is not significant in reducing RMSE although regression coefficients have the same sign as M, to recap negative the linear and positive the quadratic.

In conclusion, for underlying GBMs, increasing the number of paths decreases slowly RMSE while the order of the complete set of polynomials first decreases and then increases RMSE inducing a "U" shaped pattern for univariate GBMs or an "L" shaped one for bivariate and trivariate cases. As a matter of fact, for bivariate and trivariate cases RMSE literally explodes after reaching a critical threshold of $M = 6$.

This evidence does not confirm proposition 2 of (Longstaff and Schwartz, 2001) but it is in accordance with (Glasserman and Yu, 2004) where it is shown how MSE of the LSMC regression coefficients literally explodes when the order of the polynomial exceeds a critical threshold. There the threshold depends on the number of simulated paths. Here, we do not find much difference between RMSE for estimates derived with a different number of simulated paths. This last remark suggest not to simulate too many paths being the incremental reduction of RMSE smaller and smaller while requiring a lot of expensive CPU time, as shown in section 5.

For model 1 in (Schwartz, 1997), a geometric Ornstein Uhlenbeck motion with spring effects on the log of the normal value, the influence of the order of the polynomial on RMSE is little when it is non existent, being predominant the effect of the simulated paths. This is evident at first glance from surface plots in figure 13 where RMSE declines steadily as the number of simulated paths increases. In this case, more than in all the others examined, regressions help us to delve into the influence of the individual parameters on RMSE, see table 15.

Differently from the previous GBMs based cases, the estimates of the three value functions behave differently. As a matter of fact, coefficients change both sign and significance. Hence, while the quadratic effect of the number of simulated paths increases RMSE for the Wait to invest mode value function, the same effect decreases RMSE for the other two value functions. Instead, the linear effect of the number of simulated paths decreases significantly the wait mode value function RMSE while it is not significant in the other two cases. Finally, it is worth mentioning that the order of the polynomial generally shows non significant effect on RMSE but for Plant 1 mode value function for which the pattern previously observed

for GBMs occurs again.

For model 2 in (Schwartz, 1997), a geometric brownian motion with stochastic convenience yield generated by an arithmetic Ornstein Uhlenbeck, we observe a negative effect on RMSE of both the order of the polynomial and of the number of simulated paths, see figure 14. In this case, proposition 2 in (Longstaff and Schwartz, 2001) is confirmed. These effects are statistically significant in most of the modes value functions studied in table 16. As a matter of fact, linear effects are always negative and, in all cases but one, statistically significant. Although that is true, even in this case the (Glasserman and Yu, 2004) pattern emerges with the squared order of the polynomial term increasing RMSE in two cases out of three. The same can be observed for the number of simulated paths squared term.

For model 3 in (Schwartz, 1997), a geometric brownian motion with stochastic convenience yield and risk free rate generated by an arithmetic Ornstein Uhlenbeck, we observe patterns very similar to the previous DGP. As a matter of fact, both the order of the polynomial and the number of paths simulated are relevant for reducing RMSE. This is evident from figure 15 and from table 17. Linear effects are always negative and in most cases statistically significant. Like in many of the previous cases, here we find for the number of paths a quadratic term effect which increases RMSE.

In conclusion, LSMC accuracy depends on the underlying DGP not only for the actual size of the minimum RMSE bu also for the pattern followed in achieving it. As a matter of fact, only in two cases out of six, LSMC is a convergent algorithm.

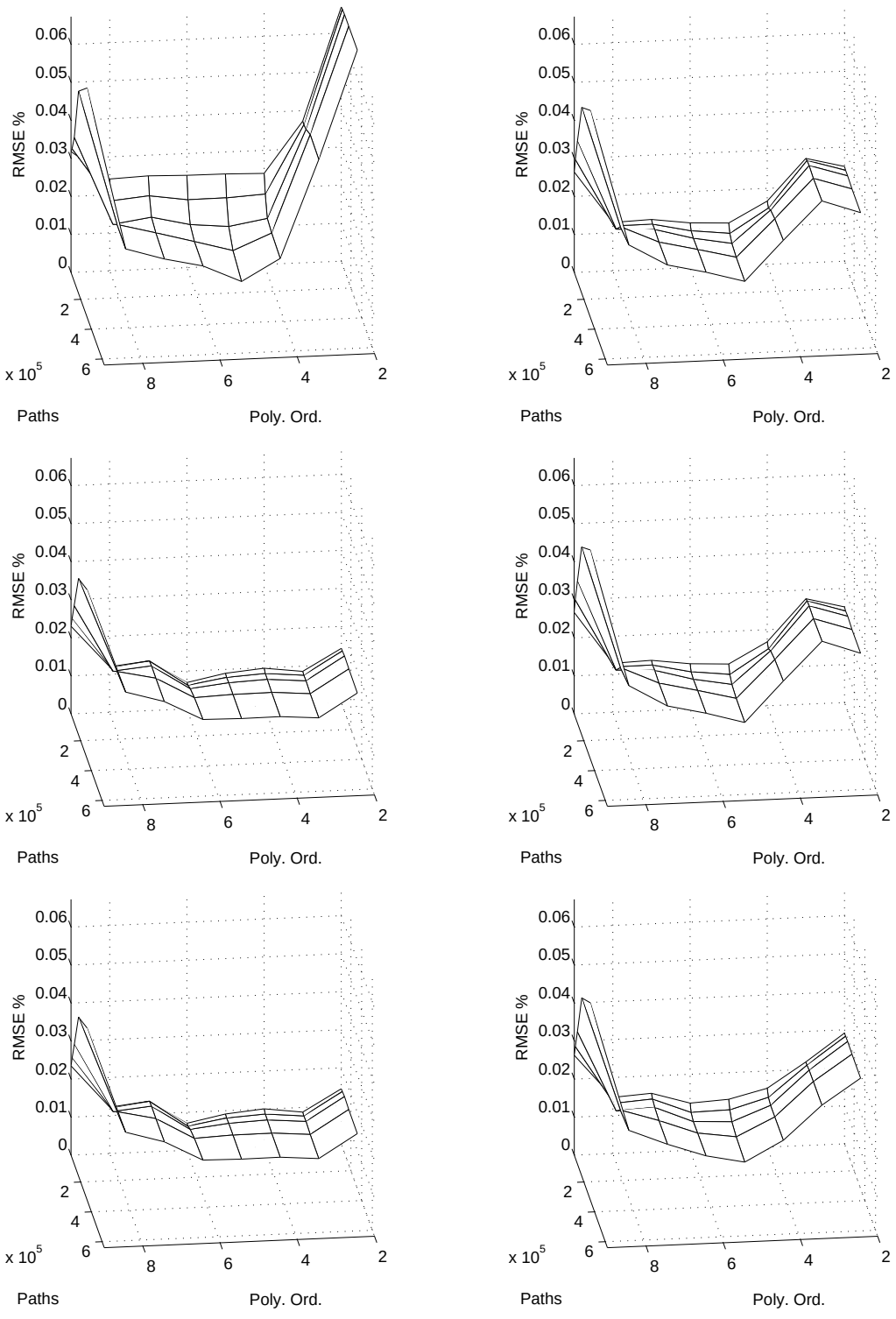

Figure 10: RMSE surface plots: Univariate GBM.

Legend: RMSE has been computed according to expression (49) for 100 estimates obtained for the different combinations of number of Monte Carlo simulated paths, $N = 20 - 640 \cdot 10^3$, and of different orders of the polynomial used in LSMC regressions, $M = 2 - 9$. Upper left hand corner graph reports RMSE for Wait Mode Value Function. Continuing row wise, RMSE for the other four value functions are reported, together with the average RMSE of the whole model, in the lower right hand corner.

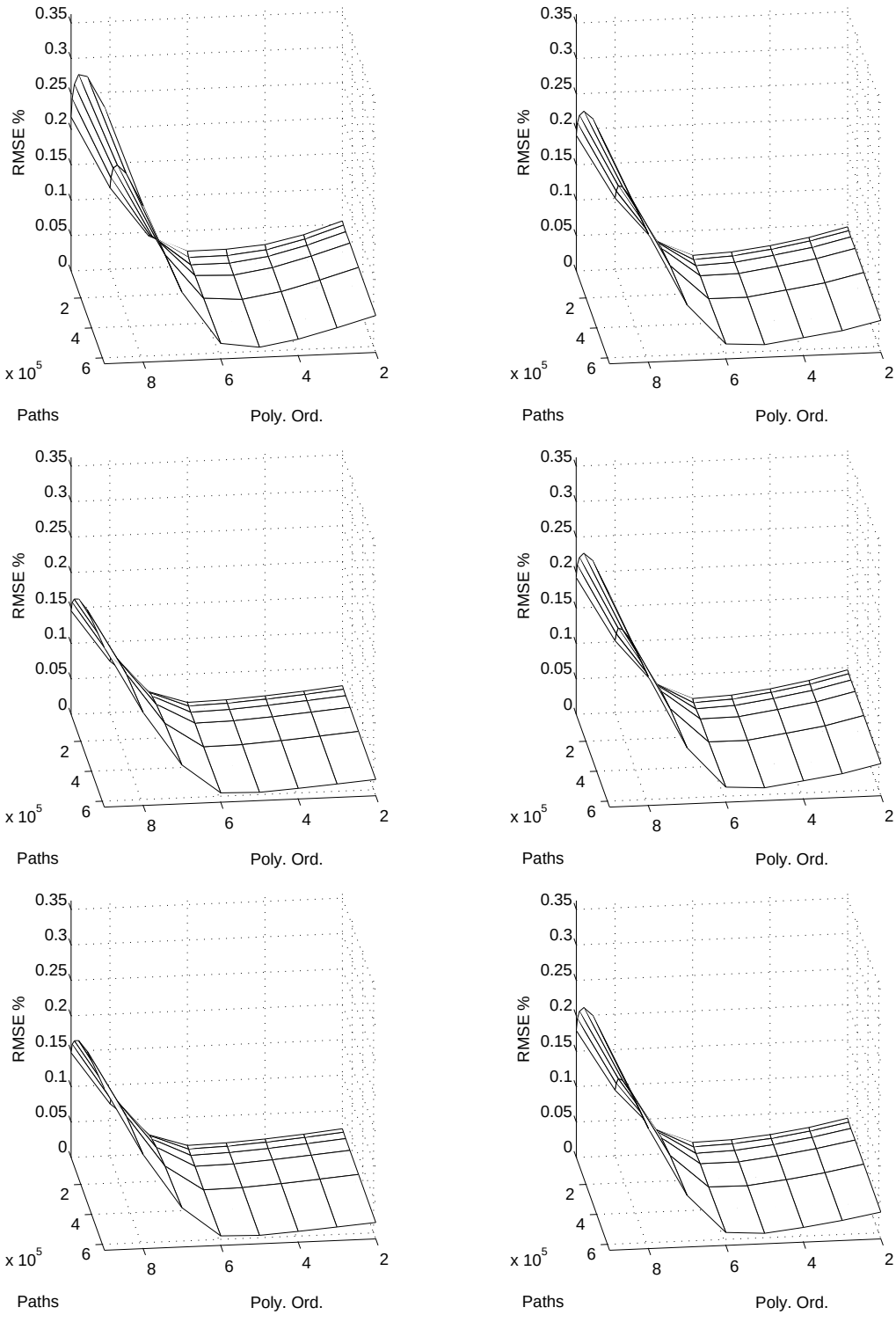

Figure 11: RMSE surface plots: Bivariate GBM.

Legend: RMSE has been computed according to expression (49) for 100 estimates obtained for the different combinations of number of Monte Carlo simulated paths, $N = 20 - 640 \cdot 10^3$, and of different orders of the polynomial used in LSMC regressions, $M = 2 - 9$. Upper left hand corner graph reports RMSE for Wait Mode Value Function. Continuing row wise, RMSE for the other four value functions are reported, together with the average RMSE of the whole model, in the lower right hand corner.

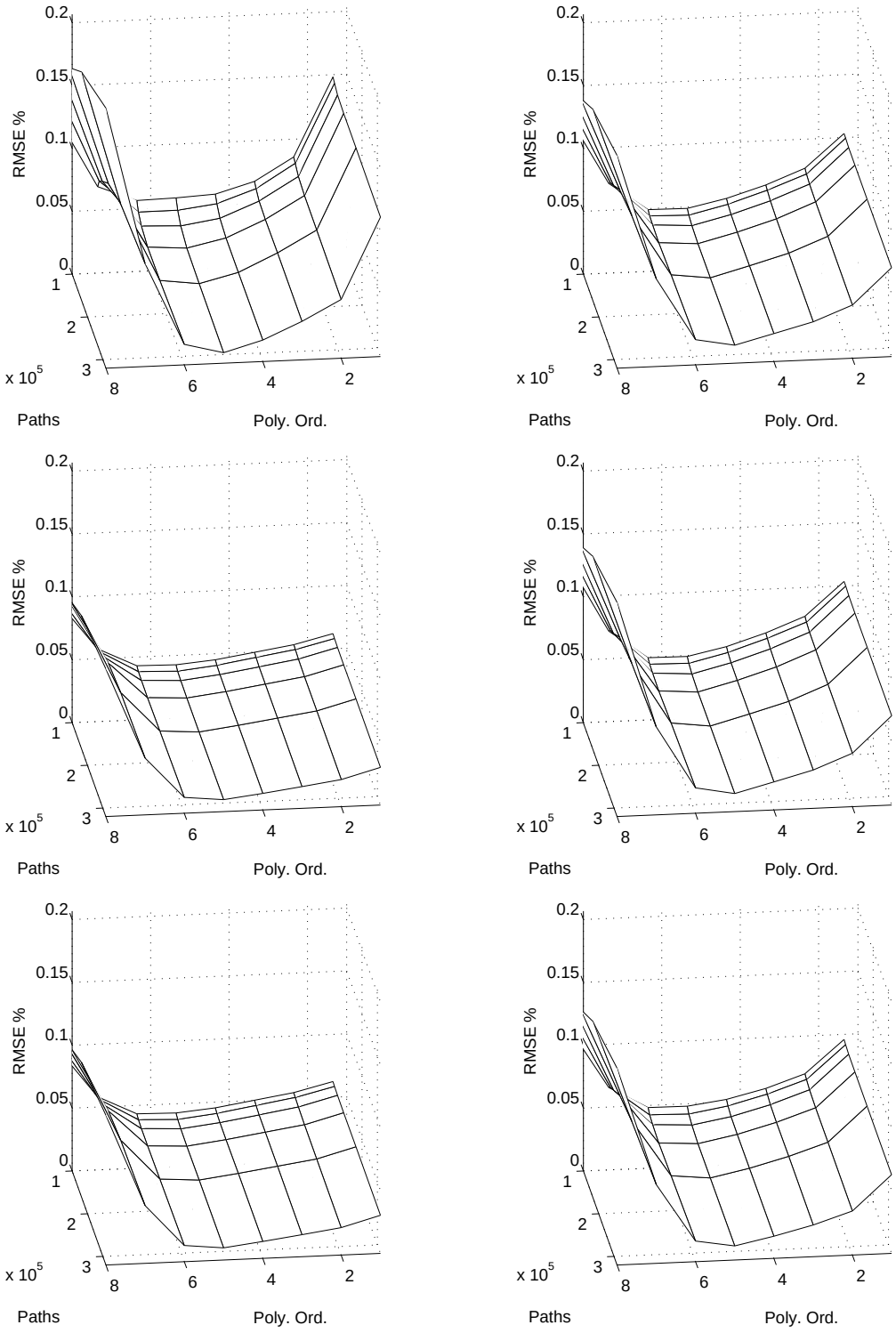

Figure 12: RMSE surface plots: Trivariate GBM.

Legend: RMSE has been computed according to expression (49) for 100 estimates obtained for the different combinations of number of Monte Carlo simulated paths, $N = 10 - 320 \cdot 10^3$, and of different orders of the polynomial used in LSMC regressions, $M = 1 - 8$. Upper left hand corner graph reports RMSE for Wait Mode Value Function. Continuing row wise, RMSE for the other four value functions are reported, together with the average RMSE of the whole model, in the lower right hand corner.

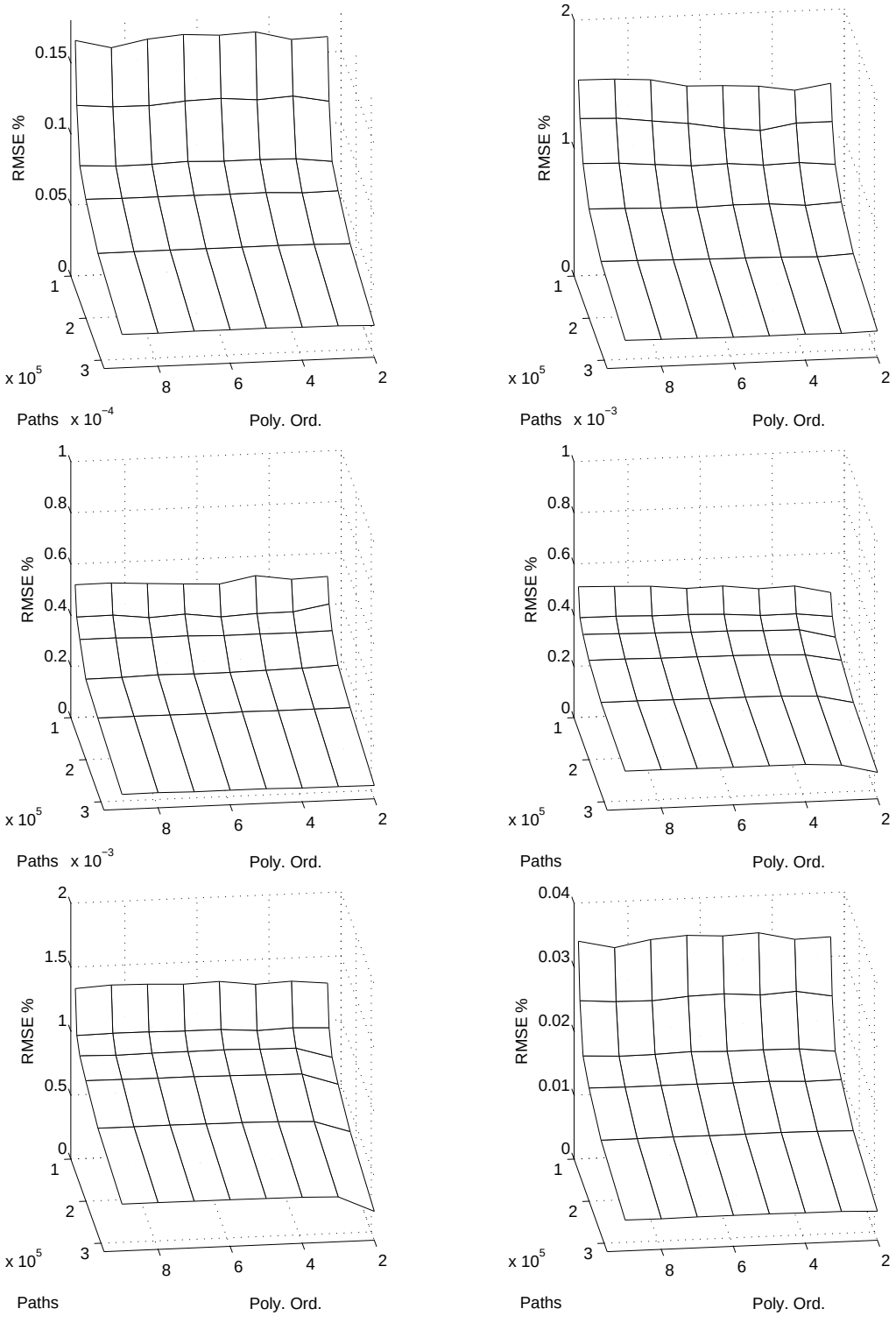

Figure 13: RMSE surface plots: Univariate GOU.

Legend: RMSE has been computed according to expression (49) for 100 estimates obtained for the different combinations of number of Monte Carlo simulated paths, $N = 10 - 320 \cdot 10^3$, and of different orders of the polynomial used in LSMC regressions, $M = 2 - 9$. Upper left hand corner graph reports RMSE for Wait Mode Value Function. Continuing row wise, RMSE for the other four value functions are reported, together with the average RMSE of the whole model, in the lower right hand corner.

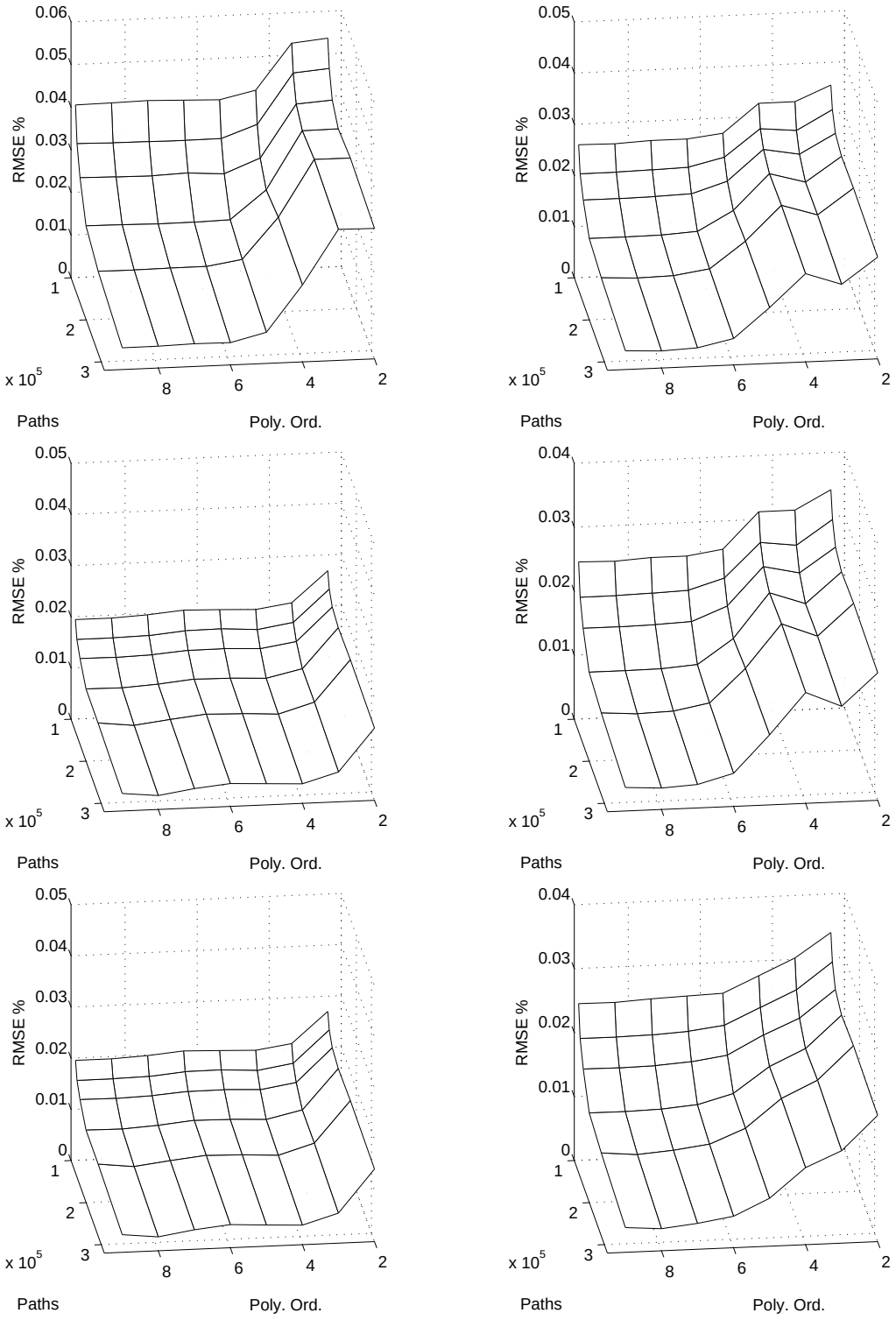

Figure 14: RMSE surface plots: Two Factor Model, Model 2 in (Schwartz, 1997).
Legend: RMSE has been computed according to expression (49) for 100 estimates obtained for the different combinations of number of Monte Carlo simulated paths, $N = 10 - 320 \cdot 10^3$, and of different orders of the polynomial used in LSMC regressions, $M = 2 - 9$. Upper left hand corner graph reports RMSE for Wait Mode Value Function. Continuing row wise, RMSE for the other four value functions are reported, together with the average RMSE of the whole model, in the lower right hand corner.

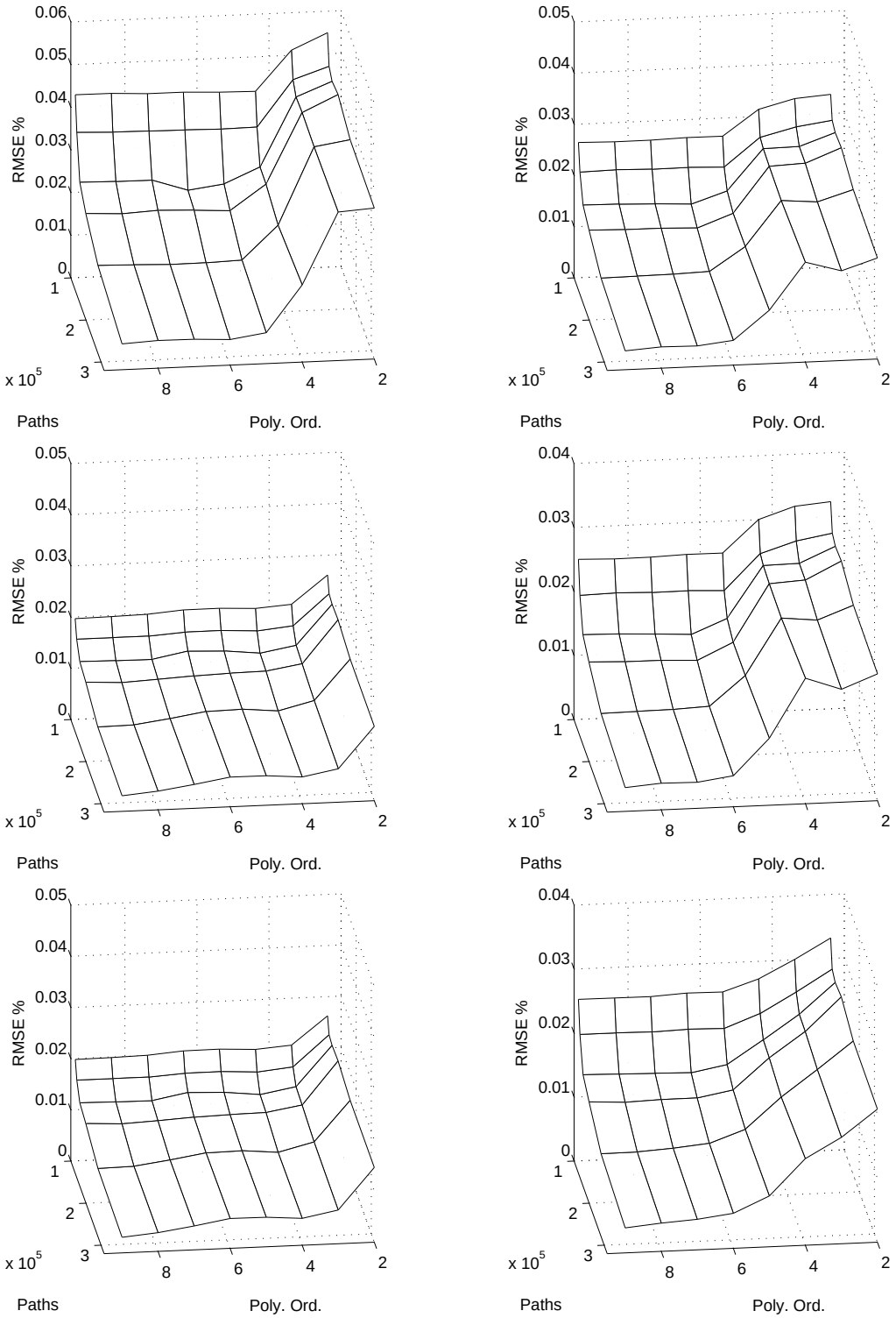

Figure 15: RMSE surface plots: Three Factor Model, Model 3 in (Schwartz, 1997).
Legend: RMSE has been computed according to expression (49) for 100 estimates obtained for the different combinations of number of Monte Carlo simulated paths, $N = 10 - 320 \cdot 10^3$, and of different orders of the polynomial used in LSMC regressions, $M = 2 - 9$. Upper left hand corner graph reports RMSE for Wait Mode Value Function. Continuing row wise, RMSE for the other four value functions are reported, together with the average RMSE of the whole model, in the lower right hand corner.

A. Wait mode Estimate:

Variable	$constant$	$poly-ord$	nms	$poly-ord^2$	nms^2	R^2
Estimate	8.3238	-6.8323	-1.1434	2.1436	0.0452	0.7340
Error	5.6343	0.6940	0.9722	0.2345	0.0417	nobs
t-value	1.4773	-9.8446	-1.1761	9.1402	1.0836	48

B. Plant 1 mode Estimate:

Variable	$constant$	$poly-ord$	nms	$poly-ord^2$	nms^2	R^2
Estimate	0.6148	-4.4460	-0.3287	1.4652	0.0160	0.4150
Error	6.6608	0.8205	1.1493	0.2773	0.0493	nobs
t-value	0.0923	-5.4189	-0.2860	5.2846	0.3242	48

C. Plant 2 mode Estimate

Variable	$constant$	$poly-ord$	nms	$poly-ord^2$	nms^2	R^2
Estimate	-2.4881	-4.5751	0.0553	1.7057	0.0001	0.8040
Error	3.5736	0.4402	0.6166	0.1488	0.0265	nobs
t-value	-0.6963	-10.3936	0.0897	11.4666	0.0030	48

Table 12: Regressing RMSE on Polynomial Orders and Number of paths: Univariate GBM.
Legend: OLS regressions of RMSE, as depicted in figure 10, on the polynomial order and the number of paths simulated. A second order term is added for each independent variable to test the existence of second order effects.

A. Wait mode Estimate:

Variable	$constant$	$poly-ord$	nms	$poly-ord^2$	nms^2	R^2
Estimate	5.1268	-9.5338	-0.5577	3.5819	0.0264	0.8230
Error	7.1061	0.8753	1.2262	0.2958	0.0526	nobs
t-value	0.7215	-10.8919	-0.4548	12.1095	0.5022	48

B. Plant 1 mode Estimate:

Variable	$constant$	$poly-ord$	nms	$poly-ord^2$	nms^2	R^2
Estimate	2.6875	-8.6341	-0.2665	3.2577	0.0149	0.8070
Error	6.9279	0.8534	1.1954	0.2884	0.0513	nobs
t-value	0.3879	-10.1178	-0.2229	11.2965	0.2900	48

C. Plant 2 mode Estimate

Variable	$constant$	$poly-ord$	nms	$poly-ord^2$	nms^2	R^2
Estimate	1.9687	-8.4946	-0.2727	3.2947	0.0150	0.8280
Error	7.0459	0.8679	1.2158	0.2933	0.0522	nobs
t-value	0.2794	-9.7877	-0.2243	11.2339	0.2876	48

Table 13: Regressing RMSE on Polynomial Orders and Number of paths: Bi variate GBM.
Legend: see table 12.

A. Wait mode Estimate:

Variable	$constant$	$poly-ord$	nms	$poly-ord^2$	nms^2	R^2
Estimate	2.7819	-3.4017	-0.8250	1.4531	0.0359	0.5400
Error	8.7975	0.4813	1.6209	0.2168	0.0740	nobs
t-value	0.3162	-7.0684	-0.5090	6.7019	0.4855	48

B. Plant 1 mode Estimate:

Variable	$constant$	$poly-ord$	nms	$poly-ord^2$	nms^2	R^2
Estimate	-0.5376	-2.5915	-0.3687	1.1586	0.0180	0.4770
Error	7.6344	0.4176	1.4066	0.1882	0.0642	nobs
t-value	-0.0704	-6.2054	-0.2621	6.1574	0.2808	48

C. Plant 2 mode Estimate

Variable	$constant$	$poly-ord$	nms	$poly-ord^2$	nms^2	R^2
Estimate	-1.2075	-2.3098	-0.4051	1.1332	0.0198	0.4700
Error	7.5574	0.4134	1.3924	0.1863	0.0636	nobs
t-value	-0.1598	-5.5871	-0.2909	6.0838	0.3114	48

Table 14: Regressing RMSE on Polynomial Orders and Number of paths: Tri-variate GBM. Legend: see table 12.

A. Wait mode Estimate:

Variable	$constant$	$poly-ord$	nms	$poly-ord^2$	nms^2	R^2
Estimate	5.3150	0.1132	-1.0224	-0.0314	0.0237	0.9940
Error	0.7019	0.0977	0.1288	0.0330	0.0059	nobs
t-value	7.5727	1.1577	-7.9391	-0.9500	4.0389	48

B. Plant 1 mode Estimate:

Variable	$constant$	$poly-ord$	nms	$poly-ord^2$	nms^2	R^2
Estimate	-6.9806	-0.1818	-0.0061	0.0845	-0.0230	0.9980
Error	0.4356	0.0607	0.0799	0.0205	0.0036	nobs
t-value	-16.0255	-2.9967	-0.0764	4.1243	-6.3151	48

C. Plant 2 mode Estimate

Variable	$constant$	$poly-ord$	nms	$poly-ord^2$	nms^2	R^2
Estimate	-8.6774	-0.1295	0.1024	0.0482	-0.0287	0.9900
Error	0.9508	0.1324	0.1745	0.0447	0.0080	nobs
t-value	-9.1262	-0.9783	0.5869	1.0780	-3.6067	48

Table 15: Regressing RMSE on Polynomial Orders and Number of paths: GOU 01. Legend: see table 12.

A. Wait mode Estimate:

Variable	$constant$	$poly-ord$	nms	$poly-ord^2$	nms^2	R^2
Estimate	4.9064	-1.4005	-0.9635	0.2076	0.0270	0.8180
Error	4.2111	0.5864	0.7726	0.1982	0.0353	nobs
t-value	1.1651	-2.3881	-1.2470	1.0474	0.7650	48

B. Plant 1 mode Estimate:

Variable	$constant$	$poly-ord$	nms	$poly-ord^2$	nms^2	R^2
Estimate	4.8133	-0.0487	-1.2518	-0.2572	0.0434	0.8180
Error	3.8126	0.5309	0.6995	0.1794	0.0319	nobs
t-value	1.2625	-0.0917	-1.7895	-1.4333	1.3592	48

C. Plant 2 mode Estimate

Variable	$constant$	$poly-ord$	nms	$poly-ord^2$	nms^2	R^2
Estimate	7.0745	-2.2449	-1.5311	0.5760	0.0555	0.9020
Error	2.4169	0.3366	0.4434	0.1137	0.0202	nobs
t-value	2.9271	-6.6699	-3.4528	5.0647	2.7437	48

Table 16: Regressing RMSE on Polynomial Orders and Number of paths: Two Factor Model, Model 2 in (Schwartz, 1997).
Legend: see table 12.

A. Wait mode Estimate:

Variable	$constant$	$poly-ord$	nms	$poly-ord^2$	nms^2	R^2
Estimate	5.3855	-1.9367	-1.0137	0.4016	0.0308	0.8010
Error	4.1886	0.5833	0.7685	0.1971	0.0351	nobs
t-value	1.2857	-3.3203	-1.3190	2.0377	0.8773	48

B. Plant 1 mode Estimate:

Variable	$constant$	$poly-ord$	nms	$poly-ord^2$	nms^2	R^2
Estimate	4.8600	-0.2073	-1.2690	-0.2003	0.0455	0.7870
Error	3.9991	0.5569	0.7337	0.1882	0.0335	nobs
t-value	1.2153	-0.3722	-1.7295	-1.0642	1.3587	48

C. Plant 2 mode Estimate

Variable	$constant$	$poly-ord$	nms	$poly-ord^2$	nms^2	R^2
Estimate	7.9343	-1.8134	-1.7899	0.4324	0.0699	0.8710
Error	2.4790	0.3452	0.4548	0.1167	0.0208	nobs
t-value	3.2006	-5.2529	-3.9352	3.7070	3.3669	48

Table 17: Regressing RMSE on Polynomial Orders and Number of paths: Three Factor Model, Model 3 in (Schwartz, 1997).
Legend: see table 12.

5 Trade off between precision and computational time

In this section we examine the trade off between computational time and accuracy. As shown in the previous section, this trade off is not always convenient. Graphs reported in figure 16 and 17 give a graphic portrayal of this. These graphs have been constructed on the same data used for surface plots and regressions on RMSE reported above. The additional variable considered here is the CPU time which has been reported on the vertical axis as the number of estimates that can be performed in one second, or

$$\left\{ \begin{array}{r} \text{Number of} \\ \text{Estimates} \\ \text{in one second} \end{array} \right\} = \frac{1}{\left\{ \begin{array}{r} \text{CPU time} \\ \text{in seconds} \\ \text{per estimate} \end{array} \right\}}.$$

The same RMSE of the surface plots is reported on the horizontal axis. This setting provides a quite intuitive portrayal of the trade off between accuracy and computational time.

In the univariate GBM case, for a very low order of the polynomial, $M = 2, 3$, increasing the number of paths simply does not affect RMSE. For $4 \leq M \leq 7$ trade off between computational time and accuracy is convenient although less than in other applications reported in extant literature, see for instance (Stentoft, 2004) and (Areal et al., 2007). For $8 \leq M \leq 9$ trade off becomes negative, i.e. a larger number of paths provides worse estimates.

In the bivariate GBM case, the RMSE-CPU trade off is generally unfavorable but for the $M = 5$. To be specific, for $2 \leq M \leq 4$, the increase in the number of paths simulated reduces RMSE only slightly. Instead, for $M = 5$ it is evident a positive trade off between accuracy and speed. Finally, contrary to most of the evidence reported in extant literature and like in the previous case, for very high order of the fitted polynomials RMSE explodes showing a negative trade off. In order to avoid cramming the picture, we did report in panel B of figure 16 an example of this pattern only for $M = 7$, being the results obtained for higher orders of the complete set of polynomials very similar.

In the trivariate GBM case, for low levels of M, $1 \leq M \leq 3$ there is a very slow trade off between precision and speed. For intermediate levels of M, $4 \leq M \leq 6$ trade off is slightly more favorable and curves become almost vertical for a very high number of simulated paths. For $M > 6$, trade off becomes negative.

In model 1 (Schwartz, 1997), as expected from what observed in section 4.2, there is not much difference in time accuracy trade off across different orders of polynomials. Although that is true, almost overlapping curves show a very favorable trade off since they do not bend down asymptotically as, for instance, in the three previous GBM cases.

In model 2 (Schwartz, 1997), instead, trade off follows the same pattern accross different orders of the

polynomial although curves are shifted and clustered on two groups. On the right side of panel B in figure 17, are clustered low orders of the polynomial, $2 \leq M \leq 3$, on the left side, high orders, $6 \leq M \leq 8$. While the curves for low order of the polynomial bend down as if they bunched into a vertical asymptote, high order of the polynomial curves show a constant reduction in RMSE, hence a favorable, although decreasing, speed precision trade off.

In model 3 (Schwartz, 1997), trade off patterns resemble those of the previous one. Although that is true, in this case it is possible to reduce much more RMSE increasing the number of simulated paths for $M > 5$.

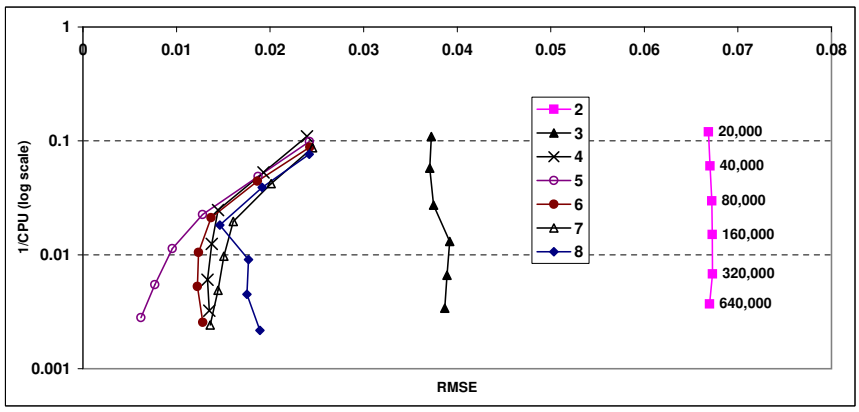

A. GBM 1.

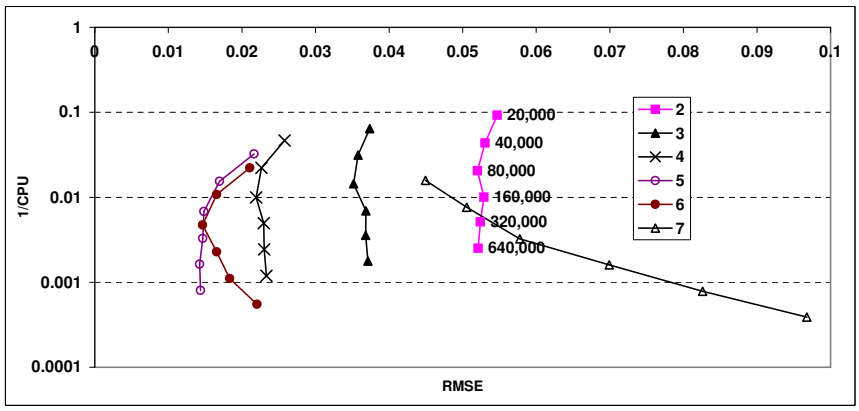

B. GBM 2.

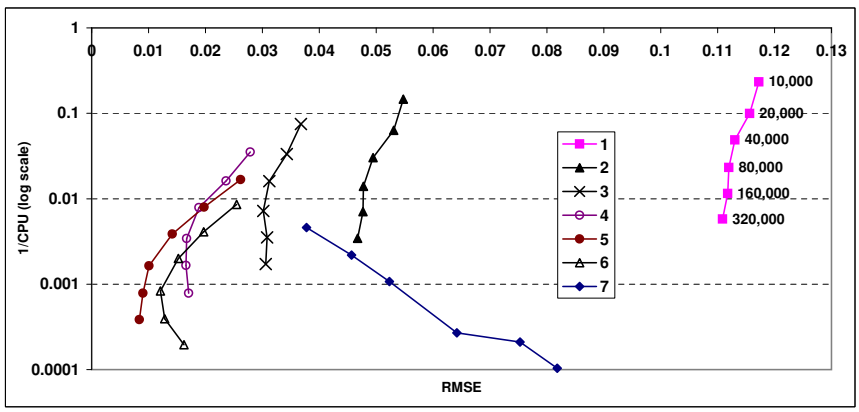

C. GBM 3.

Figure 16: Trade off CPU-RMSE: GBM 1 - 3

Legend: RMSE on the horizontal axis, the same represented in figure 10 and 12, and one divided the CPU time per individual estimate on the vertical axis, i.e. estimates per second. Each curve reports coordinates for the an individual order of the regression polynomial computed for different numbers of paths. See also inside legend.

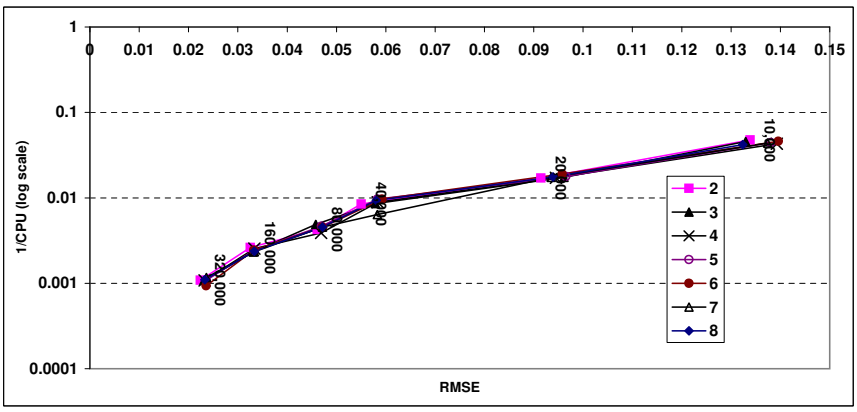

A. Model 1 in (Schwartz, 1997).

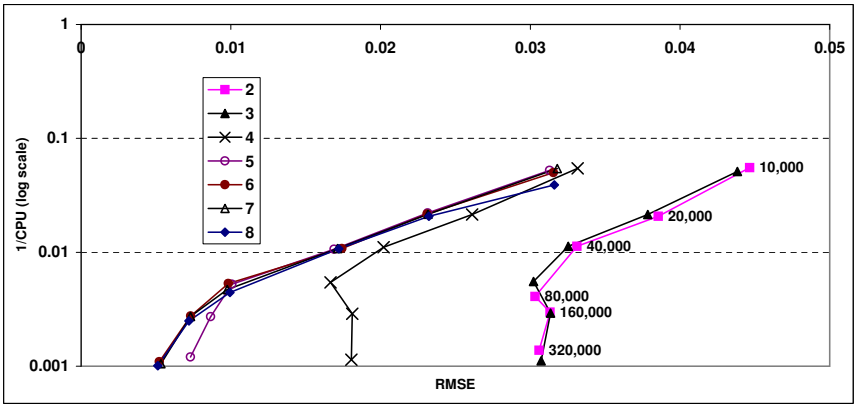

B. Model 2 in (Schwartz, 1997).

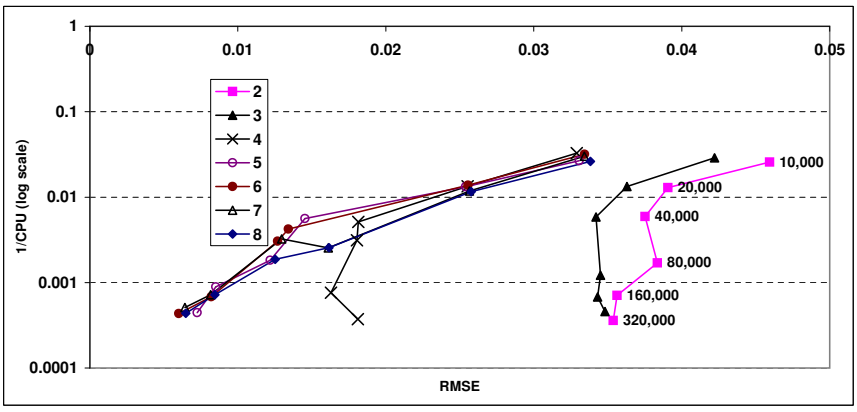

C. Model 3 in (Schwartz, 1997).

Figure 17: Trade off CPU-RMSE: Models 1,2 and 3 in (Schwartz, 1997).
Legend: RMSE on the horizontal axis, the same represented in figure 10 and 13, and one divided the CPU time per individual estimate on the vertical axis, i.e. estimates per second. Each curve reports coordinates for the an individual order of the regression polynomial computed for different numbers of paths. See also inside legend.

6 Inference about LSMC

The aim of this section is to assess the statistical significance of LSMC estimates. In other words, we aim to answer the question: are LSMC estimates of the value functions in the KT model significantly different from the lattice benchmarks which we have constructed in the previous sections ? In order to answer this question we have to consider the actual applicability of inference methods to LSMC results. In extant literature this is left as a open issue. For instance, according to Stentoft, it is not possible to make any statistical inference on LSMC estimates for both American vanilla and high dimensional options since "not much is known about the asymptotics of American prices for LSMC methods" (Stentoft, 2004) page 158.

The conclusion we reach is that generally ordinary inference methods are applicable to LSMC estimates to verify any null hypothesis. To be specific, in our case, the null that LSMC estimates are equal to lattice benchmarks is rejected in most of the cases.

This conclusion would be dismal by itself, but the statistical significance of some tests does not always imply their economic relevance. Therefore, we have analyzed how LSMC estimates distribution behaves in some economically relevant neighborhood of the lattice benchmarks. We conclude that LSMC is quite reliable in providing accurate estimates although these estimates are significantly different from lattice benchmarks.

It is quite common in extant literature about LSMC to replicate the individual estimate a number R of times and then to take the average of these estimates as the final result, see for instance (Stentoft, 2004) or (Glasserman and Yu, 2004). Although, to the best of our knowledge, no author justifies this choice, this may be due to the fact that averaging randomly sampled observations, the central limit theorem holds regardless of the form of the parent distribution, page 105 (Greene, 1994). Hence, LSMC estimates averages are expected to be normally distributed and we can state this ignoring the actual parent distribution which generated them. This, in turn, allows us to take advantage of all the nice properties of a normal distribution. In conclusion, what we analyze below is the average of R replications of LSMC and not the individual estimate as in the sections above.

In order to observe the distribution properties of the averages of R LSMC estimates replications, we have set up the following experiment design. From the evidence provided in section 4.2, we chose the combinations of simulated paths and order of the polynomial which provides the lowest RMSE. It is worth remembering that this statistics just says that for that combination LSMC provides the average estimator which minimizes the sum of the square of the bias and its variance. In other words, we have not proved that LSMC is an unbiased estimator of benchmark values derived through lattice methods. Then we have

replicated these valuations with a different initial seed of the random number generator in order to obtain a number N of different results. As shown above, in section 5, each LSMC valuation of a KT model is rather expensive in terms of both Cpu time and HD space. Hence, N has been kept low due to budget constraints and looping in the random number generator.

Therefore, in order to observe how averages obtained from different R replications are distributed, we have bootstrapped with replacement the N different results extracting a number $B = 500.000$ of batches of different sizes $R_1 = 10$, $R_2 = 100$, representing ideally small and large samples. Next, we have computed the average for each batch and we have analyzed its distribution, see histograms in figures 18-22.

Since one of the main conclusions which emerges from sections above is that LSMC behaves very differently depending on the underlying data generating process, we report this evidence per mode and not per DGP. This allows us to underline differences across DGPs in evaluating each mode value function.

To begin with, from Panels A of tables 18,20,22,24,26, we observe that LSMC averages are generally distributed normally. As a matter of fact both skewness and kurtosis are quite close to normal values. Although that is true, evidence for Two Fm DGP is an exception with a very high kurtosis, expecially for small samples, and rather negative skewness. This is true for all the modes, expecially for out of money and in the money plants and their respective mothballed modes. Skewness is generally negative when it is not significantly different from zero. A possible explanation of this pattern may be devised remembering that in LSMC the sources of errors are the Monte Carlo simulation itself and the suboptimality of the strategy approximated in the Bellman Dynamic Programming scheme. Possibly, the errors produced by Monte Carlo simulation are symmetric around the mean estimate. Instead, those produced by following a suboptimal strategy in a dynamic optimization are skewed negatively. In conclusion, these distribution confirm that in most cases LSMC errors are actually Gaussians as (Clement et al., 2002) proved.

Moreover, from the same Panel A mentioned above, we observe that average LSMC estimates are generally lower than their respective lattice benchmark. Two factor and GOU DGPs present notable exceptions for some modes. Namely, for wait mode estimates under a Two Fm DGP, lattice benchmarks fall almost in the middle of the distribution both for small and large samples. The same is true for plant 2, with in the money optionality, under a GOU DGP. In conclusion, although with the exceptions above, it is clear that LSMC produces biased low estimates, hence distributions in figures 18-22 and statistics in Panels A of tables 18,20,22,24,26 are a graphic portrayal of proposition 1 page 124 (Longstaff and Schwartz, 2001): LSMC is asmptotically biased low. As a matter of fact, lattice benchmarks are far in the upper tail of the LSMC valuations distributions, when they are not greater than the maximum average estimate obtained.

Finally, as the sample size increases, we observe that while the point estimate of the value function remains almost the same, its volatility decreases considerably. In other words, this shows convergence in mean square of the average LSMC valuation which, in turn, implies convergence in probability. This does not mean necessarily that proposition 2 page 125 (Longstaff and Schwartz, 2001) is proved. As a matter of fact, distributions converge to a spike centered on a biased low estimate as empirical distribution functions reported in figures 18-22 and boostrapped confidence intervals constructed below show.

In order to assess whether ordinary inference methods are applicable to LSMC results, we start considering as an example one individual average result, see panel B in tables 18,20,22,24,26, and apply to it one sided test under the null $H_0 : \theta_{lsmc} = \theta_{latt}$, versus the alternative $H_a : \theta_{lsmc} < \theta_{latt}$ when the result obtained through LSMC is lower than the lattice one or $H_a : \theta_{lsmc} > \theta_{latt}$ when the LSMC estimate is higher. These are the cases any practitioner would confront, having estimated a KT model $R_1 = 10$ or $R_2 = 100$ times and having averaged these results. The question is: is it appropriate to adopt ordinary inference methods and consider, for instance, the pivotal quantity distributed as a Student $t(R_i - 1)$ $i = 1, 2$?

To address this research question we rely on three different results, following (Hodrick, 1992) table 2. To begin with, we construct the distribution of the pivotal quantity under the null. This is achieved simply subtracting the average accross the B batches of size R_i results and adding back the lattice benchmarks. Then, we compute pivotal quantities $\Phi = \sqrt{R_i} \cdot \frac{\theta_{lsmc} - \theta_{latt}}{\sigma_{lsmc}}$ $\forall i = 1, 2$. Next, we analyze their distribution in three different ways, see tables 19,21,23,25,27, panels A, B and C.

To begin with, we compute most relevant quantiles, see Panels A in the mentioned tables, and compare them with $t(R_i - 1)$ for $R_1 = 10$ and $R_2 = 100$.[27] Empirical quantiles are generally quite close to those of the tabulated Student functions. This is generally true with the exception of results derived under a Two Fm DGP. For this stochastic process, empirical quantiles are rather different from tabulated ones.

Next, we compute the empirical sizes that can be observed under the null counting cases in which empirical pivotal quantitites are lower (higher) than nominal quantiles for left (right) tail tests, see Panels B in the mentioned tables. In this case too, empirical sizes are remarkably close to the corresponding nominal ones. Even in the case of Two Fm DGP, although to a lesser extent, empirical sizes are not too much far from the nominal ones.

Finally, we compute the empirical power of these tests counting the fraction of the experiments which fail to exceed the empirical critical value when the data are generated under the alternative, i.e. the pivotal quantity distributions obtained from the LSMC estimates, see Panels C in the mentioned tables. Obviously,

[27] We have not considered the normal distribution quantiles since they are generally much more different than $t(100-1)$ from the empirical ones.

these results depend on how far the alternative is from the null. Hence, results vary considerably depending on the mode. For all DGPs, wait mode results show a much higher error rate than the remaining ones. As mentioned, this may be due to the fact that estimates obtained are much closer to lattice benchmarks. Another feature of this evidence is that error rates decrease with the size of the sample R, indicating consistency, and that all the tests are unbiased, i.e. $(1-\beta) > \alpha$. GOU results for all modes show a quite high error rate due to the fact that in that case LSMC estimates are close to the lattice benchmarks. However, in most cases, error rate is nil and empirical power of these tests is one.

In conclusion, being empirical quantiles and sizes of the simple one tailed tests considered quite close to nominal ones, and being the power of these test quite high, we can conclude that it is appropriate to apply classic inference methods to LSMC estimates. Moreover, from the empirical power function evaluated at $\alpha = 5\%$ we can reject the null of LSMC estimates being equal to lattice benchmarks in most of the cases.

These results would be disappointing by themselves. Although that is true, the previous bootstrapping exercise provides us a way to study how many averaged LSMC estimates are entailed within some economically significant interval around their respective benchmarks. In order to check this specific property, we have constructed some simmetric intervals around the benchmark increasing and decreasing them for some percentages most suitable to describe empirical distributions shown above. Next, we have computed the relative frequency of the B bootstrapped experiments falling in that interval around the lattice benchmarks. For a similar procedure see chapter 25 in (Efron and Tibshirani,1993). In this context, this approach is justified by its applicability to the generality of the cases in which average LSMC estimates distributions are sometimes not even close to normal, preventing any construction of classical intervals based on the normal distribution sufficient statistics. Results are reported in tables 28-33. In this case, results have been organized per DGP process and not per mode. As a matter of fact, we aim to show that LSMC can provide reliable estimates for all the modes value functions simultaneously given an underlying DGP.

Empirical confidence intervals reported in tables 28-33 share some common features. Firstly, although not statistically significant as proved in the paragraphs above, LSMC estimates are definetly reliable: in most cases, close to 100% cases entailed in very narrow confidence intervals. These range between a minimum of $\pm.5\%$ for Two Factor model estimates and a maximum of $\pm 2.0\%$ for Trivariate GBM ones.

Secondly, as intervals shrink below the bias level, confidence levels fall abruptly. This is true with no exception of DGP and mode, although it is not observed in some cases since the simmetric intervals adopted are too coarse to single out these effect for some modes. For instance, in the Two Factor model estimates, this effect can be clearly observed for every but the wait to invest mode.

Thirdly, as the number of replications R increases, the distribution becomes less volatile. Hence, if estimates bias is less than the confidence interval, more observations are entailed in it. Else, the whole distribution shifts away from the benchmark and confidence level falls abruptly.

Fourthly, generally simmetric intervals provide different confidence levels for in the money and out of money plants. To be specific, estimates for in the money plants are more reliable – have higher probability – than out of money ones. Wait modes estimates, instead, generally follow in the money plants ones.

In conclusion, in this section we have shown that classic inference statistics is applicable to verify unbiasedness of LSMC estimates. In applying LSMC to the KT model, this provides significantly different estimates of the various modes value functions. Although these estimates are statistically different, they are economically significant falling in very close neighborhoods of the lattice benchmarks, never more than $\pm 2\%$. Being small sample estimates, $R = 10$, more volatile that large ones, $R = 100$, they are less reliable. Although that is true, when the interval chosen is very small it could be completely unreliable even for a large number of replications being the whole distribution shifted away – biased low – with respect to the lattice benchmarks.

Panel A: all experiments statistics							Panel B: one experiment example			
DGP	boot.ed	LSMC valuation					LSMC valuation		Pivotal	Nominal
latt.bench.	sample	E()	stdev()	Skewness	Kurtosis	Emp. Prob.	E()	stdev()	quantity	confidence
GBM 1	10	129.2833	0.1767	0.0117	2.9947	99.873%	129.2381	0.5226	-3.5196	0.27709%
129.8198	100	129.2836	0.0558	-0.0006	2.9972	100.000%	129.2610	0.4936	-11.3209	0.00000%
GBM 2	10	209.2701	0.6802	-0.0839	3.0991	99.989%	210.6085	2.2143	-1.6222	6.79116%
211.7444	100	209.2704	0.2152	-0.0247	3.0047	100.000%	209.5098	1.8344	-12.1815	0.00000%
GBM 3	10	211.5564	0.4529	-0.0184	3.0139	99.727%	211.9036	1.2825	-2.2267	2.50611%
212.8066	100	211.5553	0.1434	-0.0056	2.9999	100.000%	211.7200	1.5342	-7.0833	0.00000%
GOU 1	10	4.0939	0.0297	-0.0140	3.0234	86.946%	4.0895	0.0664	1.3751	9.95546%
4.0606	100	4.0939	0.0094	-0.0036	3.0145	99.977%	4.0941	0.0971	3.4497	0.02807%
Two Fm	10	282.9364	0.5534	-0.7755	6.2164	54.246%	282.8343	1.5485	-0.3569	36.43019%
283.0091	100	282.9368	0.1753	-0.2463	3.3357	65.326%	282.9586	1.6675	-0.3030	38.09355%
Three Fm	10	246.0393	0.4571	0.0111	2.9826	84.448%	247.0771	1.3195	1.3767	90.06747%
246.5027	100	246.0396	0.1450	0.0089	2.9948	99.927%	246.1414	1.5283	-2.3638	0.90440%

Table 18: Small and Large Sample examples of LSMC estimates: Wait Mode

Panel A: Empirical quantiles of the t-stat/z-stat distributions								
	$\Pr(t < q_i)$	1%	5%	10%	50%	90%	95%	99%
	$t(10-1, q_i)$	-2.8214	-1.8331	-1.3830	0.0000	1.3830	1.8331	2.8214
	$t(100-1, q_i)$	-2.3646	-1.6604	-1.2902	0.0000	1.2902	1.6604	2.3646
GBM 1	10	-2.8461	-1.8459	-1.3916	-0.0022	1.3763	1.8260	2.8090
	100	-2.3727	-1.6635	-1.2904	-0.0009	1.2881	1.6520	2.3470
GBM 2	10	-2.7250	-1.7782	-1.3469	0.0109	1.4241	1.8928	2.9050
	100	-2.3238	-1.6350	-1.2750	0.0062	1.3108	1.6875	2.4121
GBM 3	10	-2.7860	-1.8089	-1.3705	0.0026	1.4001	1.8506	2.8372
	100	-2.3580	-1.6567	-1.2897	0.0014	1.2950	1.6678	2.3777
GOU 1	10	-2.7780	-1.8188	-1.3760	0.0017	1.3901	1.8393	2.8350
	100	-2.3520	-1.6534	-1.2862	0.0004	1.2947	1.6664	2.3784
Two Fm	10	-2.7396	-1.7629	-1.3241	0.0379	1.4366	1.8894	2.8874
	100	-2.1878	-1.5437	-1.2141	0.0368	1.3856	1.7642	2.4884
Three Fm	10	-2.8957	-1.8562	-1.3932	-0.0013	1.3687	1.8115	2.7855
	100	-2.3683	-1.6649	-1.2916	-0.0027	1.2914	1.6600	2.3563

Panel B: Empirical sizes for nominal quantiles				
	sample	10%	5%	1%
GBM 1	10	10.119%	5.100%	1.041%
	100	10.160%	5.204%	1.123%
GBM 2	10	9.438%	4.572%	0.851%
	100	9.886%	4.901%	0.994%
GBM 3	10	9.809%	4.812%	0.942%
	100	10.132%	5.124%	1.086%
GOU 1	10	10.110%	5.050%	1.021%
	100	10.238%	5.227%	1.141%
Two Fm	10	9.120%	4.465%	0.875%
	100	8.769%	3.973%	0.684%
Three Fm	10	10.156%	5.188%	1.124%
	100	10.172%	5.197%	1.122%

Panel C: Type II error rates for $\alpha = 5\%$			
	sample	β	q_α
GBM 1	10	12.903%	-1.846
	100	0.000%	-1.664
GBM 2	10	3.150%	-1.778
	100	0.000%	-1.635
GBM 3	10	17.368%	-1.809
	100	0.000%	-1.657
GOU 1	10	72.647%	1.839
	100	3.147%	1.666
Two Fm	10	93.449%	-1.763
	100	88.340%	-1.544
Three Fm	10	76.742%	-1.856
	100	6.452%	-1.665

Table 19: Empirical Quantiles and Sizes and Power of the tests: Wait Mode

Panel A: all experiments statistics						
DGP	boot.ed	LSMC valuation				
latt.bench.	sample	E()	stdev()	Skewness	Kurtosis	Emp. Prob.
GBM 1	10	304.3076	0.1939	-0.0243	3.0122	100.000%
306.6760	100	304.3076	0.0612	-0.0168	2.9954	100.000%
GBM 2	10	466.1684	0.8936	-0.3110	3.2942	100.000%
472.5055	100	466.1687	0.2825	-0.0972	3.0332	100.000%
GBM 3	10	477.5856	0.4775	-0.0081	3.0138	100.000%
483.9836	100	477.5859	0.1509	-0.0047	2.9926	100.000%
GOU 1	10	180.0322	0.0012	-0.0176	2.9944	70.428%
180.0329	100	180.0322	0.0004	-0.0016	3.0015	95.680%
Two Fm	10	516.3647	0.6850	-1.9213	13.9502	96.428%
517.4022	100	516.3641	0.2166	-0.5998	4.0580	100.000%
Three Fm	10	465.5974	0.4924	-0.0045	2.9874	99.973%
467.3046	100	465.5978	0.1558	0.0018	2.9988	100.000%

Panel B: one experiment example			
LSMC valuation		Pivotal	Nominal
E()	stdev()	quantity	confidence
304.4541	0.3287	-21.3766	0.00000%
304.3754	0.5674	-40.5434	0.00000%
465.8010	2.3881	-8.8781	0.00023%
465.6654	2.9905	-22.8729	0.00000%
477.2324	1.4232	-15.0003	0.00000%
477.6580	1.4652	-43.1729	0.00000%
180.0330	0.0024	0.1298	55.03628%
180.0322	0.0041	-1.6388	5.06278%
517.0723	1.2767	-0.8171	21.64517%
516.4825	1.8860	-4.8764	0.00005%
465.7229	1.4742	-3.3929	0.34265%
465.6025	1.5764	-10.7974	0.00000%

Table 20: Small and Large Sample examples of LSMC estimates: Plant 1 Mode

Panel A: Empirical quantiles of the t-stat/z-stat distributions								
	$\Pr(t < q_i)$	1%	5%	10%	50%	90%	95%	99%
	$t(10-1, q_i)$	-2.8214	-1.8331	-1.3830	0.0000	1.3830	1.8331	2.8214
	$t(100-1, q_i)$	-2.3646	-1.6604	-1.2902	0.0000	1.2902	1.6604	2.3646
GBM 1	10	-2.7736	-1.8104	-1.3693	0.0054	1.3974	1.8520	2.8469
	100	-2.3578	-1.6585	-1.2852	0.0036	1.2926	1.6654	2.3774
GBM 2	10	-2.3655	-1.5934	-1.2277	0.0529	1.5996	2.1167	3.2488
	100	-2.2004	-1.5696	-1.2290	0.0174	1.3679	1.7764	2.5669
GBM 3	10	-2.8007	-1.8229	-1.3768	0.0023	1.3916	1.8445	2.8376
	100	-2.3570	-1.6563	-1.2882	0.0006	1.2928	1.6659	2.3602
GOU 1	10	-2.8053	-1.8208	-1.3756	0.0039	1.3963	1.8493	2.8600
	100	-2.3499	-1.6516	-1.2857	0.0015	1.2934	1.6623	2.3759
Two Fm	10	-2.6147	-1.6864	-1.2640	0.0703	1.4978	1.9641	3.0021
	100	-2.0829	-1.4488	-1.1441	0.0948	1.4710	1.8542	2.5904
Three Fm	10	-2.8398	-1.8360	-1.3794	0.0004	1.3852	1.8417	2.8442
	100	-2.3632	-1.6573	-1.2889	-0.0010	1.2923	1.6650	2.3758

Panel B: Empirical sizes for nominal quantiles				
	sample	10%	5%	1%
GBM 1	10	9.805%	4.814%	0.923%
	100	10.058%	5.129%	1.082%
GBM 2	10	7.513%	3.072%	0.386%
	100	9.043%	4.218%	0.693%
GBM 3	10	9.906%	4.921%	0.969%
	100	10.121%	5.118%	1.084%
GOU 1	10	9.893%	4.898%	0.975%
	100	10.075%	5.069%	1.062%
Two Fm	10	8.240%	3.909%	0.690%
	100	7.413%	3.097%	0.515%
Three Fm	10	9.946%	5.024%	1.031%
	100	10.128%	5.125%	1.093%

Panel C: Type II error rates for $\alpha = 5\%$			
	sample	β	q_α
GBM 1	10	0.000%	-1.810
	100	0.000%	-1.658
GBM 2	10	0.000%	-1.593
	100	0.000%	-1.570
GBM 3	10	0.000%	-1.823
	100	0.000%	-1.656
GOU 1	10	87.421%	-1.821
	100	47.567%	-1.652
Two Fm	10	45.274%	-1.686
	100	0.001%	-1.449
Three Fm	10	5.806%	-1.836
	100	0.000%	-1.657

Table 21: Empirical Quantiles and Sizes and Power of the tests: Plant 1 Mode

Panel A: all experiments statistics							Panel B: one experiment example			
DGP	boot.ed	LSMC valuation					LSMC valuation		Pivotal	Nominal
latt.bench.	sample	E()	stdev()	Skewness	Kurtosis	Emp. Prob.	E()	stdev()	quantity	confidence
GBM 1	10	525.7168	0.1843	-0.0009	2.9953	100.000%	525.7149	0.7915	-18.8706	0.00000%
530.4382	100	525.7168	0.0582	0.0009	2.9833	100.000%	525.7869	0.6043	-76.9667	0.00000%
GBM 2	10	785.2514	0.9839	-0.3865	3.3882	100.000%	784.9360	2.2602	-10.1629	0.00007%
792.1999	100	785.2512	0.3102	-0.1208	3.0385	100.000%	785.3788	2.6464	-25.7753	0.00000%
GBM 3	10	801.5168	0.4904	-0.0057	3.0105	100.000%	801.3396	1.2058	-19.2261	0.00000%
808.6709	100	801.5166	0.1550	0.0002	2.9972	100.000%	801.5752	1.5785	-44.9507	0.00000%
GOU 1	10	463.2708	0.0009	0.0041	2.9995	54.317%	463.2722	0.0018	2.4439	98.26924%
463.2709	100	463.2708	0.0003	-0.0026	3.0098	62.885%	463.2711	0.0028	0.6645	74.68137%
Two Fm	10	805.5491	0.8968	-2.4648	17.4737	99.836%	805.5813	2.3171	-2.6035	1.31655%
807.4890	100	805.5490	0.2835	-0.7855	4.4487	100.000%	805.3078	2.2756	-9.5849	0.00000%
Three Fm	10	738.7844	0.5005	0.0072	2.9821	100.000%	738.5269	1.3566	-9.7542	0.00010%
742.7113	100	738.7845	0.1584	-0.0030	2.9914	100.000%	738.8773	1.4364	-26.6923	0.00000%

Table 22: Small and Large Sample examples of LSMC estimates: Plant 2 Mode

Panel A: Empirical quantiles of the t-stat/z-stat distributions								
	$\Pr(t < q_i)$	1%	5%	10%	50%	90%	95%	99%
	$t(10-1, q_i)$	-2.8214	-1.8331	-1.3830	0.0000	1.3830	1.8331	2.8214
	$t(100-1, q_i)$	-2.3646	-1.6604	-1.2902	0.0000	1.2902	1.6604	2.3646
GBM 1	10	-2.8288	-1.8280	-1.3803	-0.0001	1.3865	1.8392	2.8319
	100	-2.3617	-1.6550	-1.2873	-0.0015	1.2913	1.6577	2.3566
GBM 2	10	-2.2636	-1.5432	-1.1949	0.0697	1.6659	2.1962	3.3637
	100	-2.1555	-1.5467	-1.2137	0.0195	1.3856	1.8025	2.6109
GBM 3	10	-2.8146	-1.8261	-1.3752	0.0001	1.3855	1.8377	2.8313
	100	-2.3633	-1.6569	-1.2879	0.0000	1.2917	1.6617	2.3715
GOU 1	10	-2.8582	-1.8520	-1.3912	-0.0027	1.3756	1.8204	2.7897
	100	-2.3797	-1.6609	-1.2922	0.0008	1.2845	1.6531	2.3496
Two Fm	10	-2.2705	-1.5163	-1.1542	0.1211	1.6957	2.2202	3.3563
	100	-1.9490	-1.3774	-1.0984	0.1291	1.5595	1.9762	2.7812
Three Fm	10	-2.8565	-1.8454	-1.3873	-0.0009	1.3768	1.8245	2.8142
	100	-2.3718	-1.6681	-1.2933	-0.0005	1.2894	1.6609	2.3556

Panel B: Empirical sizes for nominal quantiles				
	sample	10%	5%	1%
GBM 1	10	9.962%	4.961%	1.011%
	100	10.104%	5.104%	1.086%
GBM 2	10	6.945%	2.643%	0.295%
	100	8.767%	3.998%	0.579%
GBM 3	10	9.879%	4.939%	0.988%
	100	10.108%	5.117%	1.097%
GOU 1	10	10.116%	5.147%	1.064%
	100	10.185%	5.155%	1.143%
Two Fm	10	6.473%	2.606%	0.309%
	100	6.420%	2.406%	0.317%
Three Fm	10	10.060%	5.099%	1.058%
	100	10.206%	5.236%	1.115%

Panel C: Type II error rates for $\alpha = 5\%$			
	sample	β	q_α
GBM 1	10	0.000%	-1.828
	100	0.000%	-1.655
GBM 2	10	0.000%	-1.543
	100	0.000%	-1.547
GBM 3	10	0.000%	-1.826
	100	0.000%	-1.657
GOU 1	10	93.923%	-1.852
	100	90.622%	-1.661
Two Fm	10	9.605%	-1.516
	100	0.000%	-1.377
Three Fm	10	0.000%	-1.845
	100	0.000%	-1.668

Table 23: Empirical Quantiles and Sizes and Power of the tests: Plant 2 Mode

Panel A: all experiments statistics						
DGP	boot.ed	LSMC valuation				
latt.bench.	sample	E()	stdev()	Skewness	Kurtosis	Emp. Prob.
GBM 1	10	301.6550	0.1937	-0.0218	3.0101	100.000%
304.0224	100	301.6548	0.0612	-0.0098	3.0010	100.000%
GBM 2	10	463.0764	0.8927	-0.3033	3.2917	100.000%
469.4297	100	463.0778	0.2823	-0.1031	3.0305	100.000%
GBM 3	10	474.4700	0.4770	-0.0108	3.0238	100.000%
480.8921	100	474.4706	0.1508	0.0021	3.0036	100.000%
GOU 1	10	165.4120	0.0029	-0.0084	2.9795	100.000%
165.3974	100	165.4120	0.0009	-0.0053	3.0143	100.000%
Two Fm	10	514.2161	0.6885	-1.9254	13.8027	96.344%
515.2518	100	514.2183	0.2163	-0.5997	4.0550	100.000%
Three Fm	10	463.5743	0.4929	-0.0011	2.9729	99.975%
465.2815	100	463.5734	0.1556	-0.0033	3.0125	100.000%

Panel B: one experiment example			
LSMC valuation		Pivotal	Nominal
E()	stdev()	quantity	confidence
301.4179	0.7650	-10.7663	0.00004%
301.6881	0.6227	-37.4836	0.00000%
462.9786	2.9180	-6.9913	0.00188%
462.7542	3.2586	-20.4861	0.00000%
474.6356	0.9500	-20.8264	0.00000%
474.3781	1.3930	-46.7629	0.00000%
165.4087	0.0109	3.2715	0.42044%
165.4110	0.0092	14.8190	0.00000%
514.8076	1.2238	-1.1479	13.88563%
514.7340	1.9735	-2.6236	0.43498%
463.2164	1.3695	-4.7685	0.03794%
463.1720	1.5752	-13.3921	0.00000%

Table 24: Small and Large Sample examples of LSMC estimates: Mothballed 1 Mode

Panel A: Empirical quantiles of the t-stat/z-stat distributions								
	$\Pr(t < q_i)$	1%	5%	10%	50%	90%	95%	99%
	$t(10-1, q_i)$	-2.8214	-1.8331	-1.3830	0.0000	1.3830	1.8331	2.8214
	$t(100-1, q_i)$	-2.3646	-1.6604	-1.2902	0.0000	1.2902	1.6604	2.3646
GBM 1	10	-2.7696	-1.8085	-1.3677	0.0032	1.3974	1.8559	2.8569
	100	-2.3494	-1.6529	-1.2815	0.0021	1.2960	1.6676	2.3730
GBM 2	10	-2.3624	-1.5881	-1.2243	0.0516	1.6053	2.1202	3.2472
	100	-2.2014	-1.5683	-1.2281	0.0152	1.3684	1.7740	2.5585
GBM 3	10	-2.7914	-1.8152	-1.3758	0.0000	1.3893	1.8408	2.8242
	100	-2.3502	-1.6553	-1.2890	-0.0006	1.2906	1.6625	2.3775
GOU 1	10	-2.8002	-1.8165	-1.3684	0.0011	1.3956	1.8582	2.8741
	100	-2.3726	-1.6579	-1.2864	-0.0012	1.2906	1.6637	2.3749
Two Fm	10	-2.6064	-1.6829	-1.2642	0.0694	1.5043	1.9707	2.9988
	100	-2.0790	-1.4489	-1.1451	0.0949	1.4683	1.8544	2.5878
Three Fm	10	-2.8368	-1.8298	-1.3821	0.0014	1.3852	1.8412	2.8349
	100	-2.3649	-1.6557	-1.2886	0.0007	1.2878	1.6593	2.3703

Panel B: Empirical sizes for nominal quantiles				
	sample	10%	5%	1%
GBM 1	10	9.770%	4.790%	0.922%
	100	9.999%	5.081%	1.062%
GBM 2	10	7.435%	3.031%	0.381%
	100	9.036%	4.204%	0.693%
GBM 3	10	9.899%	4.858%	0.952%
	100	10.137%	5.112%	1.064%
GOU 1	10	10.177%	5.193%	1.089%
	100	10.141%	5.194%	1.126%
Two Fm	10	8.253%	3.868%	0.703%
	100	7.416%	3.093%	0.490%
Three Fm	10	9.987%	4.972%	1.024%
	100	10.129%	5.107%	1.098%

Panel C: Type II error rates for $\alpha = 5\%$			
	sample	β	q_α
GBM 1	10	0.000%	-1.808
	100	0.000%	-1.653
GBM 2	10	0.000%	-1.588
	100	0.000%	-1.568
GBM 3	10	0.000%	-1.815
	100	0.000%	-1.655
GOU 1	10	0.145%	1.858
	100	0.000%	1.664
Two Fm	10	45.384%	-1.683
	100	0.001%	-1.449
Three Fm	10	5.769%	-1.830
	100	0.000%	-1.656

Table 25: Empirical Quantiles and Sizes and Power of the tests: Mothballed 1 Mode

Panel A: all experiments statistics							Panel B: one experiment example			
DGP	boot.ed	LSMC valuation					LSMC valuation		Pivotal	Nominal
latt.bench.	sample	E()	stdev()	Skewness	Kurtosis	Emp. Prob.	E()	stdev()	quantity	confidence
GBM 1	10	516.2512	0.1846	-0.0014	2.9878	100.000%	516.3350	0.7285	-20.1591	0.00000%
520.9793	100	516.2509	0.0583	0.0034	2.9905	100.000%	516.2241	0.5836	-81.4867	0.00000%
GBM 2	10	775.6372	0.9832	-0.3849	3.3941	100.000%	775.1576	4.5953	-5.1220	0.02247%
782.6008	100	775.6381	0.3116	-0.1227	3.0390	100.000%	775.0893	4.0733	-18.4408	0.00000%
GBM 3	10	791.8971	0.4898	-0.0110	3.0139	100.000%	792.3069	1.3808	-15.5642	0.00000%
799.1029	100	791.8969	0.1553	-0.0014	3.0031	100.000%	791.8777	1.6501	-43.7862	0.00000%
GOU 1	10	172.8615	0.0105	0.0042	2.9951	98.734%	172.8601	0.0461	1.5144	8.04396%
172.8380	100	172.8615	0.0033	0.0008	2.9997	100.000%	172.8545	0.0301	5.4872	0.00000%
Two Fm	10	797.1181	0.9029	-2.4846	17.4621	99.800%	797.1214	1.8721	-3.2493	0.43652%
799.0450	100	797.1197	0.2829	-0.7724	4.4230	100.000%	796.5099	5.9434	-4.2655	0.00100%
Three Fm	10	730.6185	0.5001	0.0023	2.9842	100.000%	729.9081	1.7573	-8.2797	0.00044%
734.5092	100	730.6177	0.1583	-0.0003	3.0012	100.000%	730.6016	1.7360	-22.5089	0.00000%

Table 26: Small and Large Sample examples of LSMC estimates: Mothballed 2 Mode

Panel A: Empirical quantiles of the t-stat/z-stat distributions								
	$\Pr(t < q_i)$	1%	5%	10%	50%	90%	95%	99%
	$t(10-1, q_i)$	-2.8214	-1.8331	-1.3830	0.0000	1.3830	1.8331	2.8214
	$t(100-1, q_i)$	-2.3646	-1.6604	-1.2902	0.0000	1.2902	1.6604	2.3646
GBM 1	10	-2.8002	-1.8245	-1.3822	-0.0003	1.3858	1.8393	2.8220
	100	-2.3502	-1.6605	-1.2916	-0.0001	1.2911	1.6601	2.3689
GBM 2	10	-2.2716	-1.5416	-1.1929	0.0676	1.6660	2.1963	3.3540
	100	-2.1605	-1.5528	-1.2183	0.0209	1.3917	1.8053	2.6227
GBM 3	10	-2.8132	-1.8252	-1.3743	0.0011	1.3831	1.8362	2.8394
	100	-2.3671	-1.6576	-1.2881	-0.0005	1.2936	1.6673	2.3678
GOU 1	10	-2.8282	-1.8434	-1.3848	-0.0007	1.3827	1.8317	2.8085
	100	-2.3638	-1.6560	-1.2907	-0.0007	1.2875	1.6590	2.3641
Two Fm	10	-2.2735	-1.5131	-1.1532	0.1230	1.6980	2.2212	3.3698
	100	-1.9515	-1.3806	-1.0989	0.1287	1.5575	1.9748	2.7796
Three Fm	10	-2.8534	-1.8435	-1.3877	-0.0001	1.3752	1.8260	2.8182
	100	-2.3666	-1.6651	-1.2943	0.0009	1.2897	1.6540	2.3616

Panel B: Empirical sizes for nominal quantiles				
	sample	10%	5%	1%
GBM 1	10	9.989%	4.933%	0.968%
	100	10.175%	5.158%	1.062%
GBM 2	10	6.928%	2.663%	0.300%
	100	8.860%	4.047%	0.600%
GBM 3	10	9.870%	4.940%	0.984%
	100	10.114%	5.133%	1.108%
GOU 1	10	9.996%	4.986%	0.979%
	100	10.109%	5.146%	1.101%
Two Fm	10	6.455%	2.581%	0.322%
	100	6.452%	2.423%	0.299%
Three Fm	10	10.069%	5.086%	1.048%
	100	10.224%	5.210%	1.110%

Panel C: Type II error rates for $\alpha = 5\%$			
	sample	β	q_α
GBM 1	10	0.000%	-1.825
	100	0.000%	-1.661
GBM 2	10	0.000%	-1.542
	100	0.000%	-1.553
GBM 3	10	0.000%	-1.825
	100	0.000%	-1.658
GOU 1	10	33.781%	1.832
	100	0.000%	1.659
Two Fm	10	9.997%	-1.513
	100	0.000%	-1.381
Three Fm	10	0.000%	-1.844
	100	0.000%	-1.665

Table 27: Empirical Quantiles and Sizes and Power of the tests: Mothballed 2 Mode

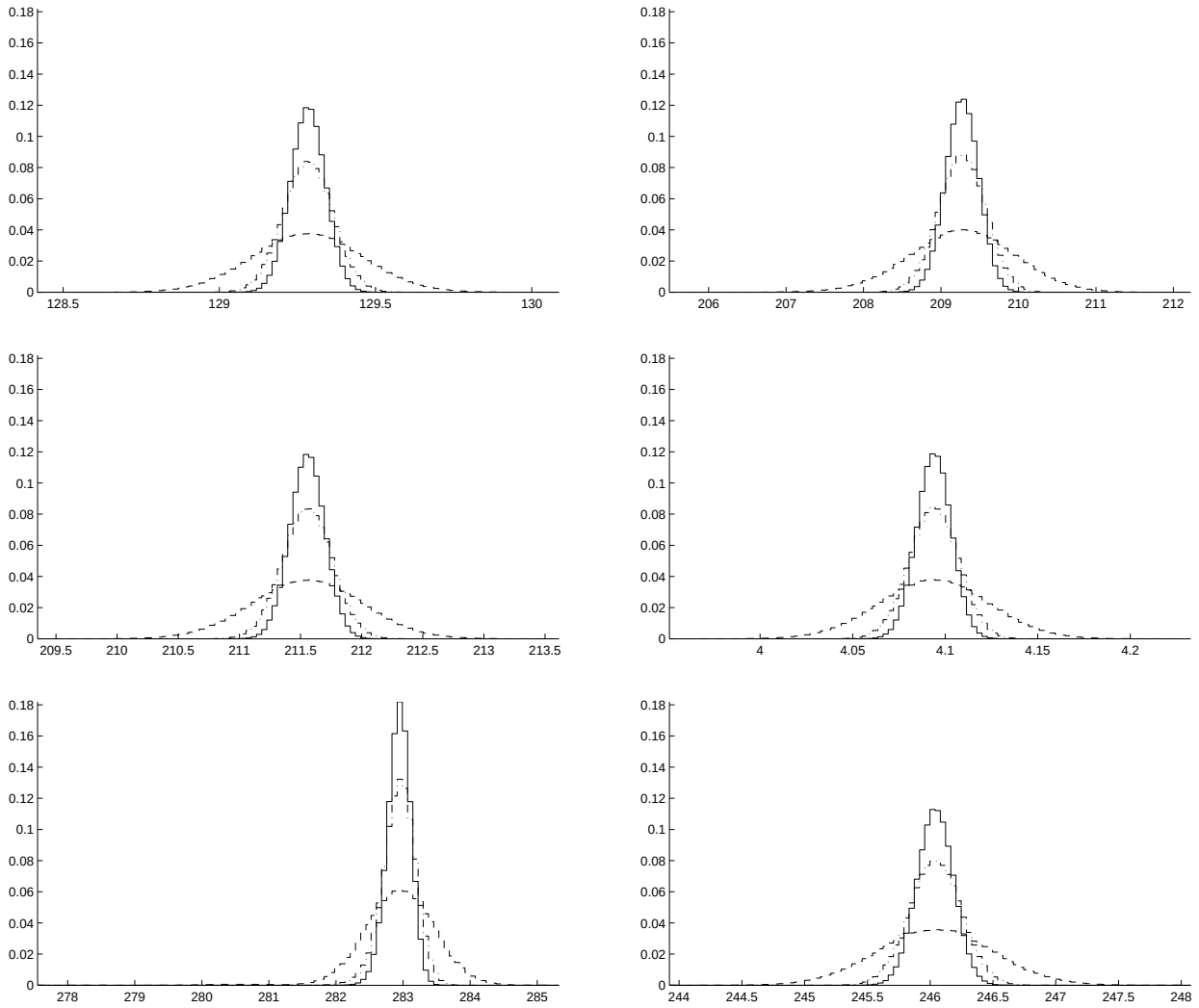

Figure 18: Distributions of Value Functions LSMC Estimates: All DGPs, Wait mode.
Legend: step functions represent the distributions of $B = 500.00$ experiments of the average estimate for a number of replications of $R = 10, 50, 100$ for the DGPs studied, beginning from the left hand upper corner GBM 1, GBM 2, GBM 3, Model 1, 2, and 3 in (Schwartz, 1997). Distribution with higher variance represents average estimates for $R = 10$, the one with lowest variance represents average estimates for $R = 100$.

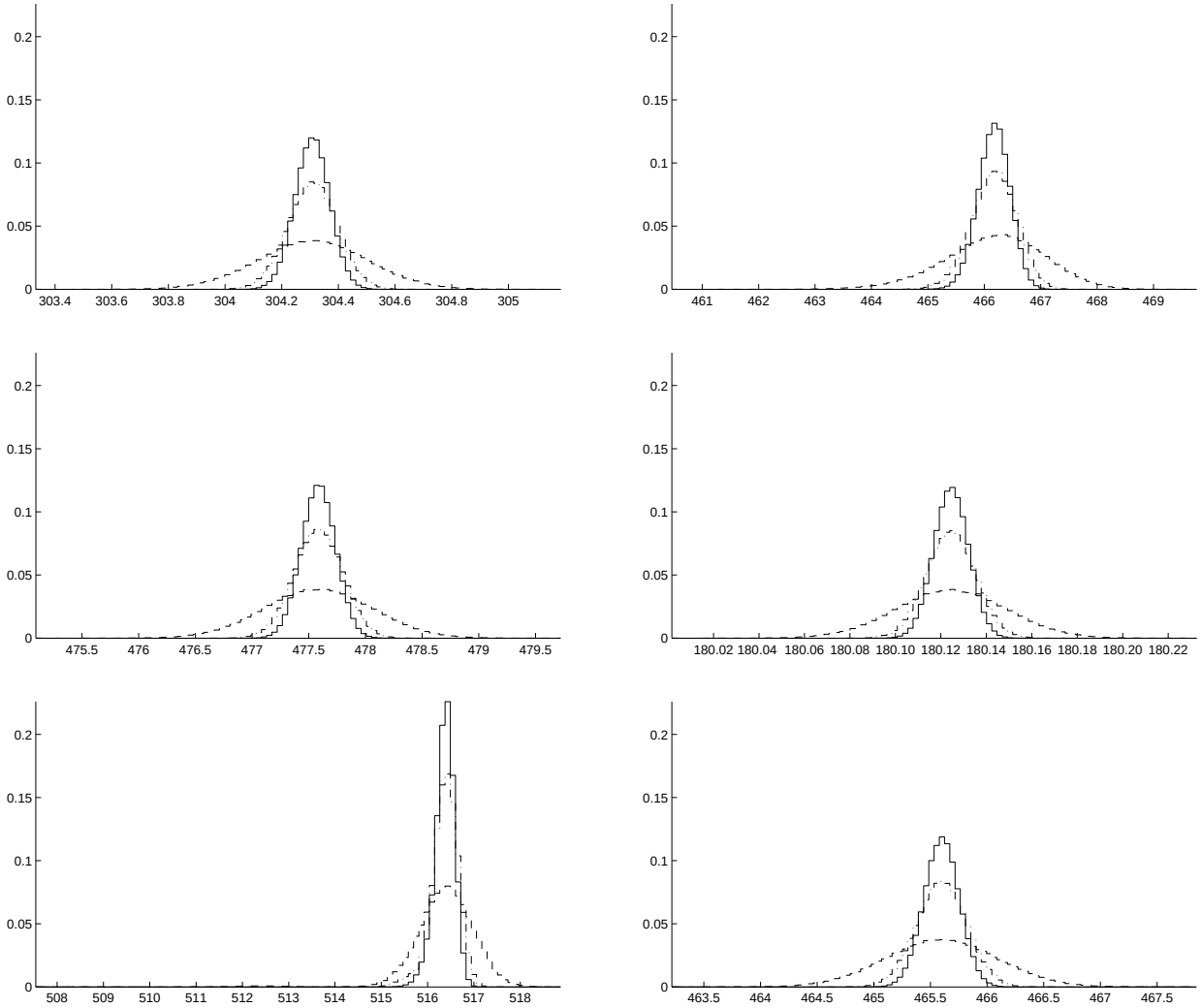

Figure 19: Distributions of Value Functions LSMC Estimates: All DGPs, Plant 1 mode.

Legend: see figure 18.

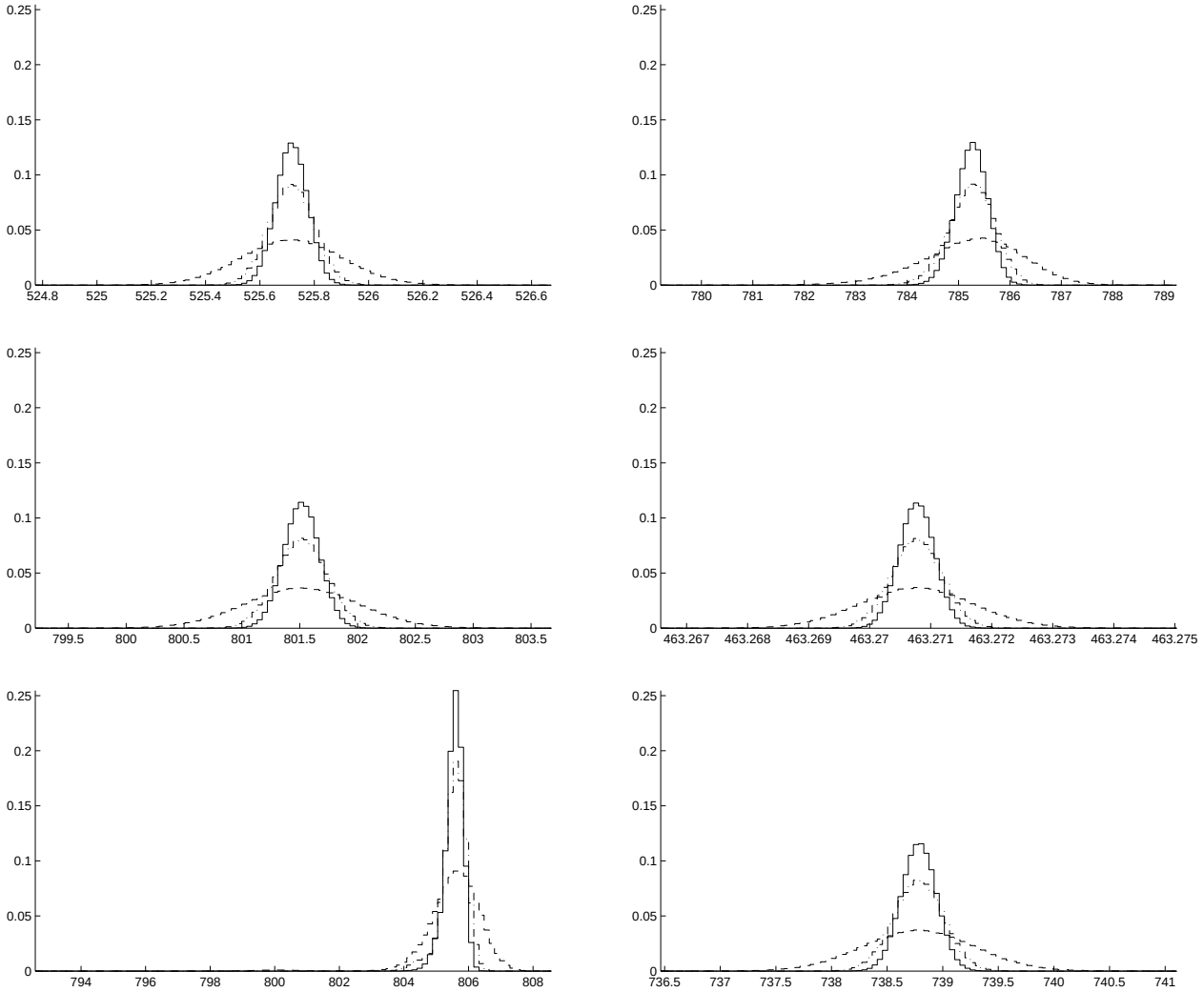

Figure 20: Distributions of Value Functions LSMC Estimates: All DGPs, Plant 2 mode.

Legend: see figure 18.

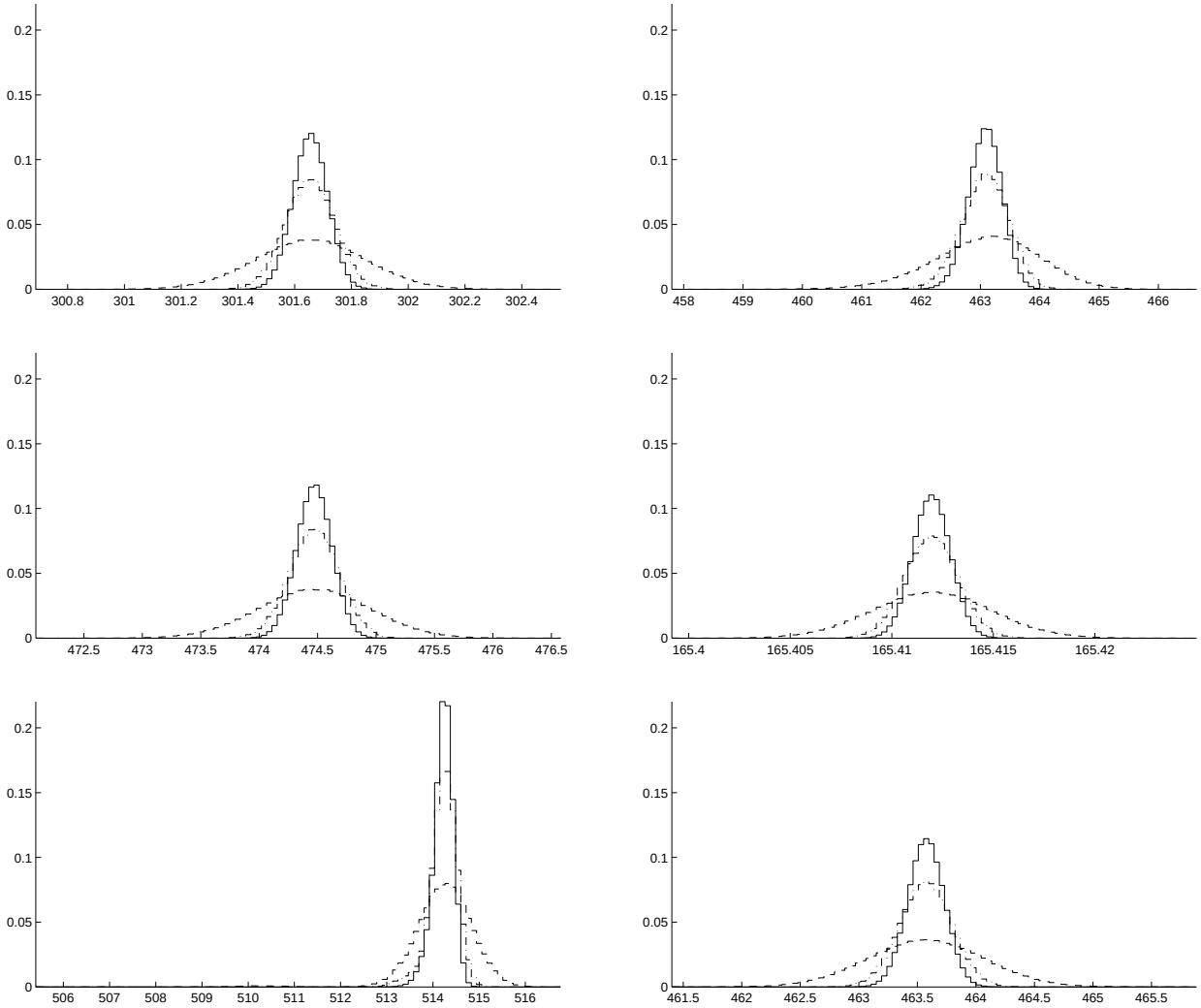

Figure 21: Distributions of Value Functions LSMC Estimates: All DGPs, Mothballed Plant 1 mode. Legend: see figure 18.

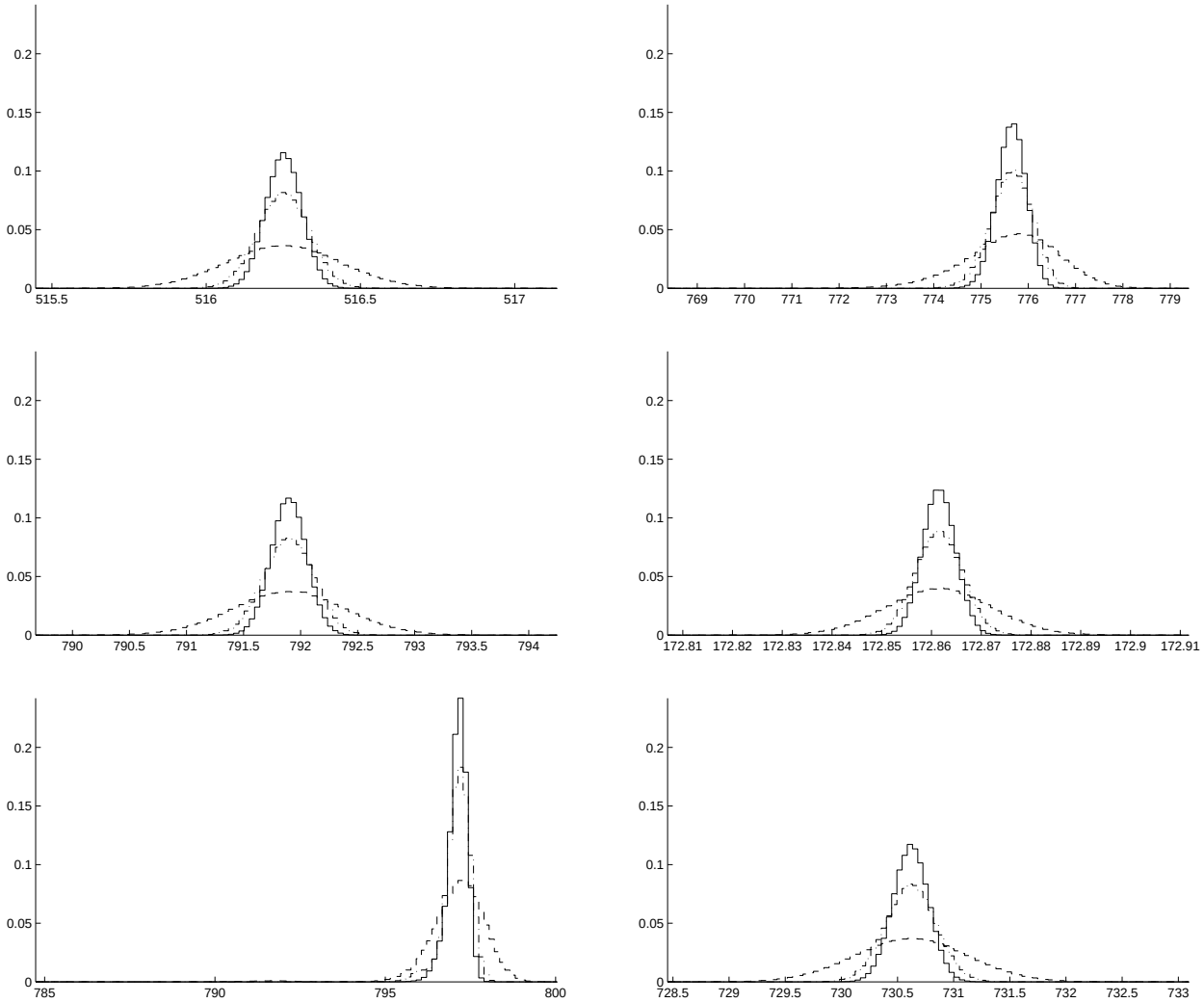

Figure 22: Distributions of Value Functions LSMC Estimates: All DGPs, Mothballed Plant 2 mode.
Legend: see figure 18.

Value Function=Wait

0	1.000%	0.900%	0.800%	0.700%	0.500%
10	100.000%	99.981%	99.778%	98.237%	73.842%
20	100.000%	100.000%	99.999%	99.872%	81.584%
30	100.000%	100.000%	100.000%	99.986%	86.704%
50	100.000%	100.000%	100.000%	100.000%	92.292%
100	100.000%	100.000%	100.000%	100.000%	97.790%

Value Function=Plant 1

0	1.000%	0.900%	0.800%	0.700%	0.500%
10	99.978%	97.733%	67.110%	12.528%	0.000%
20	100.000%	99.760%	73.370%	5.293%	0.000%
30	100.000%	99.977%	77.736%	2.304%	0.000%
50	100.000%	100.000%	83.607%	0.546%	0.000%
100	100.000%	100.000%	91.747%	0.014%	0.000%

Value Function=Plant 2

0	1.000%	0.900%	0.800%	0.700%	0.500%
10	99.932%	61.094%	0.484%	0.000%	0.000%
20	100.000%	65.717%	0.009%	0.000%	0.000%
30	100.000%	68.958%	0.001%	0.000%	0.000%
50	100.000%	73.719%	0.000%	0.000%	0.000%
100	100.000%	81.528%	0.000%	0.000%	0.000%

Value Function=Mothball Plant 1

0	1.000%	0.900%	0.800%	0.700%	0.500%
10	99.965%	97.092%	63.223%	10.878%	0.000%
20	100.000%	99.637%	67.946%	3.792%	0.000%
30	100.000%	99.935%	71.693%	1.603%	0.000%
50	100.000%	99.999%	77.158%	0.275%	0.000%
100	100.000%	100.000%	85.507%	0.000%	0.000%

Value Function=Mothball Plant 2

0	1.000%	0.900%	0.800%	0.700%	0.500%
10	99.552%	41.720%	0.113%	0.000%	0.000%
20	99.984%	38.362%	0.000%	0.000%	0.000%
30	100.000%	35.289%	0.000%	0.000%	0.000%
50	100.000%	31.728%	0.000%	0.000%	0.000%
100	100.000%	25.051%	0.000%	0.000%	0.000%

Table 28: Bootstrapped Confidence Intervals: Univariate GBM
Table entry is the relative frequency of the boostrapped B= 400.000 LSMC valuations that fall within an interval obtained increasing or decreasing the lattice benchmark for the % reported in the first row of each subsection. First column reports bootstrapped sample size.

Value Function=Wait

0	1.500%	1.000%	0.900%	0.800%	0.700%
10	85.058%	30.195%	20.251%	12.435%	7.012%
20	92.778%	22.875%	11.734%	5.020%	1.816%
30	96.183%	18.486%	7.252%	2.228%	0.509%
50	98.907%	12.204%	2.968%	0.456%	0.038%
100	99.923%	4.715%	0.343%	0.013%	0.000%

Value Function=Plant 1

0	1.500%	1.000%	0.900%	0.800%	0.700%
10	80.718%	2.615%	0.542%	0.064%	0.006%
20	88.208%	0.249%	0.007%	0.000%	0.000%
30	92.419%	0.037%	0.000%	0.000%	0.000%
50	96.696%	0.002%	0.000%	0.000%	0.000%
100	99.495%	0.000%	0.000%	0.000%	0.000%

Value Function=Plant 2

0	1.500%	1.000%	0.900%	0.800%	0.700%
10	99.995%	84.327%	59.794%	27.470%	6.371%
20	100.000%	91.523%	61.990%	19.124%	1.571%
30	100.000%	95.076%	63.822%	13.839%	0.367%
50	100.000%	98.198%	66.954%	7.708%	0.026%
100	100.000%	99.870%	72.577%	2.179%	0.000%

Value Function=Mothball Plant 1

0	1.500%	1.000%	0.900%	0.800%	0.700%
10	78.899%	2.324%	0.423%	0.057%	0.003%
20	86.531%	0.243%	0.010%	0.000%	0.000%
30	90.648%	0.023%	0.000%	0.000%	0.000%
50	95.414%	0.000%	0.000%	0.000%	0.000%
100	99.082%	0.000%	0.000%	0.000%	0.000%

Value Function=Mothball Plant 2

0	1.500%	1.000%	0.900%	0.800%	0.700%
10	99.991%	81.911%	55.951%	24.223%	5.312%
20	100.000%	89.097%	56.503%	15.555%	1.099%
30	100.000%	93.011%	57.127%	10.282%	0.227%
50	100.000%	96.957%	58.480%	4.942%	0.012%
100	100.000%	99.591%	60.951%	0.896%	0.000%

Table 29: Bootstrapped Confidence Intervals: Bivariate GBM

Table entry is the relative frequency of the boostrapped B= 400.000 LSMC valuations that fall within an interval obtained increasing or decreasing the lattice benchmark for the % reported in the first row of each subsection. First column reports bootstrapped sample size.

Value Function=Wait

0	1.200%	1.100%	1.000%	0.900%	0.800%
10	99.763%	99.134%	97.297%	92.804%	84.167%
20	99.994%	99.959%	99.680%	98.028%	92.040%
30	100.000%	100.000%	99.941%	99.410%	95.723%
50	100.000%	100.000%	100.000%	99.951%	98.726%
100	100.000%	100.000%	100.000%	100.000%	99.888%

Value Function=Plant 1

0	1.200%	1.100%	1.000%	0.900%	0.800%
10	10.669%	1.187%	0.063%	0.002%	0.000%
20	4.142%	0.069%	0.000%	0.000%	0.000%
30	1.527%	0.003%	0.000%	0.000%	0.000%
50	0.290%	0.000%	0.000%	0.000%	0.000%
100	0.006%	0.000%	0.000%	0.000%	0.000%

Value Function=Plant 2

0	1.200%	1.100%	1.000%	0.900%	0.800%
10	100.000%	99.976%	97.155%	59.652%	8.163%
20	100.000%	100.000%	99.678%	63.953%	2.420%
30	100.000%	100.000%	99.929%	66.730%	0.808%
50	100.000%	100.000%	100.000%	71.525%	0.095%
100	100.000%	100.000%	100.000%	78.677%	0.001%

Value Function=Mothball Plant 1

0	1.200%	1.100%	1.000%	0.900%	0.800%
10	8.519%	0.827%	0.047%	0.002%	0.001%
20	2.688%	0.038%	0.000%	0.000%	0.000%
30	0.960%	0.000%	0.000%	0.000%	0.000%
50	0.109%	0.000%	0.000%	0.000%	0.000%
100	0.004%	0.000%	0.000%	0.000%	0.000%

Value Function=Mothball Plant 2

0	1.200%	1.100%	1.000%	0.900%	0.800%
10	100.000%	99.932%	94.441%	48.912%	4.846%
20	100.000%	100.000%	98.831%	48.253%	0.935%
30	100.000%	100.000%	99.745%	48.040%	0.187%
50	100.000%	100.000%	99.987%	47.274%	0.014%
100	100.000%	100.000%	100.000%	46.439%	0.000%

Table 30: Bootstrapped Confidence Intervals: Trivariate GBM
Table entry is the relative frequency of the boostrapped B= 400.000 LSMC valuations that fall within an interval obtained increasing or decreasing the lattice benchmark for the % reported in the first row of each subsection. First column reports bootstrapped sample size.

Value Function=Wait

0	0.700%	0.600%	0.500%	0.200%	0.010%
10	41.499%	35.416%	29.395%	11.377%	0.538%
20	40.614%	33.154%	26.216%	9.024%	0.437%
30	38.859%	30.012%	22.279%	6.441%	0.295%
50	35.690%	25.206%	16.434%	2.853%	0.099%
100	30.333%	17.170%	8.422%	0.385%	0.002%

Value Function=Plant 1

0	0.700%	0.600%	0.500%	0.200%	0.010%
10	100.000%	100.000%	100.000%	100.000%	100.000%
20	100.000%	100.000%	100.000%	100.000%	100.000%
30	100.000%	100.000%	100.000%	100.000%	100.000%
50	100.000%	100.000%	100.000%	100.000%	100.000%
100	100.000%	100.000%	100.000%	100.000%	100.000%

Value Function=Plant 2

0	0.700%	0.600%	0.500%	0.200%	0.010%
10	100.000%	100.000%	100.000%	100.000%	100.000%
20	100.000%	100.000%	100.000%	100.000%	100.000%
30	100.000%	100.000%	100.000%	100.000%	100.000%
50	100.000%	100.000%	100.000%	100.000%	100.000%
100	100.000%	100.000%	100.000%	100.000%	100.000%

Value Function=Mothball Plant 1

0	0.700%	0.600%	0.500%	0.200%	0.010%
10	100.000%	100.000%	100.000%	100.000%	74.855%
20	100.000%	100.000%	100.000%	100.000%	82.906%
30	100.000%	100.000%	100.000%	100.000%	87.671%
50	100.000%	100.000%	100.000%	100.000%	93.423%
100	100.000%	100.000%	100.000%	100.000%	98.308%

Value Function=Mothball Plant 2

0	0.700%	0.600%	0.500%	0.200%	0.010%
10	100.000%	100.000%	100.000%	100.000%	27.946%
20	100.000%	100.000%	100.000%	100.000%	20.109%
30	100.000%	100.000%	100.000%	100.000%	15.340%
50	100.000%	100.000%	100.000%	100.000%	9.392%
100	100.000%	100.000%	100.000%	100.000%	3.229%

Table 31: Bootstrapped Confidence Intervals: Geometric Ornstein Uhlenbeck
Table entry is the relative frequency of the boostrapped B= 400.000 LSMC valuations that fall within an interval obtained increasing or decreasing the lattice benchmark for the % reported in the first row of each subsection. First column reports bootstrapped sample size.

Value Function=Wait

0	0.700%	0.600%	0.500%	0.200%	0.100%
10	99.183%	99.017%	98.550%	73.041%	41.913%
20	99.949%	99.790%	99.386%	87.221%	56.337%
30	99.993%	99.972%	99.903%	92.342%	64.642%
50	100.000%	99.999%	99.996%	96.727%	75.247%
100	100.000%	100.000%	100.000%	99.409%	86.911%

Value Function=Plant 1

0	0.700%	0.600%	0.500%	0.200%	0.100%
10	99.039%	99.012%	98.711%	52.285%	19.155%
20	99.872%	99.231%	98.333%	52.957%	11.139%
30	99.974%	99.940%	99.380%	52.807%	6.617%
50	100.000%	99.997%	99.936%	53.127%	2.572%
100	100.000%	100.000%	100.000%	52.664%	0.276%

Value Function=Plant 2

0	0.700%	0.600%	0.500%	0.200%	0.100%
10	99.032%	98.999%	98.674%	35.860%	5.343%
20	99.921%	99.278%	98.196%	29.563%	1.120%
30	99.973%	99.935%	99.291%	24.934%	0.260%
50	100.000%	99.997%	99.923%	19.114%	0.015%
100	100.000%	100.000%	100.000%	10.143%	0.000%

Value Function=Mothball Plant 1

0	0.700%	0.600%	0.500%	0.200%	0.100%
10	99.043%	99.009%	98.722%	52.442%	19.176%
20	99.911%	99.295%	98.409%	52.900%	11.198%
30	99.971%	99.928%	99.374%	53.096%	6.646%
50	100.000%	99.995%	99.941%	53.399%	2.677%
100	100.000%	100.000%	100.000%	52.775%	0.318%

Value Function=Mothball Plant 2

0	0.700%	0.600%	0.500%	0.200%	0.100%
10	99.009%	98.979%	98.627%	35.972%	5.472%
20	99.909%	99.257%	98.264%	29.394%	1.098%
30	99.978%	99.925%	99.194%	24.841%	0.279%
50	100.000%	99.996%	99.924%	18.552%	0.013%
100	100.000%	100.000%	99.998%	10.073%	0.000%

Table 32: Bootstrapped Confidence Intervals: Two Factor Model
Table entry is the relative frequency of the boostrapped B= 400.000 LSMC valuations that fall within an interval obtained increasing or decreasing the lattice benchmark for the % reported in the first row of each subsection. First column reports bootstrapped sample size.

Value Function=Wait

0	0.700%	0.600%	0.500%	0.400%	0.300%
10	99.711%	98.665%	95.353%	87.105%	71.934%
20	99.996%	99.916%	99.163%	94.772%	80.398%
30	100.000%	99.998%	99.859%	97.703%	85.340%
50	100.000%	100.000%	99.992%	99.512%	91.153%
100	100.000%	100.000%	100.000%	99.982%	97.190%

Value Function=Plant 1

0	0.700%	0.600%	0.500%	0.400%	0.300%
10	99.920%	98.696%	89.901%	62.828%	26.844%
20	100.000%	99.916%	96.440%	68.061%	19.193%
30	100.000%	99.992%	98.653%	71.755%	14.158%
50	100.000%	100.000%	99.760%	77.067%	8.345%
100	100.000%	100.000%	99.996%	85.123%	2.546%

Value Function=Plant 2

0	0.700%	0.600%	0.500%	0.400%	0.300%
10	99.505%	85.526%	33.654%	2.834%	0.028%
20	99.986%	93.344%	27.417%	0.336%	0.000%
30	100.000%	96.743%	22.935%	0.040%	0.000%
50	100.000%	99.120%	17.041%	0.001%	0.000%
100	100.000%	99.970%	8.877%	0.000%	0.000%

Value Function=Mothball Plant 1

0	0.700%	0.600%	0.500%	0.400%	0.300%
10	99.932%	98.684%	89.546%	62.223%	26.489%
20	100.000%	99.917%	96.114%	67.001%	18.676%
30	100.000%	99.991%	98.517%	70.419%	13.482%
50	100.000%	100.000%	99.747%	75.553%	7.831%
100	100.000%	100.000%	99.998%	83.584%	2.296%

Value Function=Mothball Plant 2

0	0.700%	0.600%	0.500%	0.400%	0.300%
10	99.365%	85.019%	33.328%	2.874%	0.038%
20	99.984%	92.712%	26.838%	0.320%	0.000%
30	99.999%	96.267%	22.476%	0.055%	0.000%
50	100.000%	98.905%	16.370%	0.001%	0.000%
100	100.000%	99.952%	8.356%	0.000%	0.000%

Table 33: Bootstrapped Confidence Intervals: Three Factor Model
Table entry is the relative frequency of the boostrapped B= 400.000 LSMC valuations that fall within an interval obtained increasing or decreasing the lattice benchmark for the % reported in the first row of each subsection. First column reports bootstrapped sample size.

7 Conclusions

We assess the applicability of LSMC methods (Longstaff and Schwartz, 2001) to the general model of real options by (Kulatilaka and Trigeorgis, 1994). After reviewing briefly the Kulatilaka-Trigeorgis (KT) model, we motivate the choice of LSMC among the variety of Monte Carlo methods available in current literature to price derivatives. We propose some simple correction methods to get unbiased results when using either LSMC or lattice methods to discretize a variety of data generating processes, see table 1, for the KT general model of real options. We devise several sets of experiments to assess applicability of LSMC to the KT model. First, we show which are the most effective and the most efficient parameters in honing results from LSMC. Second, we show how to make inference on LSMC results and construct confidence intervals in large and small samples.

The main conclusion of these set of experiments is that LSMC accuracy is very much dependent on the underlying DGP. We show how convergence propositions in (Longstaff and Schwartz, 2001) do not have general applicability. As a matter of fact, they are veryfied only when the underlying stochastic process contains a mean reverting feature, e.g. models 1,2 and 3 in (Schwartz, 1997), while this is not true for GBMs underlyings. We conjecture that this may be due to the fact that a least squares regression approximates better a bounded space, like the one in which a mean reverting process happens to be.[28]

We conclude that LSMC is definetly the best method to implement the KT model in multivariate frameworks being quick and accurate when compared to multivariate lattices counterparts. This paper can be considered as a building block for further extensions of the KT model.

For instance, LSMC method gives the analyst the opportunity to describe in a KT framework the investment project with real options in a more thorough way than any other numerical or symbolic solution approach. As an example, some path dependent project descriptors could be computed on each simulated path, such as Internal Rate of Return or Pay Back Period. Furthermore, given that LSMC provides an entire distributions of the expanded NPV, it is possible to compute its VaR or project at risk. In addition, with the simulated cash flows at each epoch it is possible to compute CFaR. Hence, in a multivariate LSMC framework it is easy to single out the most important sources of market risk in the risk mapping equation represented by both periodic, see equation (3), and infrequent cash flows, see expression (5).

[28] We conjecture this is the same reason why LSMC is a convergent algorithm, as $\Delta t \to 0$, in pricing an American put but not an American call, with known dividend yield of the underlying stock. In the case of models 1,2 and 3 (Schwartz, 1997) dealt in the text, the payoffs and continuation values are defined in bounded finite space since the underlying itself is bounded. In the case of an American put option this happens because the derivative has a bounded payoff.

References

Abadie, L. M. and Chamorro, J. M. (2006). Monte carlo valuation of natural gas investments. Working paper, Bilbao Bizkaia Kutxa, University of the Basque Country Dept. Foundations of Economic Analysis I, Gran Vìa 30, 48009 Bilbao, Spain.

Abdel Sabour, S. A. and Poulin, R. (2006). Valuing real capital investments using the least squares monte carlo method. *Engineering Economist*, 51:141–160.

Alesii, G. (2000). Gauss^{TM} code for real options: Kulatilaka '93: The case of a dual fuel boiler. working paper http://papers.ssrn.com, Universita' degli studi - L'Aquila, Facolta' di Economia, Dipartimento di Sistemi ed Istituzioni per Economia, L'Aquila. Posted on the Financial Economics Network in 2001.

Andersen, L. (2000). A simple approach to the pricing of bermudan swaptions in the multifactor libor model. *Journal of Computational Finance*, 3(2):1–32.

Areal, N., Rodrigues, A., and Rocha Armada, M. J. (2007). Improvements to the least squares monte carlo option valuation method. Working paper, Department of Management and Management Research Unit, School of Economics and Management, University of Minho, University of Minho, 4710-057 Braga, Portugal. Presented at the EWGFM April 2007 Rotterdam.

Bally, V., Pages, J., and Printemps, J. (2002). First order scheme in the numerical quantization method. *Mathematical Finance*, 13(1):1–16.

Barraquand, J. and Martineau, D. (1995). Numerical valuation of high dimensional multivariate american securities. *Journal of Financial and Quantitative Analysis*, 30(3):382–405.

Baule, R. and Tallau, C. (2006). Option prices of growth companies: The explanatory power of the schwartz/moon model. Working paper, Institute of Finance and Banking, University of Göttingen, Platz der Göttinger Sieben 5, D-37073, Göttingen, Germany.

Bellman, R. and Dreyfus, S. (1959). Functional approximations and dynamic programming. *Math. Tables and Other Aids Comp.*, 13:247–251.

Bertsekas, D. P. (1995). *Dynamic Programming and Optimal Control*, volume 1-2. Athena Scientific Press, Belmont Mass, first edition.

Black, F. and Scholes, M. (1973). The pricing of options and corporate liabilities. *Journal of Political Economy*, 71(2):637–659.

Borison, A. (2005). Real options analysis: Where are the emperor's clothes? *Journal of Applied Corporate Finance*, 17(2):17–31.

Boyle, P. P., Evnine, J., and Gibbs, S. (1989). Numerical evaluation of multivariate contingent claims. *Review of Financial Studies*, 2(2):241–250.

Brekke, K. and Oksendal, B. (1994). Optimal switiching in an economic activity under uncertainty. *SIAM Journal of Control and Optimization*, 32:1021–1036.

Brekke, K. A. and Schieldrop, B. (2000). *Investments in Flexible Technologies under Uncertainty*, chapter 3, pages 34–49. In (Brennan and Trigeorgis, 2000).

Brennan, M. and Schwartz, E. (1985). Evaluating natural resource investments. *Journal of Business*, 58:135–157.

Brennan, M. and Trigeorgis, L. (2000). *Project Flexibility, Agency and Competition: New Developments in the Theory and Applications of Real Options*. Oxford University Press, New York, Oxford, England.

Broadie, M. and Detemple, J. (1996). American option valuation: New bounds, approximation, and a comparison of existing methods. *Review of Financial Studies*, 9(4):1211–1250.

Broadie, M. and Glasserman, P. (1997). Pricing american style securities using simulation. *Journal of Economic Dynamics and Control*, 21(8-9):1323–1352.

Broadie, M. and Glasserman, P. (2004). A stochastic mesh method for pricing high dimensional american options. *Journal of Computational Finance*, 7(4):35–72.

Chiara, N. (2006). Real options methods for improving economic risk management in infrastructure project finance. Phd dissertation, Columbia University, Graduate School of Arts and Sciences.

Clément, E., Lamberton, D., and Protter, P. (2002). An analysis of the least squares regression method for american option pricing. *Finance And Stochastics*, 6:449–471.

Copeland, T. and Antikarov, V. (2005). Real options: Meeting the georgetown challenge. *Journal of Applied Corporate Finance*, 17(2):32–51.

Cortazar, G., Gravet, M., and Urzua, J. (2005). The valuation of multidimensional american real options using computer based simulation. Working paper, Departamento de Ingenieria Industrial y de Sistemas, Pontificia Universitad Católica de Chile, Vicuña Mackenna 4860, Santiago, Chile. Presented at the 2005 Real Options Conference, Paris.

Cortazar, G. and Schwartz, E. S. (1998). Montecarlo evaluation model of an undeveloped oil field. *Journal of Energy Finance and Development*, 3(1):73–84.

Cortazar, G., Schwartz, E. S., and Casassus, J. (2001). Optimal exploration investments under price and geological uncertainty: A real options model. *R & D Management*, 31(2):181–189.

Cortazar, G., Schwartz, E. S., and Salinas, M. (1998). Evaluating environmental investments: A real options approach. *Management Science*, 44:1059–1070.

Cox, J., Ingersoll, J., and Ross, S. (1985). An inter-temporal general equilibrium model of asset prices. *Econometrica*, 53:363–384.

Cox, J., Ross, S., and Rubinstein, M. (1979). Option pricing: A simplified approach. *Journal of Financial Economics*, 12(1):229–263.

Dixit, A. and Pindyck, R. S. (1994). *Investments under Uncertainty*. Princeton University Press, Princeton NJ.

Dixit, A. K. (1989). Entry and exit decisions under uncertainty. *Journal of Political Economy*, 97:620–638.

Duckworth, K. and Zervos, M. (2001). A model for investment decisions with switching costs. *Annals of Applied Probability*, 11:239–260.

Efron, B. and Tibshirani, R. (1993). *An Introduction to the Boostrap*. Chapman & Hall, New York.

Ekvall, N. (1996). A lattice approach for pricing of multivariate contingent claims. *European Journal of Operational Research*, 91:214–228.

Gamba, A. (2002). Real options valuation: A montecarlo simulation approach. working paper, Department of Financial Studies, University of Verona and Faculty of Management, University of Calgary - Alberta (Canada), Via Giardino Giusti 2, 37129 Verona, Italy. EFA 2002 Berlin, www.ssrn.com.

Gamba, A. and Trigeorgis, L. (2005). A log-transformed binomial lattice extension for multi-dimensional option problems. Working paper, Department of Financial Studies, Università di Verona, Department of Public and Business Administration, University of Cyprus and GSB University of Chicago. first version 2001.

Geltner, D., Riddiough, T., and Stojanovich, S. (1996). Insights on thr effect of land use choice: The perpetual option on the best of two underlying assets. *Journal of Urban Economics*, 39:20–50.

Gibson, R. and Schwartz, E. (1990). Stochastic convenience yield and the pricing of oil contingent claims. *Journal of Finance*, 45(2):959–976.

Glasserman, P. (2004). *Monte Carlo Methods in Financial Engineering*. Application of Mathematics Stochastic Modelling and Applied Probability vol. 53. Springer, New York, first edition.

Glasserman, P. and Yu, B. (2003). Number of paths versus numebr of basis functions in american option pricing. Working paper, Graduate School of Business, Columbia University, New York, NY 10027.

Glasserman, P. and Yu, B. (2004). Number of paths versus number of basis functions in american option pricing. *Annals of Applied Probability*, 14(4):2090–2119.

Gourieroux, C. and Jasiak, J. (2001). *Financial Econometrics: Problems, Models and Methods*. Princeton Series in Finance. Princeton University Press, Princeton, NJ, first edition.

Greene, W. H. (1994). *Econometric Analysis*. MacMillan, New York, second edition.

Hahn, W. J. and Dyer, J. S. (2008). Discrete time modelling of mean reverting stochastic processes for real option valuation. *European Journal of Operational Research*, (184):534–548.

Haugh, M. and Kogan, L. (2004). Pricing american options: A duality approach. *Operations Research*, 54:250–267.

Hodder, J., Mello, A. S., and Sick, G. S. (2001). Valuing real option: Can risk adjusted discounting be made to work ? *Journal of Applied Corporate Finance*, 14(2):90–101.

Hodrick, R. J. (1992). Dividend yields and expected stock returns: Alternative procedures for inference and measurement. *Review of Financial Studies*, 5(3):357–386.

Hull, J. and White, A. (1990). Pricing interest rate derivative securities. *Review of Financial Studies*, 3(4):573–592.

Hull, J. C. (2000). *Options, Futures and Other Derivatives*. Prentice Hall, Upper Saddle River, N.J., fourth edition. Third Edition 1997.

Imai, J. (2006). Evaluating the swithching options by simulation methods. Working paper, Graduate School of Economics and Management Tohoku University, 27-1, Kawauchi, Aoba-ku, Sendai Miyagi, 980-8576 Japan.

Imai, J. and Nakajima, M. (2000). A real option analyisism of an oil refinery project. *Financial Practice And Education*, pages 78–91.

Jarrow, R., Maksimovic, V., and Ziemba, W. (1995). *Finance*, volume 9 of *Handbooks in Operations Research and Management*. North Holland Elsevier, Amsterdam, first edition. Informs Institute for Operations Research and the Management Sciences.

Jiang, G. J. and Knight, J. L. (1999). Finite sample comparison of alternative estimators of itô diffusion processes: a monte carlo study. *Journal of Computational Finance*, 2(3):5–38.

Kalligeros, K. C. (2005). Framework for the optimal design of corporate facilities for contracting operations. Working paper, Engineering Systems Divisions, MIT, Cambridge MA02139.

Kamrad, B. and Ritchken, P. (1991). Multinomial approximating models for options with k state variables. *Management Science*, 37(12):1640–1651.

Knudsen, T. S., Meister, B., and Zervos, M. (1999). On the relationship of the dynamic programming approach and the contingent claim approach to asset valuation. *Finance And Stochastics*, 3(4):433–449.

Kulatilaka, N. (1988). Valuing the flexibility of flexible manufacturing systems. *IEEE Transactions on Engineering Management*, 35(4):250–257.

Kulatilaka, N. (1993). The value of flexibility: The case of a dual-fuel industrial steam boiler. *Financial Management*, 22(3):271–280.

Kulatilaka, N. (1995). *The Value of Flexibility: A General Model of Real Options*, chapter 5, pages 89–109. In (Trigeorgis, 1995).

Kulatilaka, N. and Marcus, A. J. (1988). General formulation of corporate real options. *Research in Finance*, 7:183–199.

Kulatilaka, N. and Trigeorgis, L. (1994). The general flexibility to switch: Real options revisited. *International Journal of Finance*, 6(2):778–796.

Lemelin, B., Abdel Sabour, S., and Poulin, R. (2006). Valuing mine 2 at raglan using real options. *International Journal of Mining, Reclamation and Environment*, 20(1):46–56.

Longstaff, F. A. and Schwartz, E. S. (2001). Valuing american options by simulation: A simple least-squares approach. *Review of Financial Studies*, 14(1):113–147.

Luenberger, D. G. (1998). *Investment Science*. Oxford University Press, New York, Oxford, first edition.

McDonald, R. L. (2006). The role of realoptions in capital budgeting: Theory and practice. *Journal of Applied Corporate Finance*, 18(2):28–39.

Miranda, M. J. and Fackler, P. L. (2002). *Applied Computational Economics and Finance*. MIT Press, Cambridge, Massachussets.

Mood, A., Graybill, F., and Boes, D. (1974). *Introduction to the Theory of Statistics*. Series in Probability and Statistics. McGraw-Hill, New York, third edition.

Moreno, M. and Navas, F. J. (2001). On the robustness of least squares monte carlo for pricing american derivatives. Working paper, Department of Economics and Business, Universitat Pompeu Fabra, Barcelona, Spain; Department of Finance, Instituto de Empresa, Madrid, Spain. posted on www.ssrn.com.

Mun, J. (2002). *Real Options Analysis: Tools and Techniques for Valuing Strategic Investments and Decisions*. Wiley Finance. John Wiley & Sons, Hoboken, New Jersey. with Crystal ball CD-ROM.

Neftci, S. N. (2000). *An Introduction to the Mathematics of Financial Derivatives*. Academic Press, San Diego, CA, second edition.

Oduntan, R. and Fuller, D. (2005). Valuing strategic flexibilities in nuclear power plants life cycle management using simulation. Working paper, Department of Management Sciences, University of Waterloo, 200 University Avenue, Waterloo, Ontario Canada.

Øksendal, B. (2001). *Stochastic Differential Equations: An Introduction with Applications*. Universitext. Springer Verlag, Berlin Heidelberg, 6th edition.

Rao, R. K. S. (1992). *Financial Management: Concepts and Applications*. MacMillan, New York, second edition.

Raymar, S. B. and Zwecher, M. J. (1997). Monte carlo estimation of american call options on the maximum of several stocks. *Journal of Derivatives*, 5(1):7–23.

Rodrigues, A. and Rocha Armada, M. J. (2005). The valuation of real options with the least squares monte carlo simulation approach. Working paper, Management Research Unit, University of Minho, School of Economics and Management, University of Minho, 4710-057 Braga - Portugal.

Rogers, L. C. G. (2002). Monte carlo valuation of american options. *Mathematical Finance*, 12(3):271–286.

Schulmerich, M. (2005). *Real Options Valuation: The Importance of Interest Rate Modelling in Theory and Practice*. Lecture Notes in Economic and Mathematical Systems. Springer Verlag, Berlin - Heidelberg.

Schwartz, E. S. (1997). The stochastic behavior of commodity prices: Implications for valuation and hedging. *Journal of Finance*, 52(2):923–973.

Schwartz, E. S. and Moon, M. (2000). Rational pricing of internet companies. *Financial Analysts Journal*, pages 62–75.

Schwartz, E. S. and Moon, M. (2001). Rational pricing of internet companies revisited. *Financial Review*, 36:7–26.

Sick, G. (1995). *Real Options*, chapter 21, pages 631–691. Volume 9 of (Jarrow et al., 1995), first edition. Informs Institute for Operations Research and the Management Sciences.

Stentoft, L. (2004). Assessing the least squares monte-carlo approach to american option valuation. *Review of Derivatives Research*, 7:129–168.

Tavella, D. (2002). *Quantitative Methods in Derivatives Pricing: An Introduction to Computational Finance*. Wiley Finance. John Wiley & Sons. Inc., New York.

Trigeorgis, L. (1991). The nature of option interaction and the valutation of investments with multiple real options. *Journal of Financial and Quantitative Analysis*, 28(1):1–20.

Trigeorgis, L. (1995). *Real Options in Capital Investments, Models, Strategies and Applications*. Praeger, Westport, Conn.

Trigeorgis, L. (1996). *Real Options: Managerial Flexibility and Strategy in Resource Allocation*. MIT Press, Cambridge, Mass.

Tsekrekos, A. E., Shackleton, M. B., and Wojakowski, R. M. (2006). Evaluating natural resource investments using least squares monte carlo simulation approach. Working paper, Department of Accounting & Finance, Athens University of Economics & Business (AUEB); Department of Accounting & Finance, Management School, Lancaster University.

Tsitsiklis, J. N. and Van Roy, B. (2001). Regression method for pricing complex american style options. *IEEE Transactions on Neural Networks*, 12(4):694–703.

Vasicek, O. (1977). An equilibrium caracterization of the term structure. *Journal of Financial Economics*, 5:177–188.

Vollert, A. (2002). *A Stochastic Control Framework for Real Options in Strategic Valuation*. Birkhauser, Boston, Basel, Berlin.